DEVELOPMENT OF SODIUM ALKOXIDE CATALYSTS FROM POLYOLS FOR BIODIESEL PRODUCTION

A Thesis Submitted to the College of
Graduate Studies and Research
In Partial Fulfillment of the Requirements
For the Degree of Master of Science
In the Department of Food and Bioproduct Sciences
University of Saskatchewan
Saskatoon

By

HWEE YOONG FELICIA GOK

PERMISSION TO USE

In presenting this thesis in partial fulfilment of the requirements for a Postgraduate degree from the University of Saskatchewan, I agree that the Libraries of this University may make it freely available for inspection. I further agree that permission for copying of this thesis in any manner, in whole or in part, for scholarly purposes may be granted by the professor or professors who supervised my thesis work or, in their absence, by the Head of the Department or the Dean of the College in which my thesis work was done. It is understood that any copying or publication or use of this thesis or parts thereof for financial gain shall not be allowed without my written permission. It is also understood that due recognition shall be given to me and to the University of Saskatchewan in any scholarly use which may be made of any material in my thesis.

Requests for permission to copy or to make other use of material in this thesis in whole or part should be addressed to:

Head of the Department of Food and Bioproduct Sciences
University of Saskatchewan
Saskatoon, Saskatchewan Canada
S7N 5A8

ABSTRACT

Metal alkoxide and hydroxides are popular and inexpensive base catalysts used by industry to produce fatty acid esters. However hydroxides produce water when dissolved in an alcohol based solvent. Consequently the water molecule releases hydroxide anion, which attacks triglyceride to produce free fatty acids instead of fatty acid methyl ester. Presence of free fatty acid is highly unfavorable because it reacts with the base catalyst to produce soap and hence, inactivates the catalyst. The alternative, alkoxide, is therefore, a preferred choice over hydroxide. Nevertheless, alkoxides are more expensive, their production is hazardous and they are dangerous to transport. In this study, low cost sodium alkoxide base catalysts were synthesized from 50 wt% sodium hydroxide solution and non-volatile, non-toxic polyols using an alternative route which is less expensive and hazardous. Gravimetric analysis showed that polyols effectively aid in evaporation of 50 wt% aqueous sodium hydroxide during formation of alkoxide compounds. The resulting products are strong base compounds, which were characterized using single crystal, X-ray powder diffraction and elemental analyses. Results have shown that the polyol-derived alkoxide compounds are predominately mono-sodium substituted alkoxide that occur as adducts with sodium hydroxide.

Studies of transesterification reactions catalyzed by polyol-derived sodium alkoxide/hydroxide were conducted to evaluate reaction efficiency and kinetics. The reactions catalyzed by the polyol-derived sodium alkoxide/hydroxide successfully achieved comparable biodiesel yield with sodium methoxide (0.5 wt% of equivalent biodiesel yield under reaction conditions of 6:1 methanol to oil mole ratio at 60°C). Additionally, all polyol-derived alkoxide/hydroxide catalysts investigated in these studies were capable of achieving >95 wt% of biodiesel yield after 1.5 h in a single step transesterification reaction. Initial reaction rates (2 min) differed depending on the polyol used in producing the catalyst. The reaction rates over two minutes are in order of increasing activity: sorbitol < xylitol < sodium methoxide < 1,2-propanediol < 1,3-propanediol < glycerol. This result can be associated with release of these polyols in small quantity (<0.5%) as a result of methanol solvation to liberate the methoxide ion as

catalytic agent. Presence of these polyols at the beginning of a reaction may help to stabilize the immiscible oil/methanol phase by formation of emulsifier compounds (such as glycerol esters or glycol esters), which in return facilitate the transesterification reaction. In conclusion, the polyol-derived sodium alkoxide/hydroxide catalysts have demonstrated promising qualities to the industry. These catalysts may serve as an alternative solution to lower the cost of biodiesel plant operation without compromising production efficiency.

ACKNOWLEDGMENTS

I would like to express my deepest gratitude to Dr. Martin Reaney for providing me with the opportunity to work under his dedicated supervision. I highly appreciate his constant support and guidance throughout my master program. His great enthusiasm for science and commitment to work was both inspiring and motivating. I would also like to thank my advisory committee members: Dr. Ajay Dalai, Dr. Ramaswami Sammynaiken and Dr. Phyllis Shand for their invaluable advice and assistance.

I would like to extend my appreciation to Dr. Jian Heng Shen who generously shared his valuable experience and knowledge of synthesis experimental design. I wish to specifically recognize the technical and intellectual assistance of the Saskatchewan Structural Science Centre (SSSC) with special thanks to Dr. Gabriele Schatte for sharing her expertise and knowledge of X-ray crystallographic analysis. I would also like to thank Ken Thomas and Dr. Keith Brown for their excellent technical support in analysis.

I graciously acknowledge the financial contribution of Natural Sciences and Engineering Research Council (NSERC). Many thanks go to the faculty, staff and fellow students in Department of Food and Bioproduct Sciences for their support and cooperation. Much credits and appreciation go to all Team Phat members for their cooperation and encouragement. I will not forget the joys and fun we enjoyed together as a team. Last but not least, utmost thanks to my family especially my beloved parents for their unconditional love, sacrifices, understanding and patience in shaping me into who I am today. Special thanks to Pete Christensen for his continuous motivation, moral support and a strong faith in my new life endeavors.

TABLE OF CONTENTS

LIST OF TABLES

LIST OF FIGURES

CHAPTER 1.
INTRODUCTION

As the world population continues to increase, so does the demand for energy. Simultaneously, resources for production of conventional non-renewable fossil fuels are rapidly being depleted and a search for alternative renewable fuels is under way. Biodiesel is recognized as a potential alternative renewable fuel that has many environmental benefits when compared with conventional petroleum based fuels. For example, when compared to the use of petroleum diesel fuels, biodiesel usage decreases the net emission of greenhouse gas (CO_2), polyaromatic hydrocarbons and other noxious emissions leading to a decreased environmental impact and health risk (Sharma *et al*., 2008). Biodiesel consists of long chain fatty acid alkyl esters, produced by transesterification of triglycerides (TG) and/or esterification of fatty acids with low molecular weight alcohols. Acid catalysts readily catalyze the esterification reaction used to produce esters from fatty acids while base, acid or enzymes can catalyze transesterification reactions. Homogeneous base catalysts are mostly used in industrial biodiesel production from triglyceride due to the fast reaction rate under mild reaction conditions.

Metal hydroxides are popular base catalysts used by industry due to both low cost and availability. However hydroxides produce water when dissolved in an alcohol based solvent. As illustrated in Fig. 1.1, the water of this reaction releases hydroxide anion, which may attack ester reactants like triglyceride to produce free fatty acids instead of the desired fatty acid methyl ester. Free fatty acid present in some oils react with the base catalyst to produce soap *via* a neutralization (or saponification) reaction that inactivates base catalysts and causes product losses (Basu and Norris, 1996; Liu, 1994). Neutralization of base catalysts results in loss of catalytic activity and the resulting soaps can form emulsions, which generate problems in biodiesel purification

and increase product losses. The more expensive metal alkoxides (e.g. sodium methoxide or $NaOCH_3$) dissolve in methanol to produce a solution of methoxide ion in methanol without producing water. Therefore, $NaOCH_3$ is often a preferred choice over metal hydroxide for maintaining reaction rates and yield. Nevertheless, the cost of sodium methoxide is significantly higher than the sodium hydroxide. Sodium methoxide used in commercial biodiesel production is often sold as a 25 wt% methanol solution. Due to the methanol and alkoxide this material is both flammable and corrosive and must be handled with caution adding to its cost.

The current study explores the production of low cost polyol derived alkoxide base catalysts from aqueous solutions of metal hydroxides and non-volatile, non-toxic polyols. These strong base compounds can subsequently be used in transesterification reactions that may potentially achieve the same reaction rate and yield as alkoxides produced by other more expensive and hazardous routes. Production of such strong base catalysts from readily available materials has several valuable advantages to the biodiesel manufacturer currently using either hydroxide pellets or alkoxide solutions. For example, the starting materials are comparatively inexpensive solutions of aqueous base and polyols. In addition, the catalysts are easily prepared at the site of use without involving complicated synthesis processes.

The technical objectives of this study are as follow:

1. To synthesize anhydrous sodium alkoxide catalysts using non-toxic and non-volatile polyols as starting material
2. To examine the influence of different polyol types and mole ratios of starting materials on the drying behavior of aqueous sodium hydroxide solution
3. To characterize the chemical structure and composition of the new catalysts by single crystal, X-ray powder diffraction and elemental analyses
4. To study the effect of polyol-derived base catalyst concentration on kinetics and biodiesel yield in transesterification reactions
5. To compare catalytic reactivity among polyol-derived catalysts and conventional homogeneous catalyst (sodium methoxide)

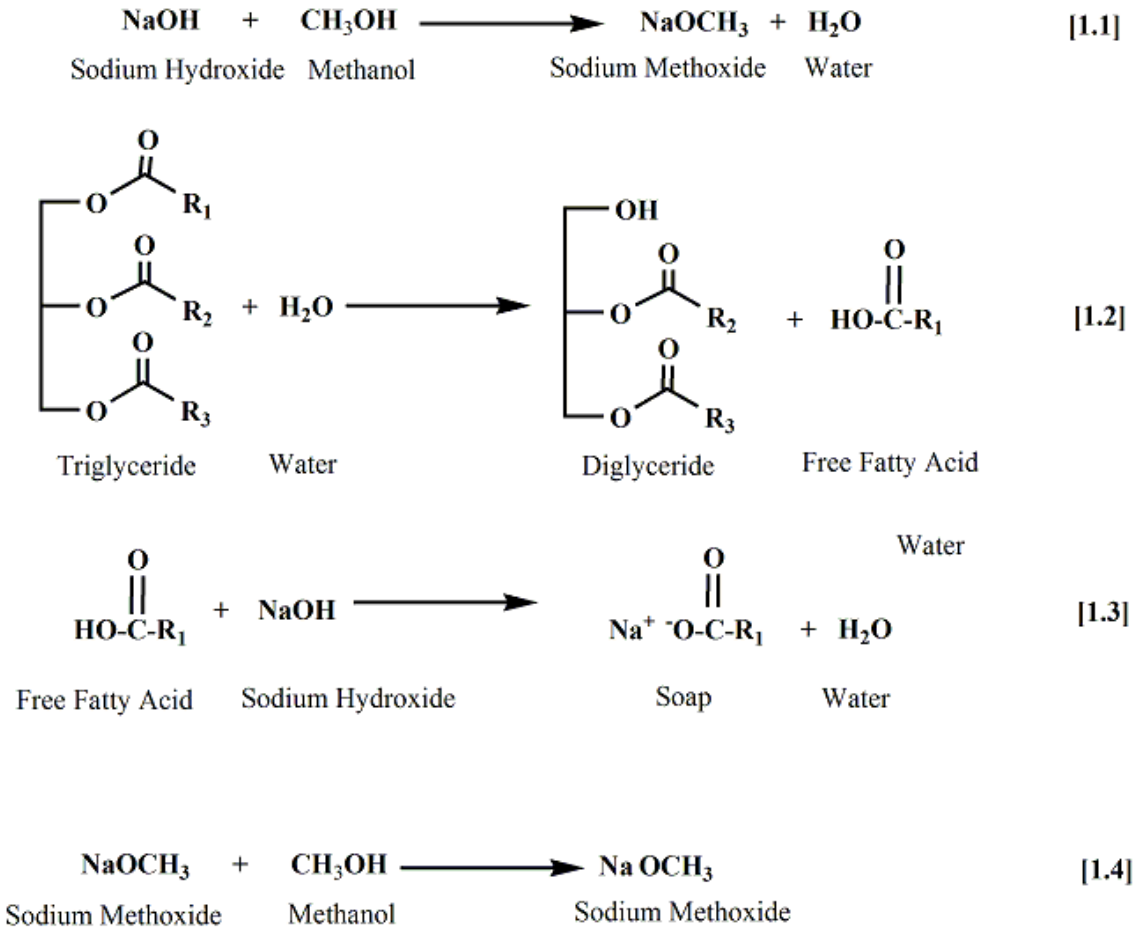

Fig. 1.1 Undesirable reactions of NaOH in triglyceride transesterification reactions. Production of water through the reaction of NaOH with methanol and saponification of triglyceride.

CHAPTER 2.
LITERATURE REVIEW

2.1 Base catalysis

Industrial production of liquid fuels and bulk chemicals requires the use of small amounts of reactive substances (catalysts) for improving the properties of the starting materials for their intended use. Such catalysts increase the chemical reaction rates and enable reactions to proceed at lower temperatures and pressures with higher selectivity towards the desired product. Moreover, a catalyst is not altered by the catalyzed reaction and thus can be recovered from the reaction products for further reactions (Crabtree, 2005; Leeuwen, 2004). Catalysts are often characterized by their chemical properties including solubility. Heterogeneous catalysts are a class of catalysts that are not soluble in the reaction medium that catalyze reactions of liquid or gaseous reagents at the surface of a solid support. Conversely, homogeneous catalysts dissolve in the reaction medium and exist in the same phase with the reactive substrate and reaction products. Therefore, all catalytic sites in a homogeneous system are available for reaction (Cole-Hamilton *et al.*, 2006).

Base-catalyzed ester hydrolysis or alcoholysis are examples of homogeneous reactions. In these reactions, Brönsted base serves two functions in organic reactions. Firstly, the compounds accept protons and thus serve in the classical function as a base. This reaction consumes the base and is not catalytic. Secondly, basic alkoxides produce a nucleophilic anion that can react with a carbonyl of a carboxylic ester (Bender, 1960). Both of these functions can be observed in the reactions of ester methanolysis by sodium hydroxide. First, the solvation of sodium hydroxide in methanol (CH_3OH) generates catalytic methoxide anion ($^{-}OCH_3$) by replacing the methanolic proton with sodium cation. This first reaction is not catalytic in nature. Subsequently, the methoxide

ion attacks the carboxylic ester compound *via* nucleophilic substitution to produce a new ester compound. The methoxide anion is released after the reaction and thus this reaction is catalytic.

2.2 Metal alkoxides: classification and general history of development

Metal alkoxides can be defined as compounds that are constituted from one or more alkyoxy groups (R) attached to metal (M) through the oxygen atom (Horn and Horns, 2000). These compounds are typically derived from alcohols by replacement of hydroxyl hydrogen with metal. The metal alkoxide derivatives for almost all the elements of the periodic table have been studied extensively to expand their applications in organic and inorganic reactions (Turnova and Novoselova, 1965). Metal hydroxides, being the inorganic metal analog to alkoxides, have been utilized in similar applications. For instance, both sodium hydroxide and methoxide may be used as homogeneous catalysts in transesterification reactions. However, unlike the hydroxide counterpart, properties of alkoxides are not determined solely by the electronegativity of the metal element. The reactivity and specificity also depends on acidity characteristics of the corresponding alcohol radical. In this context, metal alkoxide derivatives can be classified into three groups based on different types of metal and alcohol radical combination (Fig. 2.1).

Liebig first observed the interaction of potassium and sodium with alcohols 170 years ago and made the earliest observations of alkoxides. The first synthesis of metal alkoxide was published in 1837 when sodium ethoxide synthesis was described (Liebig, 1837). In 1872, Letts prepared the mono-sodium alkoxide derivative from glycerol and removed the alcohol of crystallization by heating in a current of hydrogen (Letts, 1872). In the 1880s, deForcrand prepared glycerol derived alkoxide by reacting three moles of sodium hydroxide with one mole of glycerine heated in an atmosphere of hydrogen at 100^{o}C (deForcrand, 1887). In the same year, deForcrand published another work related to di-sodium substituted glycerolate prepared by further reacting mono-substituted glycerolate with sodium ethoxide at elevated temperatures; *i.e.* 180 – 190°C

(deForcrand, 1887). In most of the alkaline alkoxide synthesis work reported, these compounds were described as a complex product instead of the pure alkoxide. The compounds are often derived as an adducts or solvates with neutral ligands like alcohols ($M(OR)_n$. xROH; x= 2 or 3) which require further purification steps to obtain unsolvated alkoxides (Fisher and McElvain, 1934).

In the 20th century, an enormous amount of alkoxide research was directed to discover physicochemical properties of alkoxides derived from multivalent metals (group III to group VIII). Their volatile properties made them attractive alkoxide precursors for depositing pure metal oxide films by chemical vapour deposition. These thin films of metal oxide are widely used in the electronics industry as insulators and high dielectric materials. Such compounds also have utility as nonlinear optical materials, high temperature superconductors and fast ion conductors (Bradley, 1989). In addition, these multivalent metal alkoxides can also be used as molecular precursor for preparing ceramic oxide materials and speciality glasses using sol-gel processes (Brinker and Scherer, 1990; Wright and Sommerdijk, 2001). The latter method provides a relatively low temperature mechanism for producing solid oxide materials as compared to the traditional method.

2.2.1 General techniques for synthesis of alkali alkoxides

For more than a century, various alkoxide derivatives have been prepared utilizing a wide range of synthetic approaches. In general, the technique selected for preparation of a particular metal alkoxide depends on the electropositive character of the metal of interest. Metals with more electropositive nature, such as group I alkaline metals, react spontaneously with alcohols. Alkoxides are prepared from much less electropositive metals (*eg*. Group III to VIII metals) using their metal chlorides with alcohols either alone or in the presence of a base acting as hydrogen chloride acceptor (Mehrotra, 1988). The present review will be devoted to the derivatives of the alkaline metals and aliphatic alcohols, which are characteristic of the metal alkoxide (category three) illustrated in Figure 2.1.

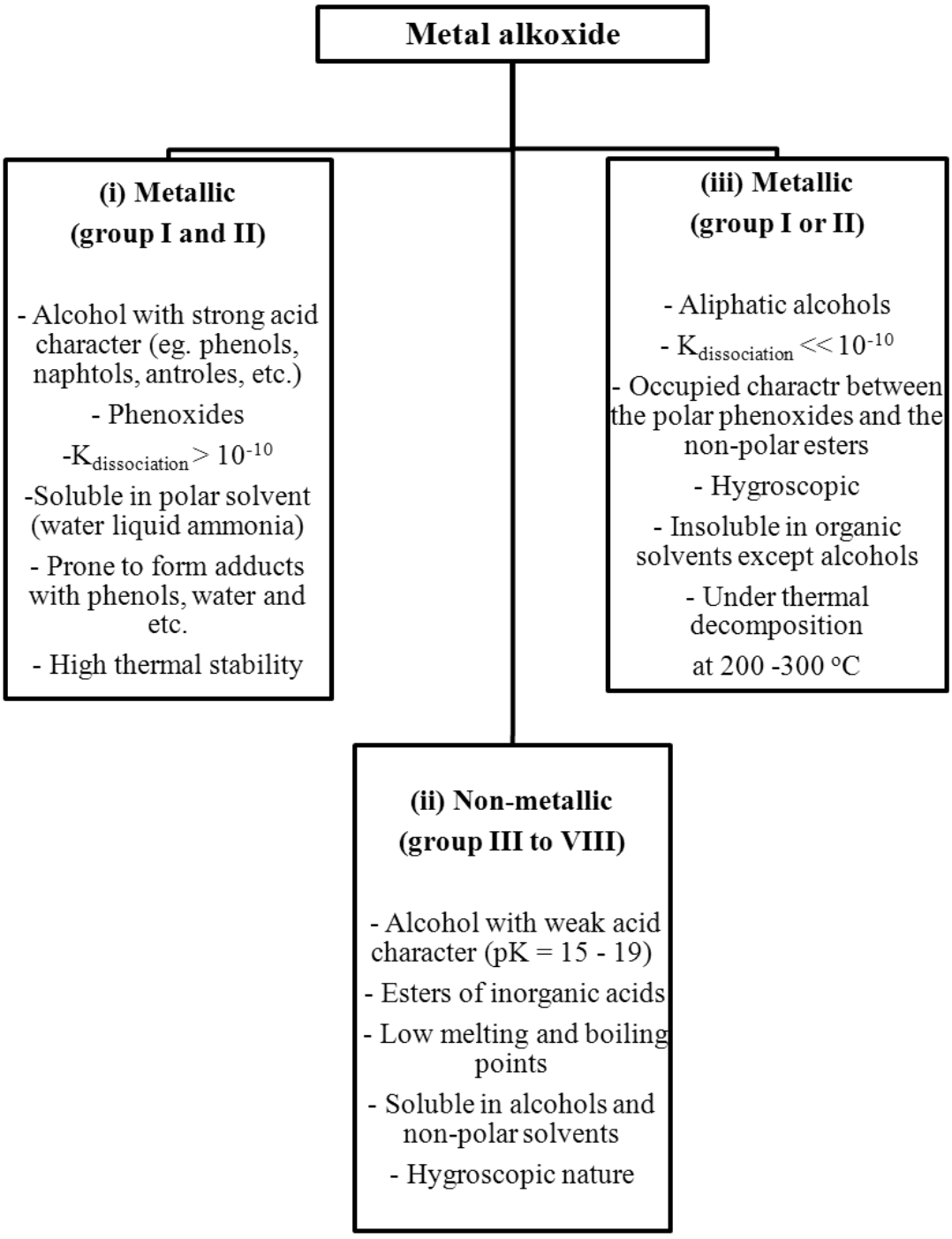

Fig. 2.1 Classification and properties of metal alkoxides (Turova and Novoselova, 1965)

2.2.1.1 Reaction of alcohol with metal

Generally, strongly electropositive elements such as group I and II and lanthanides may be reacted with alcohols with the release of hydrogen as described in equation [2.1]. Where the reaction is slow it may be driven to completion by dissolving the metals in an excess of alcohol while heating the reaction mixture.

$$M + nROH \longrightarrow M(OR)n + n/_2\ H_2 \qquad [2.1]$$

Reaction conditions such as the presence of catalysts and solvents may be varied to favour the formation of the alkoxide. In addition, the chemical properties of the alkoxide can significantly affect approaches required for separation of the product from the reaction mixture. Alkoxides produced in this way often crystallize in the form of solvates, for examples LiOEt•2EtOH, NaOPr•3PrOH, NaOPh•H_2O, KOMe•3MeOH, $Mg(OMe)_2$•3.5MeOH and *etc.* (Turova, 2002) but non-solvated alkoxides are much more reactive particularly for use in organic synthesis. Therefore, heating under an inert atmosphere (150 – 200°C), which can sometimes cause pyrolysis, may be required to evaporate the alcohol of crystallization. For direct preparation of metal alkoxide without the formation of solvent adducts, Fisher and McElvain (1934) proposed the use of hydrocarbon and ether media in which metal alkoxides are not soluble. This technique involves reaction of metal with the stoichiometric amount of alcohol in a mixture of high boiling inert solvent such as xylene or dioxane. The solvated alkoxide produced initially in this reaction continue to bind with the free metal and precipitated as non-solvated alkoxide from the inert solvent.

Liquid ammonia may also be used as a medium to facilitate the reaction between alkaline and alkaline earth metal with an alcohol. The reaction occurs with liberation of hydrogen while the alkoxide forms an insoluble precipitate from ammonia. The equilibrium reaction stoichiometry in ammonia is provided in equation [2.2]. Chablay (1905) first reported using this method for the synthesis of sodium alkoxides. Subsequently, alkoxides derived from other alkali metals and alkaline earth metals were

produced (Bradley *et al*., 1978). The versatility of the method allows the production of alkoxides from a wide range of unsaturated and polyatomic alcohols including alkoxides of carbohydrate compounds such as monosaccharides and polysaccharides (Rendleman, 1966).

$$M + NH_3 \longrightarrow [Na((NH_3)_6]^+ + ROH \overset{-NH_3}{\rightleftharpoons} M(OR)n + 1/2\ H_2 \qquad [2.2]$$

As alkali metals are highly reactive and explosive, the reaction of alcohol with metal may utilize a mixed metal product like a metal amalgam (mercury alloy) to slow the reaction of metal with alcohol. Industrial production of sodium alkoxides using sodium amalgam with alcohol is one good example. Sodium amalgam is produced from electrolytic reaction of aqueous sodium chloride (brine) solution. In the reaction chlorine is collected at a graphite anode; whereas sodium is discharged at a moving mercury cathode and is removed from the cell as amalgam. Sodium amalgam reacts with alcohol to produce alkoxide (NaOR•nROH), which is subsequently isolated from the electrode mercury. Sodium residue in the amalgam may then be hydrolysed to sodium hydroxide to generate heat. Meanwhile the mercury and alkaline solution are recycled to the electrolyser and the heat generated is used to initiate the reaction of the amalgam with alcohol (Turova, 2002). Sodium methoxide ($NaOCH_3$) powder sold in industry typically is assayed to have 97.5% purity with 0.5% sodium hydroxide; 0.4% sodium carbonate; 0.4% sodium formate and 0.5% free methanol. Another $NaOCH_3$ product is offered in the form of a 30% solution in methanol with purity 29 – 30% (Horn and Horns, 2000). This solution is sold to the biodiesel industry due to its ease of use and compatibility with processing.

The nature of alcohol may also affect the reaction rate for formation of alkoxide. Hydrogen atoms in the various alcohol molecules have different lability. Proton lability determines the reaction rate of a metal with an alcohol. In general, alcohols with more hindered and complex alkyl group react more slowly than lower aliphatic n-alcohols. Alkoxides synthesized from tertiary alcohols form slowly requiring several hours to

react while secondary and primary alcohols react quickly. The multiple alkyl substituent partially releases electrons and thus increases the electron density on the alcoholic oxygen by electrostatic induction (Huheey, 1971). This inductive effect hinders the breaking of O-H bond and, thus, delays deprotonation processes associated with metal alkoxide formation.

2.2.1.2 Reaction of alcohol with metal hydride or hydroxide

Alcoholysis of metal hydrides is also used in alkoxides synthesis. These reactions rely upon the interaction of the active hydrogen atom of the alcohol with the anion of the metal hydride and subsequent formation of gaseous H_2. The stoichiometry of this reaction is shown in equation [2.3] below with n = 1 or 2 for reaction with electropositive metal (Group I and II) hydride:

$$MH + ROH \longrightarrow MOR + H_2 \qquad [2.3]$$

The metal hydride reagents react more slowly with alcohol than the corresponding metal, thus, lowering the risk of fire and explosions that may occur during the release of hydrogen and the heat of reaction. Metal hydride reagents are normally prepared in solution with benzene or tetrahydrofuran with cryptands added to bind the alkaline metal into a more stable chelate complex. When the alkoxide production reaction is completed the solvent is removed under vacuum at ≤90°C due to low solvent volatility.

Alkoxides are also prepared by reacting hydroxides of alkaline metal with alcohol. Although this reaction typically produces a weaker base such reactions are commonly used for the commercial production of alkaline alkoxides from inexpensive raw materials. The chemical reaction stoichiometry is provided in equation [2.4]:

$$MOH + ROH \rightleftharpoons MOR + H_2O \qquad [2.4]$$

Reaction [2.4] is reversible and the metal alkoxide formed is soluble in alcohol. Therefore, if the desired product is an anhydrous alcoholate, water must be removed to force the reaction equilibrium to completion. Where low boiling alcohol is used in alkoxide synthesis, water can be removed as an azeotrope with inert solvents such as benzene or xylene at atmospheric or elevated temperature (Halbig, 1931). Nevertheless, removal of water azeotrope can be challenging, as precise boiling point control is required to form an azeotrope. Moreover, this technique is not applicable when methanol is in use for methoxide synthesis (Kyrides, 1929). Tower *et al*. used calcium carbide to remove water of reaction to prepare anhydrous calcium methoxide (Tower, 1963). However, calcium carbide is expensive and its production requires considerable energy. In addition, the by-product of this approach is acetylene, which requires special handling during purification. Despite these disadvantages, this method was widely applied for industrial production of sodium ethoxide and methoxide in Germany during the 1930's (Ullmann, 1953).

Olson and Twining (1931) proposed shifting the reaction equilibrium of metal hydroxide with alcohol towards alkoxide production by precipitating the alkoxide from the reaction medium during the reaction. For example, sodium ethoxide may be produced by reacting sodium hydroxide with ethanol in the presence of anhydrous acetone, the ethoxide precipitates from the reaction medium (Olson and Twining, 1931). Loder *et al.* (1939) proposed a reaction involving alkali metal salt of a weak acid with an alcohol, e.g. anhydrous sodium sulphide and methanol to form sodium methoxide and sodium hydrogen sulphide. The subsequent handling of the toxic and foul smell of hydrogen sulphide was reported to be problematic (Loder and Lee, 1939). Sodium hydroxide may also be reacted with alcohol in a continuous counter-current flow process using fractional column separations and subsequently distillation techniques for product purification (Kramis, 1959; Meyer and Johnson, 1957).

Metal hydroxides may be converted to alkoxides of high boiling alcohols by heating the alkaline mixture at high reaction temperature. This approach is efficient for synthesis of alkoxides with polyol with boiling points higher than 100°C (Turova,

2002). In such reactions water is eliminated to obtain anhydrous alkoxide without losing the alcohol reactants. Gross and Jacobs (1926) developed a new method for the preparation of sodium glycerolates without the use of expensive sodium metal or absolute alcohol. The method requires only sodium hydroxide and glycerol, both of which have boiling points greater than 100^{o}C. This method readily produced monosodium glycerolate but not disodium glycerolate. In addition, Gross and Jacobs (1926) also reported that 1,2-propanediol and 1,3-propanediol produce a similar alkoxide compound when reacted with caustic soda followed by heating at 135^{o}C. In these reactions disodium alkoxides were not produced when higher mole ratios caustic soda were employed. Despite the successful synthesis of the alkoxides of polyols the structure of the base was not reported. Only recently Reaney and co-workers (Reaney *et al*., 2010; Schatte *et al*., 2010; Schatte *et al*., 2011) have reported the structure of alkoxides of polyols.

The low solubility of alkali hydroxide in higher alcohols with lower polarity requires the use of multistep reactions to achieve alkoxide synthesis. One approach is to prepare a solution of metal hydroxide in aqueous solutions prior to mixing the alkali hydroxide with the higher alcohol. Subsequently the water may be distilled at high temperatures to produce an alkoxide. Reaney and Westcott (2007) achieved the synthesis of alkoxide catalysts by reacting aqueous solutions of metal hydroxide (40 – 50 wt% solution) with polyether alcohols. The reaction mixtures were heated to 130°C under a vacuum pressure of 0.001 mmHg. The resulting alkoxide compounds were effective in isomerisation of alkyl esters of linoleic and linolenic acid to yield fatty esters with conjugated double bonds. This process has been used for commercial synthesis of conjugated linoleic acid (Reaney *et al*., 2002).

2.2.2 Physicochemical properties of alkali alkoxides

The alkali metal alkoxides are colorless substances that are sensitive to moisture and carbon dioxide. These alkoxides are strongly associated by intermolecular forces and their stability is dependent on the size and ramifications of the alkyl groups (Bradley, 1960). The alkali metal methoxides are solid, non-volatile compounds due to the small size of the methyl group and lack of stearic effects on the metal atom. Due to the proximity of an electronegative oxygen and electropositive metal, M--O—R bonds are polarized with a dipole moment generated by a partial negative charge near the oxygen atom and a partial positive charge near the metal atom.

The extent of this polarization depends upon the electropositive nature of the metal element "M" (Allred, 1961). In the case of electronegative metals like germanium and selenium, the derivatives possess a covalent nature that leads to volatile products. Conversely, alkali and lanthanide metal derived alkoxides are electropositive and produce electrovalent ionic solids. For derivatives of the same element, the covalent character of metal oxygen bond increases with the ability of the alkyl group to release electrons. For example, when comparing a series of butoxide isomers of a particular element, the tertiary butoxide shows the highest covalent behavior due to its highest electron donating capability (Huheey, 1971).

Alkali metal alkoxide solubility is also affected by the character of the alkyl group. Alkoxides of *n*-alcohol are insoluble in liquid ammonia, sulfur dioxide and other non-polar solvents. With increase size and complexity of the alcohol radicals, the solubility in non-polar solvent increases. Alkoxide derived from *n*-alcohol radicals are generally soluble in polar solvent like alcohol. For instance, n-alcohol derived sodium alkoxides are readily soluble in alcohols. As the branching of radicals is increased, the solubility of the corresponding sodium alkoxide decreased considerably as depicted in Table 2.1.

Dissolution of alkoxides often induces formation of solvates. Isolation of individual compounds is reportedly difficult but still the solvate composition can be determined by thermal analysis. Drakin *et al.* determined the exact methanol solvate compositions by thermogravimetric approaches (Drakin *et al*., 1967). According to their study, lithium, sodium, potassium, rubidium and cesium ions form in alcoholic and aqueous solution with coordination numbers of 4, 6, 6, 8, and 8, respectively. Formation of such complex compounds is mostly due to the electronic interaction between the metal ions with the surrounding molecules. Such interaction depends slightly on the nature of solvent but is highly influenced by the charge, radius and electronic structure of the ion in solution. Drakin *et al.* (1967) reported that the coordination compounds of alkoxides with alcohol exist in solution form. Metal alkali alkoxides may be reactive with molecular oxygen (O_2) especially under uncontrolled conditions. Oxidation produces peroxide groups which decompose to radicals. This reaction leads to the production of water, oxo- (-OOR) and carboxylic groups (-OOH) in the lattice of metal atoms. The formation of these side products is accompanied by the appearance of yellowish brown color (Turova, 2002).

The structures of lithium, sodium and potassium methoxide were elucidated by x-ray powder diffraction in the 1960's (Wheatley, 1960). While most of these alkoxides were originally reported to have an amorphous nature, x-ray powder diffraction revealed adequately sharp reflections for interpretation of the structures. Wheatley (1960) reported the x-ray powder diffraction of $LiOCH_3$, $NaOCH_3 \bullet 2CH_3OH$ and $KOCH_3 \bullet nCH_3OH$ (n = 1 or 3) in which he identified the compounds as a layered structure (Fig. 2.2). Taking $LiOCH_3$ as an example, each Li atom in the lattice is surrounded by a distorted tetrahedron of oxygen atoms. Meanwhile, the coordination polyhedron of oxygen is a pyramid with four Lithium atoms constituting the base. The alkyl groups are always found on the outside of the layers. This structure explains the low volatility and insolubility of these complexes in non-polar solvent (Weiss, 1993).

Table 2.1 Solubility of sodium alkoxides (NaOR) in alcohols with increased ramification at 20^{o}C (Gjaldbaek, 1948)

Alcohol types (R)	**Solubility (moles NaOR litres^{-1})**
n-C_3H_7	>1
iso-C_3H_7	0.22
n-C_4H_9	>1
iso-C_4H_9	0.63
s-C_4H_9	0.66
t-C_4H_9	0.34 (27°C)

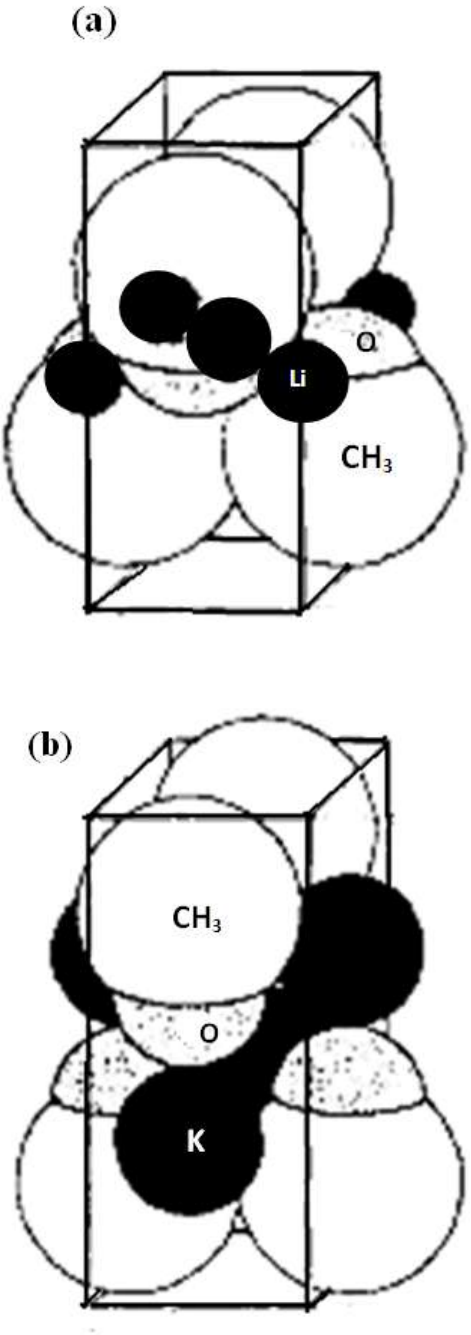

Fig. 2.2 The layered structures of (a) $LiOCH_3$ and (b) $KOCH_3$ (Redrawn from Weiss, 1993)

2.3 Polyols

Polyols contain multiple hydroxyl groups. The monomeric compounds have the general formula $R(CH_xOH)n$, where $n \geq 1$ and R is an alkyl group or CCH_xOH (x = 1 or 2); the dimers and trimers are also commercially significant. Some common polyol examples are sugar alcohols such as glycerol, erythritol, xylitol, sorbitol and mannitol. These alcohols can potentially be used as starting material for synthesis of the alkaline metal alkoxide due to their low cost and availability.

Sugar alcohols are produced from reduction of simple sugars from which their names are often derived from. One good example is xylitol where the name is derived from xylose. Most polyols contain straight carbon chains with each carbon atom attached to a hydroxyl group. These sugar alcohols have the common basic structure $HOCH_2(CHOH)n\text{-}CH_2OH$, where n = 2-5. In general, polyols are hydrophilic compounds that are water soluble and possess a sweet taste. The acidity of polyols decreases with the number of hydroxyl groups, as indicated by the pKa values in aqueous solution at 18°C (Table 2.2).

Sugar alcohols may form complexes in solution with many metal ions *via* chelation. Formation of chelated complexes is accompanied with the release of protons from the polyol molecule. These protons are not liberated in aqueous medium due to the weak acidity of the alcohols (PospIsilová *et al*., 1997). Group 2 alkaline metals (*eg.* calcium, strontium, and barium) form more stable complexes with polyols in aqueous solution than group 1 alkali metals like sodium and potassium (Mills, 1962). Magnesium forms less stable complexes than other group 2 metals. Sodium ferric tartrate forms a stable metal-chelating complex upon addition of sorbitol and mannitol. Precipitation of ferric oxide from solutions of sodium ferric tartrate with these polyols is inhibited after production of the complex.

Table 2.2 pKa values of sugar alcohols (Thamsen, 1952) in aqueous solution at 18°C.

Polyol	**pKa**
Glycerol	14.16
Xylitol	13.73
Sorbitol	13.57
Dulcitol	13.46

Rendleman (1966) confirmed formation of carbohydrate alcoholate in ethanolic media and later reviewed the polyol and carbohydrate complexes of alkali and alkali earth metals (Rendleman, 1967). In these publications, it was shown that the metal ion (associated with anionic oxygen) is chelated to the neighbouring donor groups (hydroxyl or carbonyl) within the same carbohydrate moiety. This chelation increased the stability of the alcoholate anion. Therefore, the chelate effect acts as a driving force to enhance formation of mono-metal alcoholate.

Hartman (1974) studied metal complex synthesis from sugar alcohol by preparing solid magnesium complexes with sorbitol and other polyols using magnesium ethoxide as a starting material. The resulting complexes are useful as antacids and catalysts in organic reactions including the isomerisation of glucose and fructose. The exact structures were not determined in Hartman's study (1974) though it was proposed that the catalyst was a mixture of mono-magnesium substituted alkoxides.

2.3.1. Glycerol

Glycerol or 1, 2, 3-propanetriol has a sweet warm taste and is hygroscopic. Historically glycerol was produced as a co-product of soap (saponification of triglycerides) and fatty acid production. More recently, the oleochemical industry has become the major source of glycerol production where it is obtained from splitting triglycerides with water, to produce fatty acids, and transesterification of triglyceride (TG) to produce biofuels (Morrison, 2000). With improvements in enzyme technology, glycerol can also be produced after hydrolysis or alcoholysis of TG with enzymes. In a biodiesel plant, 10% of the raw oil mass is released as a glycerol co-product. With the large increase of biodiesel production globally, glycerol has been overproduced leaving a glut in the market.

The utilization or disposal of this glycerol is complex, expensive and has become an increasing impact factor in the economics of the biodiesel industry (Engelhaupt, 2007). There is a worldwide demand for technologies that convert glycerol

into various value added products. Kapicak and Schreck (2008) reported synthesis of an anhydrous basic metal (sodium, potassium and calcium) salt of glycerine and use of the product as catalyst for biodiesel production. According to this work, 90% to 98% conversion of TG to biodiesel can be achieved using the metal salts of glycerine. Despite this patent information, catalyst reactivity and efficiency have not been reported (Kapicak and Schreck, 2008).

2.3.2 Xylitol and Sorbitol

Xylitol is a five-carbon pentitol. It is a non-chiral and occurs in an all-*threo* configuration in which all its hydroxyl moieties occur on the same side of the C5 chain in a zigzag configuration. Xylitol is found naturally in primrose *(Oenothera biennis)* and in small quantities in mushrooms *(Boletus edulis)* (Lawson, 2000) . Synthetic xylitol is also produced through the chemical or enzymatic conversion of glucose and D-xylose. Onishi *et al*. (1969) described production of xylitol using glucose as starting material by a sequential fermentation process that produced D-arabinitol and D-xylulose as intermediates (Onishi and Suzuki, 1969). In addition, D-xylose may be reduced to xylitol using Raney Nickel (Karabinos and Ballun, 1953) or *via* an electrolytic process (Creighton, 1926). Woody biomass such as corncobs, cottonseed hulls, almond shells or olive waste containing carbohydrate compounds like xylan and hemicellulosic substances can also be processed as sources of xylitol. For example, hydrogenation of the acid hydrolysate of cottonseed hulls is a route to the production of xylitol (Kohno *et al*., 1971).

Sorbitol is a hexitol with six hydroxyl moieties. The vicinal diol pairs from C2 to C5 are configured in the sequence of *threo*, *threo*, *erythro* for each group respectively. Sorbitol was first discovered in 1872 in mountain ash berries though it is also found in the fruits of apples, plums, pears, apricot, dates, peaches and cherries. It is also abundant in the leaves and bark of many of the fruit species mentioned above (Lawson, 2000). Sorbitol is prepared commercially by reduction of glucose. Typically glucose is hydrogenated under alkaline condition to produce sorbitol using metallic

heterogeneous catalysts like nickel, cobalt, platinum and ruthenium. At higher pH (4-8), glucose isomerizes to fructose and mannose after which hydrogenation will yield sorbitol and mannitol. Sorbitol can also be synthesized from biomass resources like cotton cellulose and starch *via* hydrolysis and subsequent hydrogenation (Kool *et al*., 1952). Sugar alcohols are bio-alcohols that are readily available from plant resources. The abundance of biomass renewable resources and well-researched conversion chemistry has made sugar alcohol synthesis economically feasible.

2.3.3 Glycols; pinacol, propylene glycol and trimethylene glycol

Glycols are diols compounds containing two hydroxyl groups attached to separate carbon atoms in an aliphatic chain. Examples of commercially available glycols include ethylene glycol, propylene glycol and pinacol (2,3-dimethyl-2,3-butanediol). Pinacol is a white solid organic compound. It is mainly produced by reduction of acetone with a base metal such as sodium amalgam or electrolysis. Pinacol is widely used in organic chemistry after reaction with borane or boron trichloride to produce the useful synthetic intermediates pinacol borane and pinacol chloroborane respectively. The tertiary alcohols structure of pinacol may contribute to the production of alkoxides with greater base strength than alkoxides from lower glycols. Also the hydrophobic alkyl groups of pinacol can potentially be used to produce alkoxides with improved solubility and potential catalytic activity in organic phases. In addition, the tertiary alcohol groups are comparatively unreactive and are not likely to form esters if used in the presence of acids or esters.

Propylene glycol (PG) and trimethylene glycol (TMG) are common terms for 1,2-propanediol and 1,3-propanediol respectively. PG is a three-carbon diol with a steriogenic center at the central carbon atom. Thus, there are two enantiomers: (R)-1,2-propanediol and (S)-1,2-propanediol. As for TMG, it is a single isomer due to its molecular symmetry. PG is a major commodity chemical with an annual production of over 1 billion pounds in the United States (Dasari *et al*., 2005).

Table 2.3 Physical properties of sugar alcohols (Lawson, 2000)

Sugar alcohol type	**CAS registry number**	**Melting point, °C**	**Solubility g/100 g H_2O[a]**	**Boiling point, °C[b]**
Glycerol	[56-81-5]	18.17	Very soluble	290
Xylitol	[87-99-0]	61-61.5 (meta-stable) 93-94.5 (stable)	179	216
Sorbitol	[50-70-4]	93 (meta-stable) 97.7 (stable)	235	296

[a]At 25°C unless otherwise stated
[b]At atmospheric pressure 100kpa and temperature 25°C

Some typical uses of PG and TMG are as components of unsaturated polyester resins, functional fluids (antifreeze, de-icing, and heat transfer), pharmaceuticals, foods, cosmetics, liquid detergents, tobacco humectants, flavours and fragrances, personal care items, paints and animal feed.

The most widely used glycol, ethylene glycol, is toxic to humans and animals raising concerns about its use in many applications. Both PG and TMG are seen as alternative to ethylene glycol in the antifreeze market. Propylene glycol is produced by hydration of propylene oxide derived from propylene by either the chlorohydrin process or the hydro-peroxide process (Parsons, 2000). Alternate routes to propylene glycol synthesis are possible with renewable feedstocks. The most common alternative route of production of both glycols is through high temperature and pressure hydrogenolysis of glycerol, sugars or sugar alcohols in the presence of a metal catalyst (Haas *et al*., 1995; Ludwig and Manfred, 1997).

2. 4 Base catalyzed transesterification reaction

Transesterification is also known as alcoholysis. This reaction occurs when the alkoxy group of an ester is exchanged by another alcohol. This reaction is similar to hydrolysis except that an alcohol is used instead of water (Srivastava and Prasad, 2000).

Alcoholysis

$$RCOOR' + R''\text{-}OH \rightleftharpoons R'COOR'' + ROH \qquad [2.5]$$

Hydrolysis

$$RCOOR' + H\text{-}OH \rightleftharpoons R'COOH + ROH \qquad [2.6]$$

One prominent application of transesterification reactions is for biodiesel production as illustrated in Fig. 2.3 where transesterification reactions between fats or oil (TG) and methanol produce fatty acid methyl ester (biodiesel) and glycerol. Biodiesel is a biodegradable and non-toxic alternative fuel for diesel engines. It has been gaining

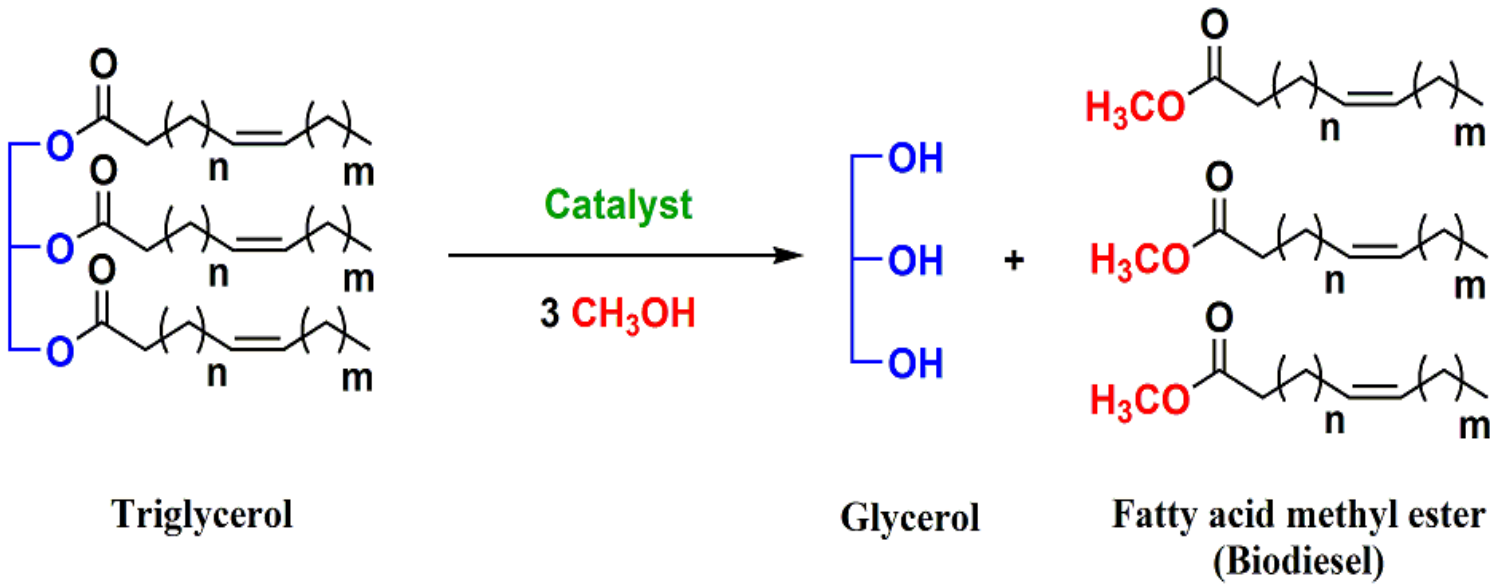

Fig. 2.3 Transesterification of vegetable oil for biodiesel production

global interest because it can be derived from renewable resources and is an environmental friendly alternative to petrochemical sources.

Biodiesel is commonly produced by catalytic reactions. A strong acid or base is commonly used to enable transesterification reactions employed for biodiesel production. Freedman *et al*. (1984) reported that base catalysts enabled higher reaction rates than acid catalyzed reactions. Moreover, homogeneous base catalysts are typically less corrosive to industrial equipment. Hence, base catalysts are preferred in industrial biodiesel manufacturing processes. Nevertheless, if the reaction feedstock has high concentrations of free fatty acids (> 20 wt%), pre-treatment of feedstock with acid catalyst may be required before proceeding to further transesterification using base catalyst (Ma *et al*., 1998). Sodium hydroxide (NaOH), potassium hydroxide (KOH) and their corresponding alkoxides such as sodium methoxide ($NaOCH_3$) and potassium methoxide ($KOCH_3$) are used commercially as catalysts for the production of biodiesel. In many studies, sodium methoxide is preferred for its high yield and reaction efficiency. Vicente *et al*. (2004) reported lower biodiesel yield (85.9 wt%) in sodium hydroxide catalyzed reactions than reactions catalyzed with sodium methoxide (98 wt%) due to substantial yield losses through TG saponification. However, methoxide base is more expensive than hydroxide base and it is more difficult to handle due to its hygroscopic and flammable nature.

Transesterification of TG with methanol is a three-step reversible reaction that converts TG with intermediate formation of diglycerides (DG) and monoglycerides (MG) to three moles of methyl esters (ME) and 1 mole of glycerol (GL) as depicted in reaction equations [2.7], [2.8] and [2.9] below:

$$TG + MeOH \rightleftharpoons DG + ME \qquad [2.7]$$

$$DG + MeOH \rightleftharpoons MG + ME \qquad [2.8]$$

$$MG + MeOH \rightleftharpoons GL + ME \qquad [2.9]$$

Each of these reactions is initiated with an attack on the carbonyl group of the TG, DG and MG molecule by the methoxide ion (CH_3O^-). Fig. 2.4 shows the alkali-catalyzed transesterification of TG with methanol and methoxide. The methoxide ion is the catalytic agent in base catalyzed transesterification reactions with methanol, as it is not consumed by the reaction. When an alkali hydroxide is used as the catalyst it participates in a reaction that liberates methoxide ion. This reaction is dependent on the alkali metal dissociation constant and quantity of hydroxide ion. Sodium and potassium are highly electropositive elements and hence, their dissociation constants are also high. As for hydroxide ion quantity, the catalyst concentration and molecular weight play a substantial role in determining the overall catalytic activity of the corresponding reactions (Vicente *et al*., 2004).

A substantially anhydrous feedstock with free fatty acid less than 0.5 wt% is required for production of biodiesel from oil by transesterification (van Gerpen *et al*., 2004). Lower quality oils will produce low biodiesel yield. Water molecules present in the reaction medium, particularly at high temperatures, can hydrolyze the TG to DG and form free fatty acids (FFA). Once FFA forms it quickly reacts with alkali catalysts causing soap formation, which is undesirable. Excessive soap produced in a biodiesel reaction acts as an emulsifier, which inhibits glycerol separation and complicates biodiesel refining. The soaps of saturated fatty acids tend to solidify at ambient temperatures. These soaps form a viscous semi-solid mass with the reaction mixture that interferes in the reaction as well as recovery of pure biodiesel. Low yields and complicated washing procedures increase the cost of biodiesel production. In order to avoid these problems, feedstock low in FFA (<0.5 wt%) and moisture content (<0.3 wt%) is required (Granjo *et al*., 2009). Furthermore, the base catalysts should be maintained in anhydrous state and prolonged contact with air should be avoided to mitigate the possibility of catalyst interaction with moisture and carbon dioxide (CO_2).

Pre-step: Generation of methoxide ion, $^-OCH_3$ from base catalysts

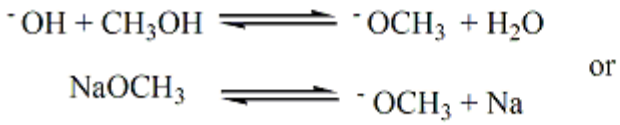

Step 1:

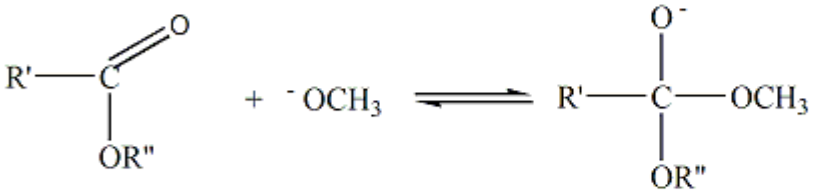

(triglyceride) (methoxide ion)

Step 2:

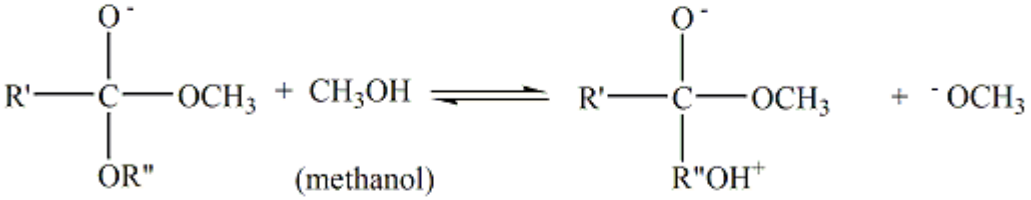

Step 3:

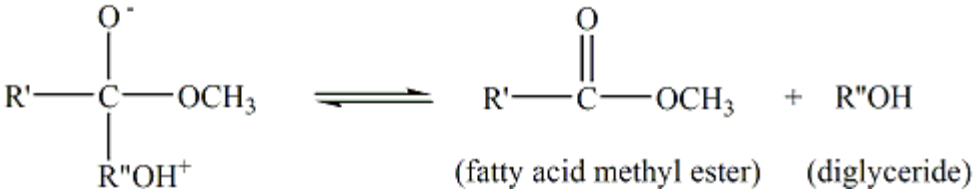

(fatty acid methyl ester) (diglyceride)

Where R'= long chain alkyl group; R"= glycerol backbone attached to fatty acids

Fig. 2.4 Mechanism of alkali-catalyzed transesterification of triglyceride with methanol (Ma and Hanna, 1999)

2.4.1 Optimized conditions for homogeneous base-catalyzed transesterification reaction

Transesterification is a reversible reaction that can be shifted to completion by optimizing the reaction conditions. Alkaline catalyst loading of 0.5 to 1 wt% may lead to a yield of 94 - 99 wt% methyl ester from vegetable oil. Further increase of catalyst concentration does not affect the conversion. Instead, excessive catalyst addition increases the cost of transesterification and increases the cost of separating the catalyst from the reaction products (Feuge and Gros, 1949; Krisnangkura and Simamaharnnop, 1992; Saka and Kusdiana, 2001). Patil and Deng (2009) reported that maximum yield was obtained using 1 wt% of KOH loading in a transesterification reaction of canola oil with methanol and that yield decreased with an increase of KOH loading. Decreased yield was associated with soap formation due to excessive base catalyst.

Another important factor affecting the biodiesel yield is the molar ratio of alcohol to vegetable oil. According to the stoichiometry of the TG transesterification, three moles of alcohol are required to react with 1 mol of TG for a complete reaction. Nevertheless, a large excess of alcohol is typically necessary to drive the reaction to completion. A molar ratio of 6:1 (alcohol:TG) is reportedly used in the industrial processes to achieve biodiesel yield of higher than 90 wt% (Freedman *et al*., 1986). Literature methods suggest that the reaction is conducted close to the boiling point of methanol (60 – 70°C) at atmospheric pressure and 6:1 molar ratio of alcohol to TG to optimize the reaction rate (Murugesan *et al*., 2009). The reaction will proceed close to completion even at room temperature but the reaction is said to be slow. A process at lower temperature might be too slow for commercial production.

Freedman *et al.* (1984) recommended the optimum conditions for ester formation by transesterification of vegetable oils or refined oils, which are substantially anhydrous with a free fatty acid content of less than 0.5%. The common conditions applied in industry for homogeneous base-catalyzed reaction are described as follow: A molar ratio of alcohol to oil of 6:1; 0.5 wt% sodium methoxide (for laboratory use) or 1

wt% sodium hydroxide (for larger scale reactions); reaction temperature of 60°C for methanol, 75°C for ethanol and 114°C for butanol for 1 hr reaction time with 0.5 wt% sodium methoxide.

2.4.2 Kinetics of homogeneous base catalyzed transesterification reaction

Knowledge of the rate of transesterification reactions is essential in process assessment and development. Studies of reaction kinetics enable the prediction of the reaction progress under particular reaction conditions (Darnoko and Cheryan, 2000). Freedman *et al*. (1984) first studied the kinetics of acid and base catalyzed alcoholysis of soybean oil using 1-butanol and methanol at 30:1 and 6:1 alcohol to TG molar ratios. In Noureddini and Zhu (1997) reported the kinetics of base-catalyzed alcoholysis of soybean oil with methanol at 6:1 molar ratio. Their study demonstrated that the reaction conducted using 6:1 (alcohol:TG) molar ratio demonstrated second-order kinetics. Pseudo-first order kinetics provided a satisfactory mechanism with experimental results at larger molar excess of alcohol.

In most of the kinetic studies of methanolysis of TG, three phases of the reaction are usually observed as a sigmoidal curve in the plot of biodiesel yield *vs.* time. The initial lag phase is due to the mass transfer limitation between two immiscible phases (TG and methanol). Jeong *et al.* (2004) concluded that the heterogeneous effect of TG-methanol mixing is more pronounced for low intensity mixing rates. However, with high mixing intensity of N_{Re}>6000, the reaction becomes more chemically controlled and thus reducing the mass transfer resistance. In this context, the reactant mixture can be considered as pseudo-homogeneous (Granjo *et al*., 2009). The second phase of TG methanolysis is more chemically controlled in which the reaction rate increases rapidly when the two immiscible phases are converted to miscible materials. Finally, in the last stage of the reaction, reaction rate slows as the reaction approaches equilibrium. This occurs as glycerol separates from the methyl ester. The catalyst is soluble in glycerol, therefore, its concentration decreases at this stage of the reaction. Furthermore, the

presence of glycerol by-product tends to contribute to the reverse reaction and equilibration (Marjanovic *et al*., 2010).

2.4.3 Quantification of biodiesel yield by Nuclear Magnetic Resonance Spectroscopy

Over the past two decades, Nuclear Magnetic Resonance (NMR) has played an increasing role in the study of oil chemistry especially in providing insights into transesterification reactions. In 1995, Gelbard *et al*. (1995) was the first to describe the use of nuclear magnetic resonance, particularly ^{1}HNMR, for monitoring transesterification reaction yield (Gelbard *et al*., 1995). As illustrated in Fig. 2.5, methoxy groups of the methyl esters at 3.7 ppm (singlet) and the α-carbonyl methylene groups present in all fatty ester derivatives at 2.3 ppm (triplet) were used to monitor the reaction progress. A multiplet at 2.1 ppm is also well resolved and is related to allylic protons. The yields for the transesterification reactions are obtained directly from the areas of the selected signals using equation [2.7] below:

$$Y\% = 100 \times (2A_1/3A_2) \qquad [2.10]$$

where A_1 = areas of the methoxy group (3.7 ppm, singlet); and A_2 = area of the α-carbonyl methylene group (2.3 ppm, triplet). Values are calculated at ±2% according to the reproducibility of integration.

Carbon ^{13}C NMR may also be used to monitor the TG transesterification (Dimmig *et al*., 1999). The signal of the terminal methyl groups at 14.5 ppm, which are not affected by reaction, was chosen as internal standard, and the glyceridic carbons at 62–71 ppm along with methoxy carbon of fatty esters at 51 ppm were selected to determine the conversion rate. Neto *et al.* (2004) was able to monitor soybean oil ethanolysis as well as to quantify the content of fatty ethyl esters in mixtures of biodiesel using ^{1}H NMR methods. The region of 4.05–4.40ppm (ester ethoxy and glycerol methylene hydrogen) was chosen for the quantification of the reaction. The

authors stated that the method is more rapid and simple than gas chromatography (GC) and high performance liquid chromatography (HPLC). Moreover, a small amount of sample is required and it can be analyzed without purification. Morgenstern *et al.* (2006) developed a ^{1}H NMR method to monitor transesterification reactions of soybean oil. Through NMR analysis, they were able to establish the average degree of fatty acid unsaturation and methyl esters in biodiesel (Morgenstern *et al*., 2006). In addition, NMR methods may also be correlated to Fiber-Optic Near Infrared (NIR)(Knothe, 2000) and Fourier-Transform (FT)-Raman spectroscopy (Ghesti *et al*., 2007) to validate the method accuracy in monitoring the progress of vegetable oil methanolysis. NMR quantification of biodiesel yield is rapid and reliable. It has advantages over other analytical methods like GC or HPLC where internal standard and calibration of the NMR instrument are not required.

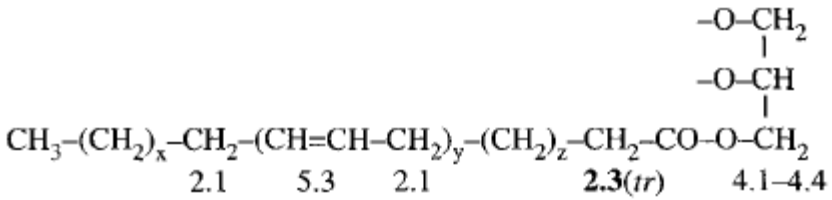

Triglyceride (TG)

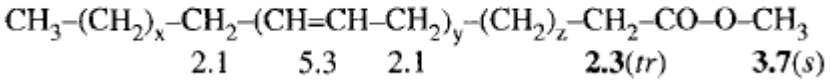

Fatty acid methyl ester (FAME)

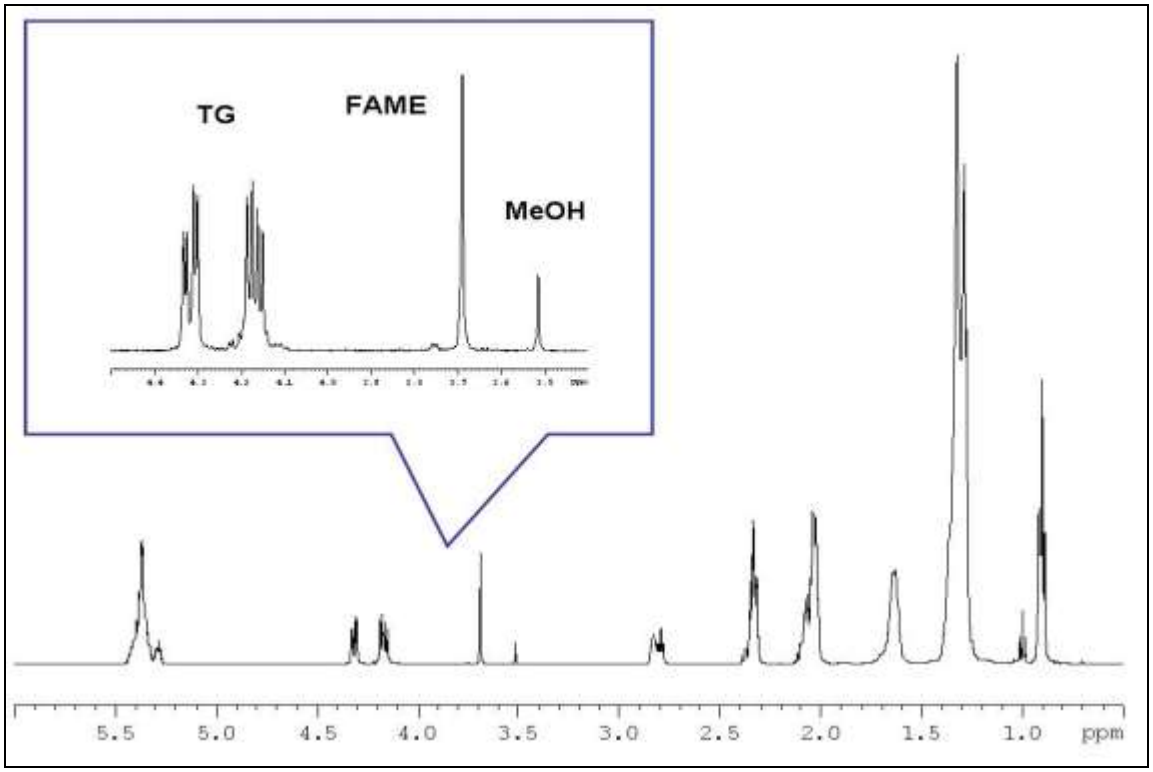

Fig. 2.5 NMR spectra for monitoring a progressing transesterification reaction using canola oil

CHAPTER 3.
SYNTHESIS OF METAL ALKOXIDE CATALYSTS FROM POLYOLS

3.1 Abstract

Base catalysts can be synthesized when aqueous solutions containing polyols and sodium hydroxide are heated under vacuum pressure. The combined high boiling point and stability of polyols allow these alcohols to withstand the alkalinity, heat and dehydration conditions. The influence of different polyol chemistry and the mole ratios of sodium hydroxide to polyol affect the drying processes and can be, in part, quantified by measuring water loss. Gravimetric analysis of water mass loss shows that drying under heat and vacuum removes all of the solution water plus additional water produced during formation of sodium alkoxide compounds. The drying process is more rapid for higher molecular weight polyols like sorbitol and xylitol while lower molecular weight polyols glycerol, 1,2-propanediol, and 1,3-propanediol dried more slowly. The drying trend is influenced by the ability of the polyols to form ion chelating complexes. The availability of vicinal hydroxyl groups plays an important role in formation of a stable metal-ion chelate. The study has demonstrated the dehydration rate of 50 wt% aqueous NaOH solution added with polyols is, in decreasing order, Xylitol > sorbitol > glycerol > 1,2-propanediol > 1,3-propanediol.

3.2 Hypothesis

Alkoxide base catalysts can be synthesized when polyols undergo a series of dehydration reactions with sodium hydroxide upon heating under vacuum pressure. The combined high boiling point and stability of polyols enable these alcohols to withstand heating and dehydration in aqueous sodium hydroxide solution.

3.3 Methods

3.3.1 Synthesis of alkoxide from solutions of pinacol and sodium hydroxide

Sodium hydroxide (NaOH) solution (50 wt%) was prepared by dissolving 16.000g (0.4 mol) sodium hydroxide pellets (EMD chemicals, Gibbstown, USA) in distilled water (16.000g). Pinacol (23.630g (0.2 mol), Sigma Aldrich, Oakville, Canada) was added to a round bottom flask (TS24/40 ground glass fitting) containing 50 wt% sodium hydroxide solution. The flask was connected to a distillation column (TS24/40; 200mm) wrapped in aluminum foil and connected to a condenser. The experimental apparatus is shown in Fig. 3.1 (except that a distillation column was connected to the sample flask before condenser). Vacuum pressure (28 inch Hg) was applied using a pump (model 8907A; Welch Vacuum Technology; Niles, USA) while heating the round bottom flask to 100°C under constant stirring with a Teflon coated magnetic stirrer. A clear crystal-liked substance was observed on the walls of the distillation column and in the water trap flask during evaporation under vacuum pressure. The crystals were dissolved in deuterated chloroform (Sigma Aldrich, Oakville Canada) for Nuclear Magnetic Resonance (NMR) analysis to confirm their identity. ^{1}H NMR spectra were recorded from 500MHz Avance NMR spectrometer using ^{1}H NMR probe 5mm (Bruker, Milton Canada) (spectral width, 10330.58 Hz; data points, 32768; pulse width, 6.05 µs (90^{o}); pulse delay, 1.79 s and number of scans, 128). The unprocessed free induction decay (fid) data were then converted frequency domain by Fourier transform (ACD Labs version 11).

3.3.2 Synthesis of sodium alkoxide catalysts by two-stage vacuum dehydration

A series of base catalysts were synthesized by mixing 50% aqueous sodium hydroxide (NaOH) solution and polyols according to three different mole ratios (NaOH: polyol ratio 1:1, 2:1 and 3:1) and was calculated based on stoichiometric concentration as indicated in Table 3.1. The amount of NaOH (0.700 g or 0.0175 mol) was held constant while polyols were added at molar amounts to create the desired ratio of NaOH

Table 3.1 Polyols weight and moles used in synthesis of sodium alkoxide catalyst at different molar ratio.

Polyols ([1]b.p)	**Mol. weight ($gmol^{-1}$)**	**Weight (±0.001g)**		
		NaOH: alcohols molar ratios (alcohol mol concentration)		
		1:1 (0.0175mol)	**2:1 (0.00875mol)**	**3:1 (0.00583mol)**
1,2-propanediol (188.2°C)	76.09	1.331	0.666	0.443
1,3-propanediol (210 – 212°C)	76.09	1.331	0.666	0.443
Glycerol (290°C)	92.09	1.611	0.805	0.537
Xylitol (216°C)	152.15	2.663	1.331	0.888
Sorbitol (296°C)	182.17	3.188	2.125	1.063

[1]b.p = boiling point at a vacuum pressure of 100 kpa (Budavari, 1996)

to polyol (0.0175, 0.035 and 0.0525 mol). Xylitol and sorbitol (in powder form; Sigma Aldrich, Oakville Canada) were initially dissolved in water to prepare a 50 wt% solution before adding a 50 wt% NaOH solution. The mixtures were then heated in an oil bath to evaporate water at 120^{o}C under vacuum pressure (28 inch Hg) for 2 h. The temperature, 120°C is above the boiling point of water, but below boiling point of the polyol. The experimental apparatus is shown in Fig. 3.1. Following evaporation, the catalysts were further dehydrated for an additional 24 h under vacuum pressure (28 inch Hg) in a vacuum oven (model 280A; Fisher Scientific, Ottawa Canada).

3.3.3 Gravimetric analysis during alkoxide catalysts synthesis

The drying behavior of alkoxide catalysts was measured by evaporation of the reaction mixture using a modified rotary evaporator (model Rotavapor R200; Buchi, New Castle, USA) for 2 h period. The vacuum line of the rotary evaporator unit was connected to a 5 L round bottom flask through a three-way joint, which was also connected to the vacuum pump (model V-710; Buchi, New castle USA) *via* rubber tubing. The modification provides additional air volume for the vacuum pump, thereby controlling the pressure fluctuation range within ±10%. The evaporation process was conducted under regulated vacuum conditions (250 mbar) using a vacuum controller (model V-809; Buchi, New Castle USA). The integrated aeration valve and precision pressure sensor of the vacuum controller provided a defined and regulated vacuum pressure for maintaining consistent evaporation.

A solution of NaOH (50 wt%) was prepared by dissolving approximately exactly 7.000g of NaOH pellets (EMD chemicals, Gibbstown USA) in approximately exactly 7.000g (0.175mol) of water. The solution was then added to the polyol based on mass according to Table 3.2. Polyols used in this study were obtained from Sigma Aldrich (Oakville Canada). According to the certificate of analysis from the supplier, these polyols had relatively low water content (glycerol <2%; 1,2-propanediol <0.2%; 1,3-propanediol <0.1 % Karl Fischer titration). A teflon coated magnetic stirrer was used to facilitate mixing of the reagents. Evaporation occurred when the chemical

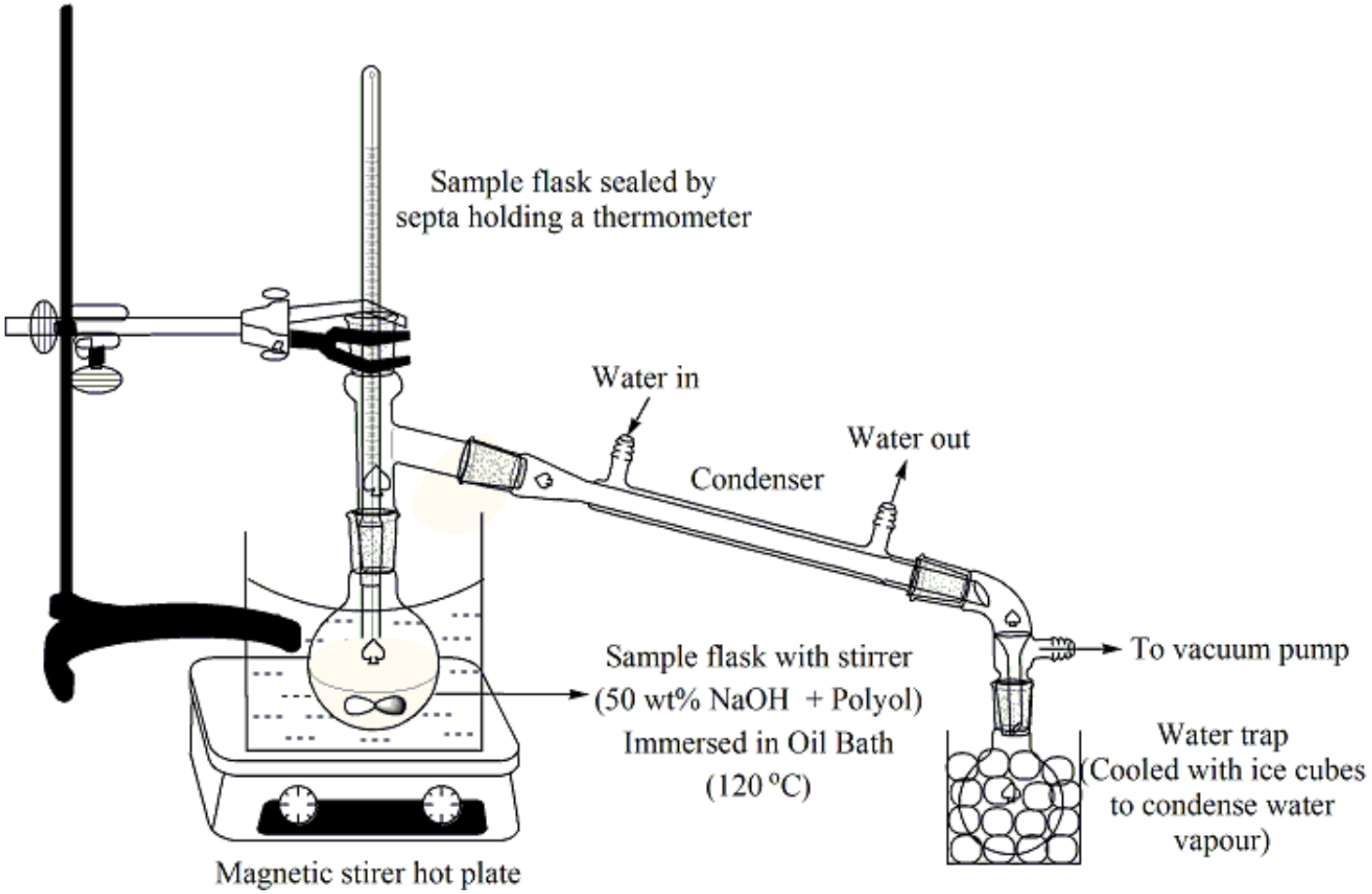

Fig. 3.1 Laboratory apparatus for synthesis of polyol catalysts under vacuum and heating conditions

Table 3.2 Polyol weight (g) and mole content in gravimetric analysis

Polyols	**Mol. weight ($gmol^{-1}$)**	**Weight (±0.001g)**	
		Molar ratio (NaOH: alcohols)	
		2:1	**3:1**
		(0.175 mol: 0.0875mol)	**(0.175 mol: 0.0583mol)**
1,2-Propanediol	76.09	6.651	4.436
1,3-Propanediol	76.09	6.651	4.436
Glycerol	92.09	8.058	5.369
Xylitol	152.15	13.313	8.870
Sorbitol	182.17	15.939	10.621

mixture was heated to 120°C in a rotating round bottom flask (immersed in an oil bath) and vacuum pressure was applied. The initial flask weight was recorded to allow calculation of mass loss due to water evaporation. The flask was disconnected and weighed at 15 min intervals throughout the 2 h experiment. After 2 hours of heating, the flask containing the sample mixture was further evaporated under lower vacuum pressure (68 mmHg) for 18 hours. The final sample weight was recorded for calculation of total water mass loss. A control without polyol, using 50 wt% sodium hydroxide solutions, was analyzed for comparison. Control solutions of each polyol were also studied to determine the drying behaviour in the absence of NaOH.

3.4 Results & discussions

3.4.1 Alkoxide catalysts derived from various polyols

Crystal-like substances accumulated in the water trap during the evaporation of solutions of pinacol and sodium hydroxide. The substances were subjected NMR analysis and the NMR spectrum was identical to that of the starting reagent, pinacol. The boiling point of pinacol at 50 mmHg (27.5 in Hg vacuum gauge pressure) is reported as 105°C (Cornils *et al*. 1983) thus explaining why pinacol distilled at 100°C as vacuum pressure (28 in Hg) generally lowers the boiling point. The trap on the evaporator is cool relative to the heated flask and it is expected that pinacol would accumulate in the trap if it evaporated. The NMR spectra in Fig. 3.2 displays the chemical shifts of pinacol in which the methylene (CH_2) and hydroxyl group can be found at 1.23 ppm; and 2.11 ppm respectively. Figure 3.3 demonstrates qualitative identification of the clear, crystal-like compound in the water trap where the compound has the exact chemical shift and integration ratio of pinacol. Based on the relatively low boiling point of pinacol compared to the rest of the polyols, it was determined that pinacol was not a suitable starting material for quantitative production of base using the vacuum pressure method.

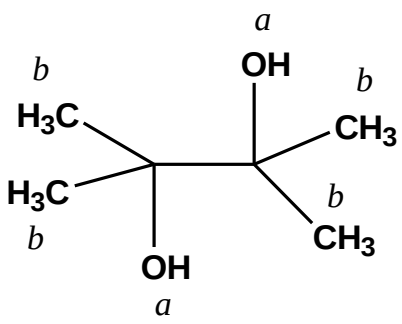

pinacol (2,3-dimethyl-2,3-butanediol)

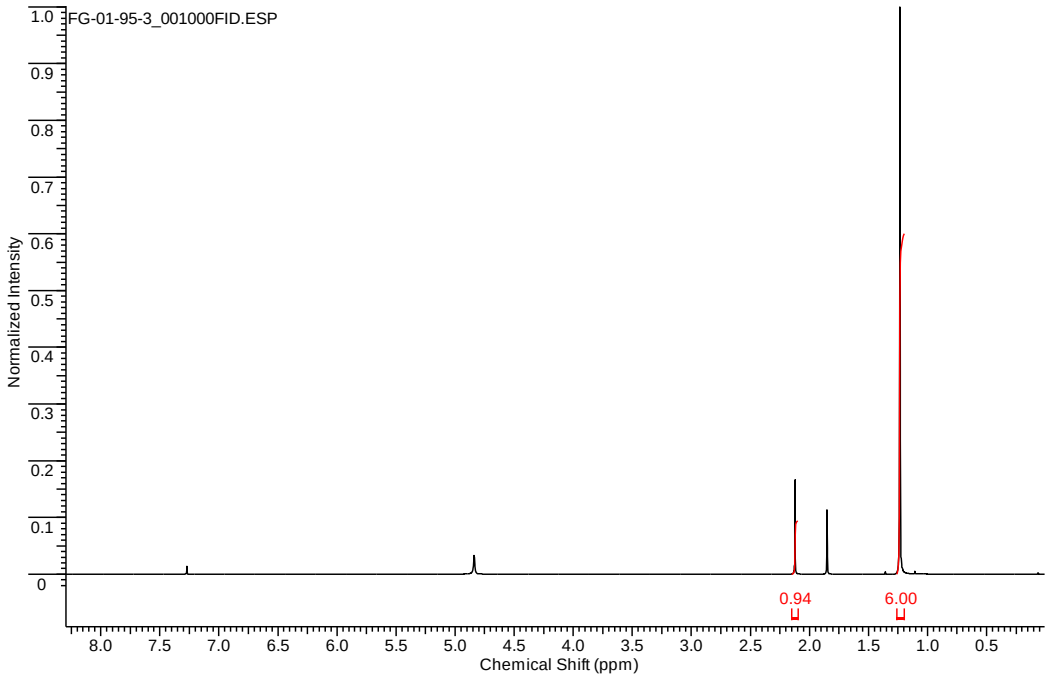

Fig. 3.2 NMR spectra of crystal-like substances (pinacol) formed in water trap; OH group *(a)*: 2.11ppm; CH_3 group *(b)*: 1.23ppm

Dehydration of sodium hydroxide solutions with 1,2-propanediol, 1,3-propanediol, glycerol, xylitol and sorbitol produced solid products by the end of the first dehydration stage, which persisted after the second stage of vacuum dehydration. The solids derived from 1,2-propanediol, 1,3-propanediol, glycerol and xylitol were hygroscopic, anhydrous powders while the solid derived from sorbitol had a white, foamy and pasty texture. The powder from 1,3-propanediol was slightly yellowish, whereas, those powders from other compounds were white. The nature of the alkoxide catalyst produced by mixing aqueous solutions of sodium hydroxide with glycerol (3:1 molar ratio) followed by vacuum dehydration could theoretically produce an alkoxide as shown in Fig. 3.3 (glycerol is the polyol used in this example). This proposed reaction sequence is based on an ideal theoretical reaction where free water and three chemically bounded water molecules are removed from the reaction mixture. The actual final product composition was determined using elemental analysis (Chapter 4).

Brönsted acid-base theory may be used to describe the deprotonation reactions to produce alkoxides. In this context, polyol served as an acid (proton donor); whereas $^{-}$OH from NaOH served as base (proton acceptor). Since alcohols are weakly acidic (pKa >12), interaction with metal ions are generally weak in neutral aqueous medium. Furthermore, polyols compete with water molecules to dissolve cations in neutral aqueous solution (Lawrance *et al*., 2002). However, with increasing pH, the alkaline medium enables deprotonation of alcoholic hydroxyl groups to occur. Once deprotonated, the polyols behave as a much stronger base with the ability to bind with the metal ions (PospIsilová *et al*., 1997) to produce metal alkoxide.

Randleman (1966) observed that the hydroxides of lithium, sodium, potassium and caesium reacted with simple non-acidic sugar alcohols at room temperature in anhydrous alcoholic media. The resulting products were colorless, amorphous, hygroscopic precipitates that were predominantly mono-substituted carbohydrate alkoxides. Such compounds are stabilized through chelation processes. It was also reported that the metal ion attached to the deprotonated hydroxyl moiety is chelated to

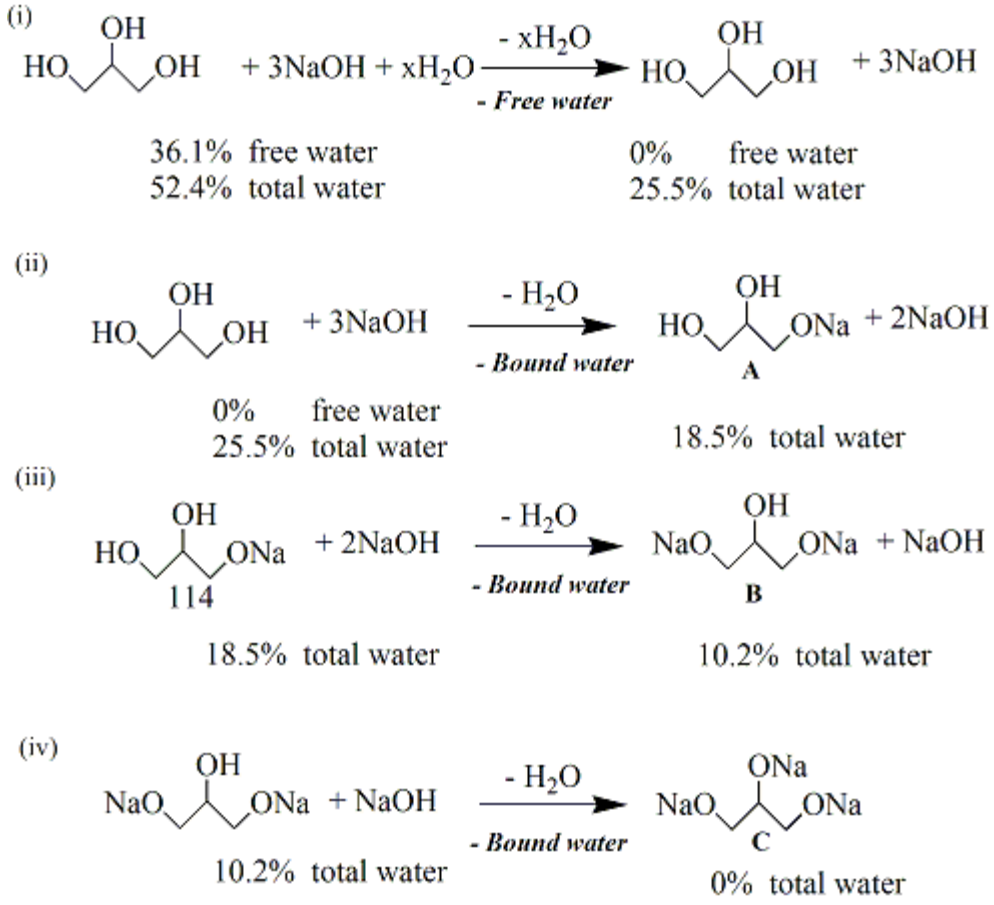

Fig. 3.3 Possible synthesis pathway of sodium glycerolate catalyst at 3:1 mole ratio (A = mono-sodium substituted; B = di-sodium substituted; C = tri-sodium substituted)

neighbouring donor groups such as vicinal hydroxyl moieties within the same sugar alcohol structure. Therefore, it is understood that chelation increases stability of the metal alkoxide formation which subsequently acts as a driving force to enhance the formation of alkoxide (Rendleman, 1966). In the current experiment, all the polyols used possess multiple hydroxyl donor groups, which are located adjacent to each other. Therefore, it is highly possible that the formation of metal alkoxide compounds is promoted by intermolecular metal chelation. Meanwhile, heating under reduced pressure facilitates displacement of water molecules by dehydration of hydroxyl groups.

3.4.2. Drying behaviour of aqueous sodium hydroxide solutions under vacuum pressure

In general, an aqueous solution containing solutes has a lower vapour pressure than that of pure water at the same temperature. Consequently, for a given pressure the boiling point of a solution is higher than that of 100% water. Fig. 3.4 illustrates the effect of solute concentration on the boiling point of aqueous NaOH solutions. As the solute concentration increases, the boiling point of the aqueous solution rises exponentially. Such boiling point elevation phenomenon is a colligative property, which means that it is dependent on the quantity of dissolved particles rather than on their identity (Moore, 1962). In the current experiment, 50 wt% of an aqueous solution of sodium hydroxide (50%) was prepared. According to Fig. 3.4, the boiling temperature of this solution would have been approximately 144°C under atmospheric pressure.

Duhring's rule states that the boiling point of a solution at various concentrations increases linearly with the boiling point of pure water. McCabe *et al*. (1993) has developed a plot of NaOH/water system as stated by Duhring's rule (McCabe et al., 1993). Based on the Duhring plot of NaOH/water system, the boiling point of water and 50 wt% sodium hydroxide under different vacuum pressure conditions is provided in Table 3.3. While 50 wt% NaOH solution boils at 144°C under

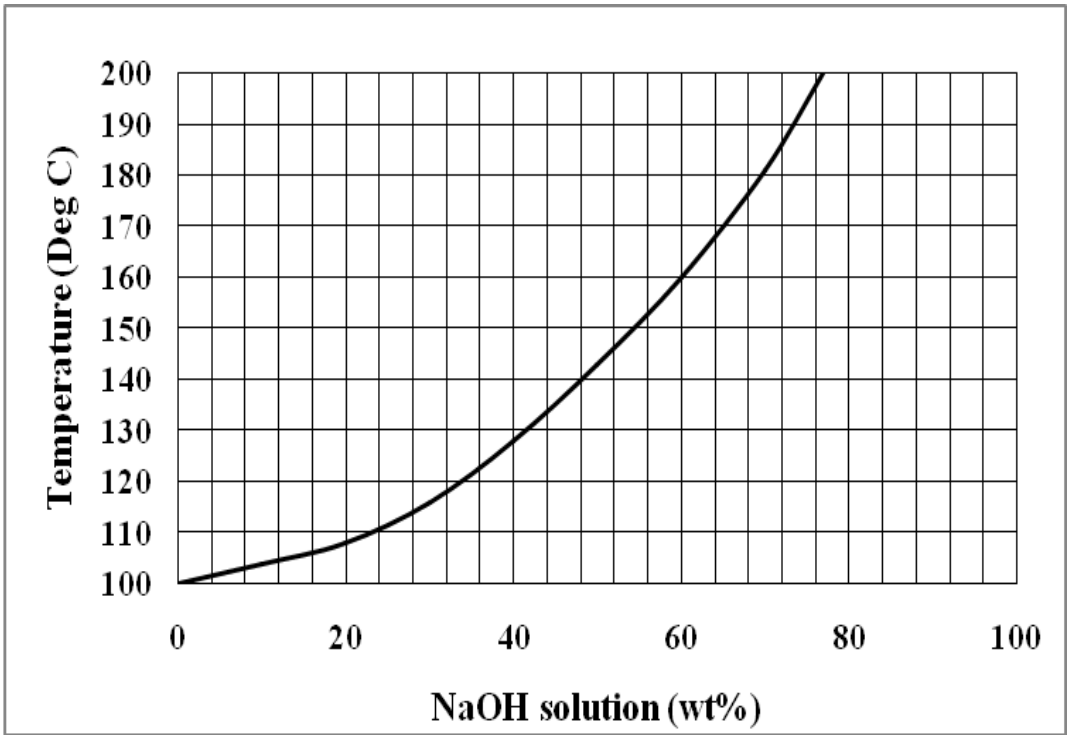

Fig. 3.4 Boiling temperatures of aqueous sodium hydroxide solutions under atmospheric pressure (redrawn from McCabe *et al*., 1993)

Table 3.3 Boiling point of water and 50 wt% NaOH solution at various pressures

Pressure (mbar)	**Boiling point (water, °C)**	**Boiling point (50 wt% NaOH solution, °C)**
1013.25 (Atmospheric)	100	144
250 (vacuum[1])	65	107
68 (vacuum[2])	38.7	67

[1] Atmospheric pressure in vacuum rotary evaporator (first stage drying)
[2] Atmospheric pressure in vacuum oven (second stage drying)

atmospheric pressure the boiling point is lowered to 107°C by applying a vacuum pressure of 250 mbar to accelerate catalyst drying. Lower vacuum pressure (68 mbar) in the second stage lowers the boiling point of 50 wt% NaOH solution to 67°C. Therefore, the combined heat and applied vacuum pressure will dehydrate aqueous NaOH solution to promote the formation of sodium hydroxide or alkoxide compounds.

3.4.3 Influence of different polyols

Before commencing evaporation water that was added (known as free water) to dissolve the solid reagents was quantified so that water loss from alkoxide formation could be measured. In a control study, it was shown that polyols heated to the same experimental conditions did not experience substantial mass loss (0.08 wt% for glycerol; 0.8 wt % for 1, 2-propanediol and 0.2 wt% for 1, 3-propanediol). The negligible mass loss could be associated with evaporation of moisture present in each reagent. Therefore, it can be assumed that sample mass loss in excess of losses of added water is attributable to the formation of alkoxide compounds. After the two-stage drying process the water mass loss exceeded the added mass of free water (see Table 3.4). The excess loss of mass is best explained (in most examples) as evaporation of water, which is produced from the reaction of polyols (hydroxyl group) with sodium hydroxide *via* deprotonation to form sodium alkoxide compounds.

The drying behaviour of aqueous sodium hydroxide added with polyols at different molar ratio is illustrated in Fig. 3.5 and 3.6. The blank NaOH solution, without addition of polyol, dried more slowly with only 20% free water mass loss after 2 h of vacuum dehydration (figure 3.6). Therefore, polyols play a substantial role in aiding the evaporation of solutions of aqueous base. As discussed earlier, polyols may act as ligands to bind metal ions through the formation of stable complexes. Therefore, the presence of polyols in the base aqueous solution has improved dehydration rates by lowering the concentration of solute during drying.

Table 3.4 Measurement of free water mass loss for base-polyol mixtures at different mole ratio

Time (min)	**50 wt% NaOH**	**2:1 mole ratio of base: alcohol Free water mass loss (±0.0002g)**					**3:1 mole ratio of base: alcohol Free water mass loss (±0.0002g)**				
		Glycerol	**1,2-PD**	**1,3-PD**	**Sorbitol**	**Xylitol**	**Glycerol**	**1,2-PD**	**1,3-PD**	**Sorbitol**	**Xylitol**
0	7.2648	7.2648	7.2648	7.2648	7.2648	7.2648	7.2648	7.2648	7.2648	7.2648	7.2648
15	5.8113	2.1620	4.1490	3.9340	1.3000	0.9430	4.0413	4.2763	5.3016	1.7600	1.1077
30	5.8082	1.3210	3.9060	3.0630	0.7820	0.4850	3.8990	3.9580	5.2157	1.1746	0.7656
45	5.5836	0.9760	3.1200	3.4140	0.4510	0.3770	3.0626	3.6406	5.1583	0.9529	0.6790
60	5.4938	0.6960	1.8770	3.2660	0.2340	0.3000	2.9527	3.4778	4.8545	0.8612	0.6286
75	5.4295	0.5220	1.4140	3.1430	0.1230	0.2390	2.9046	3.2949	4.8444	0.8104	0.4350
90	5.3735	0.4310	1.2330	2.8360	0.0650	0.1260	2.8098	3.0135	4.6195	0.7390	0.2582
105	5.3645	0.2920	1.0450	2.5730	0.0310	0.0640	2.7283	2.8558	4.6114	0.6832	0.1736
120	5.1161	0.1820	0.9760	2.4760	0.0310	0.0380	2.6595	2.5318	4.5343	0.6238	0.1458
24 hours		**-1.8980**	**-2.2360**	**-4.7230**	**-2.4290**	**0.9420**	**-1.4270**	**-1.9080**	**2.8420**	**-0.4390**	**0.6000**

*PD = propanediol

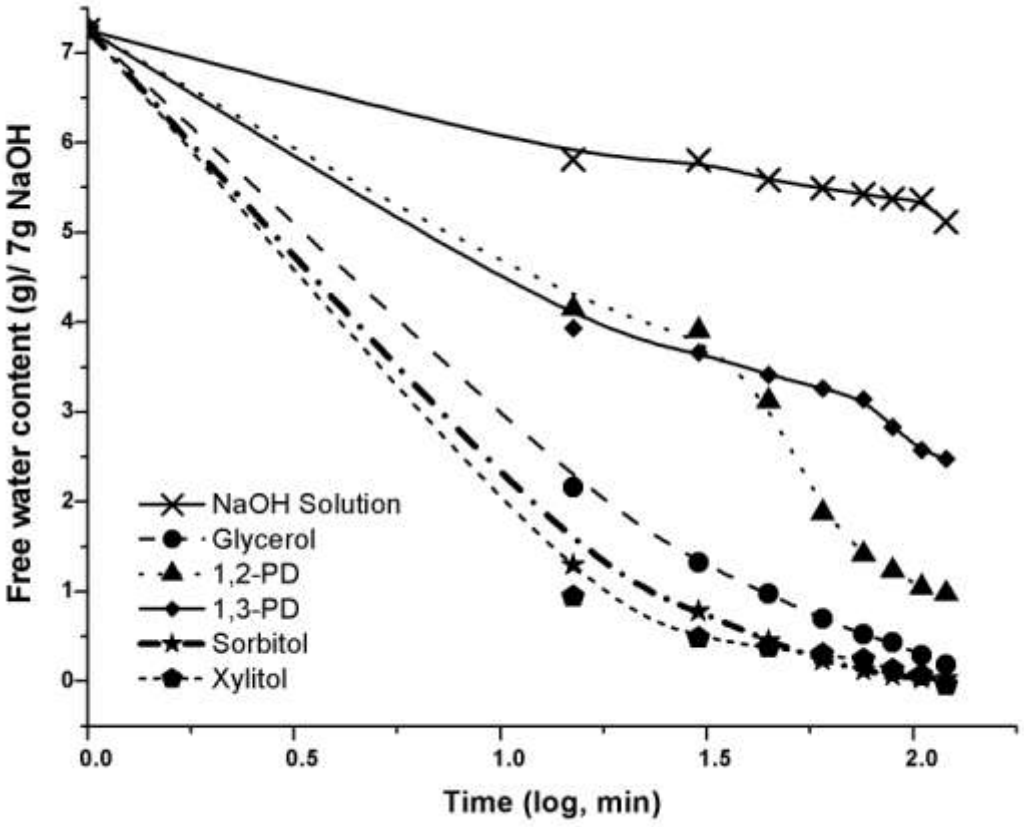

Fig. 3.5 Mass loss of aqueous sodium hydroxide: polyol solutions (2:1 molar ratio) during first stage vacuum dehydration

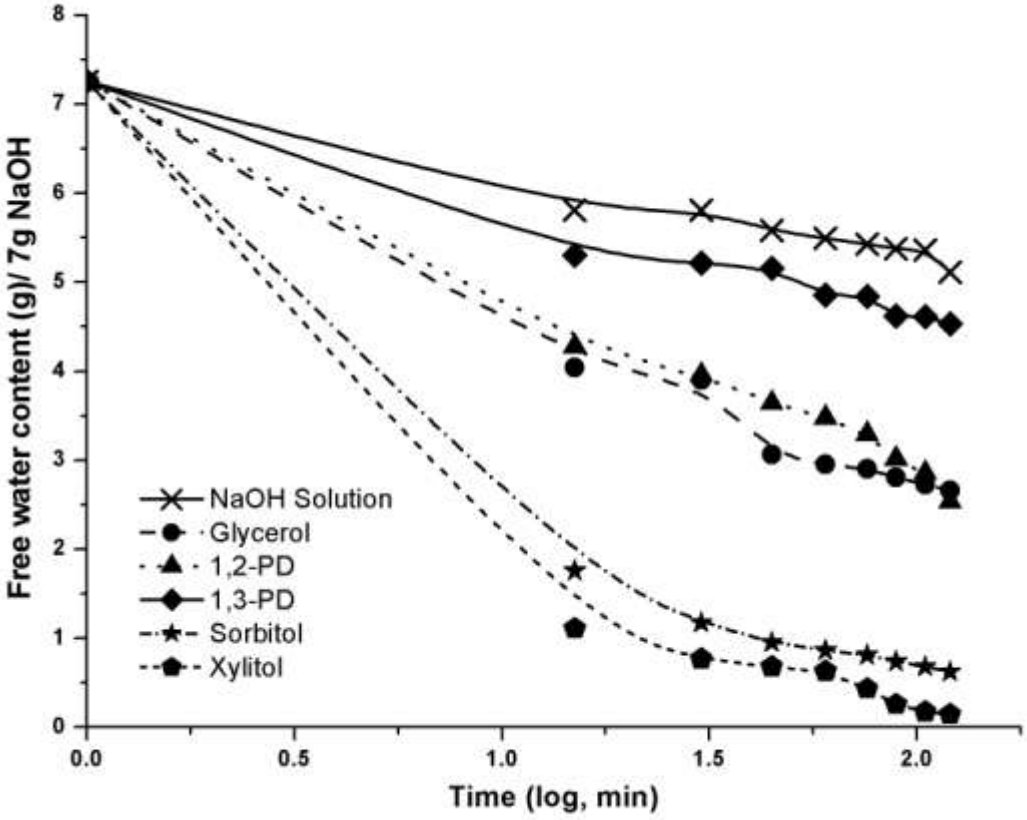

Fig. 3.6 Mass loss of aqueous sodium hydroxide: polyol solutions (3:1 molar ratio) during first stage vacuum dehydration

The alkaline reaction medium enables deprotonation of polyols, which then tend to bind with the sodium ion. The resultant alkoxide complex replaces 3 moles of solute (Na^+, OH^- and polyol) with one polyol alkoxide, which will further enable improved evaporation. Therefore, drying of aqueous solutions of sodium hydroxide is more effective in the presence of polyols.

The chemical properties of the polyols and their solutions vary and these properties may affect the drying behaviour of the aqueous base solution. Dehydration of solutions of sodium hydroxide and polyols with three and more hydroxyl groups (glycerol, sorbitol and xylitol) was more rapid than dehydration of similar solutions with diol compounds. The drying trend is possibly related to the chelating ability and stability of the polyols. Gyurcsik and Nagy (2000) studied the relationship between the structure of sugar alcohol and the stability of metal complexes with the sugar alcohol. They observed that at least three hydroxyl groups in a favourable steric arrangement are necessary for stable complex formation. The chelating ability of ligands with only two OH groups is inferior compared to glycerol (Rich *et al*., 1991). The present experiment supports this hypothesis as the evaporation of the polyols from base solution occurs more rapidly than for solutions with diols. In addition, availability of the 1,2-diol structure (vicinal hydroxyl group) is also an important factor since the adjacent hydroxyl donor group stabilize the metal complex (Rich *et al*., 1991). The present data show that 1,3-propanediol base solutions dry more slowly than other solutions possibly due to the lack of a vicinal hydroxyl structure in which a stable metal complex is formed to facilitate water loss.

Multiple hydroxyl moieties in polyols have the tendency to increase water removal by providing various metal-binding sites. Deprotonation of primary alcohol (terminal hydroxyl group) occurs more readily than for secondary alcohols. However, the presence of secondary or vicinal alcohol may help in stabilizing the alkoxide. Based on Table 3.5, xylitol and sorbitol possess the highest number of hydroxyl groups per mole compared to other polyols. These compounds also have a high ratio of secondary alcohols to primary alcohols and vicinal alcohols to total alcohols. Therefore, both

Table 3.5 Classification of primary and secondary hydroxyl group in polyols

Polyols	Fischer Projection	Primary OH	Secondary OH	Total OH
(R)-1,2-Propanediol	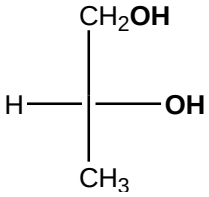	1	1	**2**
1,3-Propanediol	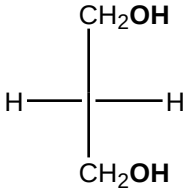	2	0	**2**
Glycerol	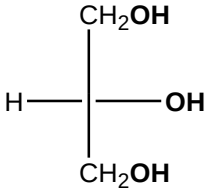	1	1	**2**
Xylitol (*threo, threo, threo*-)	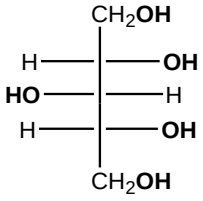	2	3	**5**
(D)-Sorbitol (*threo, threo, erythro-)*	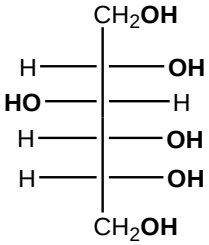	2	4	**6**

compounds dehydrate more rapidly than the other polyols investigated. Consequently, removal of water molecules is more efficient when utilizing xylitol and sorbitol.

Another important factor that affects formation of a stable metal-polyol complex is the regioselectivity of the polyol compounds. Formation of a stable complex requires a *threo-threo* arrangement of hydroxyl groups while the *erythro* arrangement is not observed in alkoxides (Fraser-Reid *et al*., 2008). Xylitol is a non-chiral, all-threo-configured pentitol, which allows grouping of all its hydroxyl functions on the same side C5 chain with zigzag conformation. Therefore, the configuration of the complex formed from this carbohydrate would be free of stearic hindrance. As for sorbitol, it is a hexitol with its vicinal hydroxy groups from C2 to C5 configured with the sequence *threo, threo, erythro*. The configuration of these polyols may explain more rapid dehydration of xylitol base solutions than sorbitol containing base solutions despite the greater number of hydroxyl groups per molecule in sorbitol as compared to xylitol.

Comparison of drying process for respective polyol–NaOH combinations at different molar ratio shows that the base: alcohol ratio of 2:1 (mol: mol) is more efficient than that of 3:1 (mol: mol). The experiment was designed such that a constant amount of sodium hydroxide (0.176 mol) was reacted with polyols at two mole ratios: 0.088 mol for 2:1 mole ratio and 0.058 mol for 3:1 mole ratio. The data strongly suggests that higher ratios of sodium hydroxide to glycerol, 1,2-propanediol and 1, 3-propanediol improved the drying of 50 wt% aqueous sodium hydroxide solutions (see Fig. 3.7). A similar effect was not observed in xylitol and sorbitol dehydration. This observation may be highly associated with the presence of multiple hydroxyl groups in their chemical structure. Since these polyols contain more than three OH groups and potentially form a stable chelating ligand, a 3:1 mole ratio is sufficient to form a stable alkali complex. Additional hydroxyl groups may not improve the chelating effect.

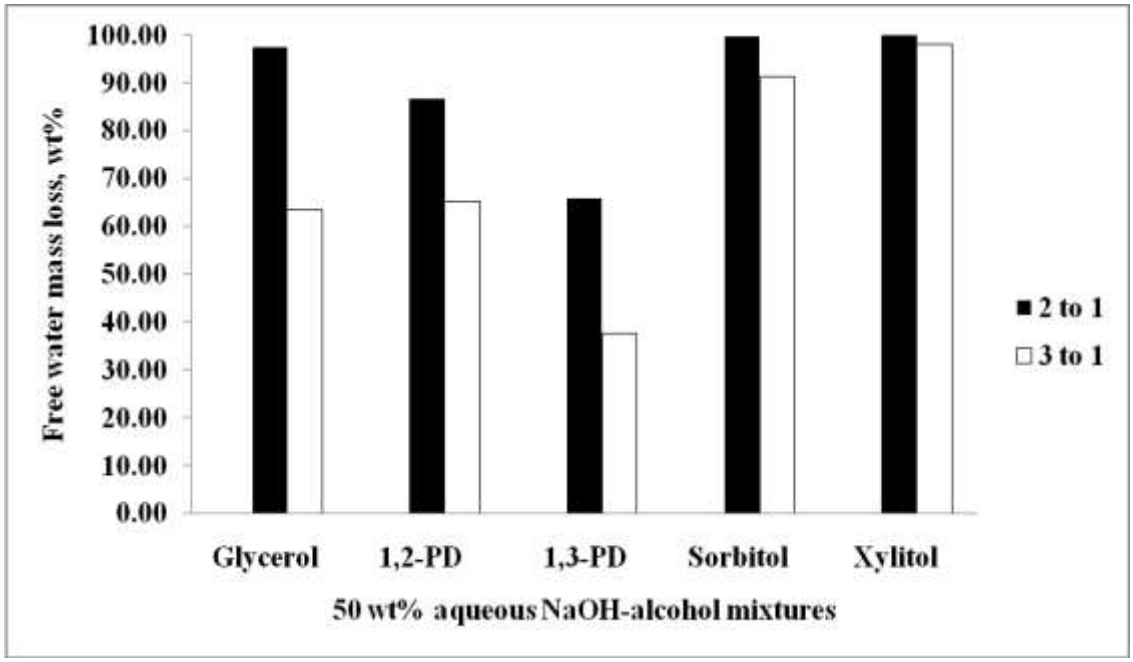

Fig. 3.7 Drying of 50 wt% aqueous NaOH-polyol after first stage of vacuum dehydration

3.5 Connection to the Next Study

Sodium hydroxide is produced as a 50 wt% solution by electrolysis of sodium chloride brine and sold as an inexpensive source of industrial base. Unfortunately, due to the high water content 50% NaOH is not a suitable catalyst for biodiesel production and other transesterification reactions. Evaporation of the water from 50 wt% NaOH solution to produce substantially anhydrous NaOH requires high temperatures (315°C) to achieve a solid that is 94 wt% NaOH and 6 wt% water. Solid sodium hydroxide and sodium methoxide are preferred catalysts for the production of biodiesel. The literature describes the spontaneous formation of alkoxides from aqueous solutions of polyols and sodium hydroxide without evaporation or heating. Chapter 3 describes the drying behavior of various aqueous solutions of polyols and 50 wt% NaOH under vacuum pressure and mild heating conditions (120°C). The mixed solutions, which contained both polyol and NaOH, dried more rapidly and thoroughly than aqueous NaOH solution alone. This improved drying was likely due to the formation of solid alkoxide products as shown in the proposed synthesis mechanism (Figure 3.3). The nature of the alkoxide compounds produced by drying will be explored using single crystal x-ray diffraction, x-ray powder diffraction and elemental analyses. The chemical structure and empirical formulae of the dried products will be discussed based on these analyses.

CHAPTER 4.
CHARACTERIZATION OF SODIUM ALKOXIDE CATALYST

4.1 Abstract

The empirical formulae of powders produced by drying aqueous solutions of sodium hydroxide with polyols were determined. Sodium content was determined using inductively coupled plasma atomic emission spectrometry (ICP-AES) while carbon, and hydrogen (CH) content determined by combustion gas analysis. Anhydrous dried products derived from different polyols were crystalline powders suitable for x-ray powder diffraction analysis. The diffraction patterns obtained from these powders indicate that new materials were obtained as all patterns differed from the original reagents. Nonetheless, the presence of spectral lines corresponding to NaOH(s) indicates that the powders of some compounds may be adducts that incorporate one or more moles of NaOH. Empirical formulae were consistent with the formation of alkoxide compounds or complexes. The powders were mainly mono-sodium alkoxides or adducts of mono-sodium alkoxide with water and/or sodium hydroxide. In addition, single crystal X-ray structures were obtained for glycerol and xylitol derived alkoxides. The diffraction pattern of the powder produced by dehydration of glycerol in the presence of sodium hydroxide (1:1 Mol ratio) was in agreement with those simulated from a single crystal unit cell of sodium glycerolate. Therefore, sodium glycerolate crystal chosen for the single crystal X-ray structure was representative of the bulk sample.

4.2 Hypothesis

Dehydration of aqueous solutions of sodium hydroxide and polyol will, potentially produce novel crystalline compounds. The composition of these compounds

will readily be determined by obtaining x-ray diffraction patterns and empirical formulae. Under sufficiently powerful dehydration conditions, alkoxide compounds, derived by deprotonation of polyols, that exhibit bonding between the sodium metal and oxygen atoms of the polyol may be observed.

4.3 Methods

4.3.1 Crystal growth for X-ray crystallography

Polyols were mixed with sodium hydroxide at various ratios and the samples were allowed to dry slowly in an attempt to produce individual crystals. The sample mixtures were composed of 50 wt% of NaOH solution and the polyols at a 3:1 mole ratio. The sample mixtures were stored in vials (covered by perforated aluminum foil) for several weeks in a desiccator containing sodium hydroxide pellets as a drying agent. The strong alkali absorbed water and, thereby, increased the concentration of the reagents to facilitate crystal growth.

Glycerol (92 g; 1 mol) was slowly added into 50 wt% sodium hydroxide solution which was freshly prepared by dissolving 120 g (3 mol) NaOH pellets in 120 g water. The mixture was stirred vigorously and allowed to cool to room temperature. Colorless crystals formed were only stable in the mother liquor at ambient temperatures. Xylitol (3.043 g) and sodium hydroxide pellets (3.200 g, ground to powder) were mixed together in a 50 mL vial. Sufficient (approximately 30 mL) methanol was slowly added to the mixture and stirred vigorously until the solute just dissolved. The vial was then stored in a 400 mL tall beaker filled with hexane. The beaker was sealed using parafilm (VWR International; Mississauga, Canada) and stored to allow crystal growth. Slow diffusion of hexane vapour into the inner vial caused crystals to form.

A colorless plate-like crystal (glycerol derived alkoxide) with approximate dimensions of 0.25 x 0.25 x 0.13 mm was removed from the solution and quickly coated with oil (Exxon Paratone 8277; Houston, USA), collected onto the nylon fiber

Cryoloop™ (Hampton Research; Aliso Viejo, USA) and immediately transferred to the cold stream of the X-ray diffractometer (Bruker AXS Proteum R Smart 6000; Milton, Canada). The data collection was performed at -90 °C. All measurements were performed on the diffractometer using monochromated Cu K_α radiation (α = 0.71073 Å) from Bruker-AXS FR591 rotating-anode generator equipped with Montel200 multilayer graded optics. For xylitol derived alkoxide, a colorless rod shape crystal with approximate dimensions of 0.16 x 0.09 x 0.04 mm was analyzed using the same procedure except that the data collection was performed at -100 °C and monochromated Cu K_α radiation at wavelength 1.54184 Å.

4.3.2 Hygroscopic material transfer procedure

All alkoxide powders synthesized were stored in sealed airtight containers to prevent exposure to air and moisture. For subsequent characterization, the moisture sensitive powders were carefully weighed and transferred in an inflatable polyethylene isolation chamber (AtmosBag™ Sigma-Aldrich; Saint Louis, USA) with built-in gloves. The chamber was placed in a fume hood for added safety. Residues in the air that could react with the powders were eliminated by a series of 5 vacuum/argon gas purge cycles to ensure an inert atmosphere in the chamber for appropriate transfer of a hygroscopic material.

4.3.3 Powder diffraction

Where a reaction did not produce a larger crystal that could be mounted individually, a small amount of the sample powder was suspended in oil (Exxon Paratone 8277; Houston, USA) so as to produce a thick paste. The sample was then placed onto the aperture of a mounting loop Micromount™ (diameter of the aperture: 100 microns; *MiTeGen* - Microtechnologies for Structural Genomics; Ithaca, USA). A Micromount™ consists of a thin microfabricated polyimide film attached to a solid non-magnetic stainless steel pin.

Data was collected at 295 ºK using a Proteum R CCD detector cooled to -50 ºC (Smart 6000; Bruker-AXS, Milton Canada) using Cu-K_α radiation from a Bruker-AXS FR591 rotating-anode generator equipped with Montel200 multilayer graded optics. The system uses a horizontal-oriented D8 goniometer base with 2-theta, omega and phi drives and a fixed chi stage with an angle of 54.74º. The detector distance was adjusted manually. Powder diffraction data were collected using an exposure time of 600 s, a scan width of 2º and different sets of phi scan as listed in table 4.1. A total of nine frames were collected and the total data collection time was 1.5 hours for each sample. Data processing was performed by merging the frames into a composite image using the Phase ID module (Noiroj, Intarapong *et al*., 2009) as embodied in the Bruker ApexII software tools. After defining the area for analysis, the image was integrated and integration results were displayed graphically as intensity *vs.* 2-theta. Background correction, calculation of *d*-spacing, 2-theta and intensities were calculated using *PowderX* software (Dong 1999).

The powder diffraction pattern of sodium glycerolate (Schatte *et al*., 2010) and starting materials such as sodium hydroxide (Stehr, 1967), glycerol, xylitol and sorbitol were calculated from single crystal X-ray data using the program *POUDRIX* (Bochu, 2004). The Crystallographic Information Files (CIF) for the starting materials were downloaded from the Cambridge Crystallographic Database and converted into a format (shelxl.ins files) suitable for interpretation by the POUDRIX program using the program WinGX (Farrugia, 1999). The powder diffraction data for NaCl was obtained from Mineral Powder Diffraction File: Data Book, International Centre for Diffraction Data. Microsoft Office Excel 2007 and OriginPro 7.0 program were used to generate the diffraction patterns from the raw data points.

Table 4.1 Powder diffraction instrument settings (phi scans) for data collection

Axis	**dx/mm**	**2θ/°**	**ω/°**	**ϕ/°**	**χ/°**	**Width/°**	**Frames**
Phi	100.000	-14.00	171.00	0.00	54.74	180.00	1
Phi	100.000	-24.00	167.00	0.00	54.74	180.00	1
Phi	100.000	-34.00	162.00	0.00	54.74	180.00	1
Phi	100.000	-44.00	157.00	0.00	54.74	180.00	1
Phi	100.000	-54.00	152.00	0.00	54.74	180.00	1
Phi	100.000	-64.00	147.00	0.00	54.74	180.00	1
Phi	100.000	-74.00	142.00	0.00	54.74	180.00	1
Phi	100.000	-84.00	137.00	0.00	54.74	180.00	1
Phi	100.000	-94.00	132.00	0.00	54.74	180.00	1

4.3.4 Compositional characterization

4.3.4.1 Inductively Coupled Plasma- Atomic Emission Spectrometry (ICP-AES)

Stock solutions of powdered samples were prepared by dissolving approximately exactly 100 mg of dry powder in 10 mL of distilled water. Prior to analysis, dilutions were made by taking aliquots from these stock solutions. Calibration was conducted using certified sodium chloride standard solution (EMD chemical, New Jersey USA) in the concentration range of 10 mg/L to 1000 mg/L. A sodium-free blank was measured prior to sample analysis. The samples were analyzed for sodium content using Inductively Coupled Plasma Atomic Emission Spectrometer (Model IRIS Intrepid, Thermo Jarrel Ash; Massachusetts USA). Sodium content (ppm) was converted into wt% according to equation 4.1.

$$\text{Sample Content (wt\%)} = \frac{\text{Sodium content (ppm)x 0.01 L x 100\%}}{\text{Sample weight (mg)}} \qquad [4.1]$$

4.3.4.2 Elemental analysis by CHN Analyzer

Approximately 2-3 mg of dry sodium containing powder was loaded in tin capsules (8x5 mm) (UIC, Inc.; Joliet, USA) that were subsequently loaded in the CHNS elemental analyzer (Perkin Elmer 2400 CHN; Waltham, USA) for determination of carbon and hydrogen contents. Samples were subjected to combustion and the exhaust gasses were quantified by thermal conductivity. The analyzer was calibrated with tin blanks and four acetanilide samples (2-3 mg) with an analysis error within ±2%. Oxygen content was calculated in wt% by subtracting carbon, hydrogen and sodium content from 100 %. Best fitting of the final compound composition was estimated by mathematical models, which were optimized using the Marquardht-Levenberg algorithm as embodied in the Excel Solver program (Microsoft Office Excel 2007; Microsoft Corporation; Redmond, USA). Refer to Appendix C for application details.

of the Solver Program. The product composition is expressed in mole ratios of each constituent element and can be calculated from equation [4.2], with assumption that total sample weight is 100 g:

$$\text{Product Composition} = \frac{\text{Solver composition (wt \%)x Total sample weight (g)}}{\text{Molecular weight (g mol} - 1)} \quad [4.2]$$

4.4 Results and Discussion

4.4.1 Crystal structure of sodium glycerolate

Colorless plate-like crystals were observed when the mixture of sodium hydroxide solution and glycerol was cooled to room temperature in a closed glass vial. Colorless rod shape crystals were obtained from sodium hydroxide and xylitol mixtures. The crystals were only stable in the mother liquor at ambient temperatures (Fig. 4.1). Schatte *et al.* (2010) reported the same crystal structure of sodium glycerolate in which sodium was attached to a deprotonated hydroxyl group of a primary carbon atom of glycerol and stabilized by chelation to other electron donor groups. Hence, basic conditions were necessary for deprotonation to occur since both glycerol and xylitol are weak acids with pKa values of 14.16 and 13.73, respectively (Thamsen, 1952). According to Schatte *et al.* (2010), the crystal structure was elucidated as:

> "A mono-sodium glycerolate with molecular formula $[Na(C_3H_7O_3)]_n$ or $Na[H_2gl]$. The H_2gl^- anion behaves as a multifunctional ligand in the glycerolate structure. In the first mode, the H_2gl^- ligand is coordinating to the sodium atom by one oxo- (O_1) and one hydroxo (O_2) group."

This structure is shown in Fig 4.2 (a). A mono-sodium xylitolate with molecular formula $Na[H_4xl]$ also formed with a similar intra-molecular bonding (Fig. 4.2 b). The $M^{\delta+}$--$O_1^{\delta-}$--C bonding in alkali metal alkoxides are usually assumed to be dominated by 80% ionic character in view of the strongly electronegative nature of oxygen (3.5 on the Pauling scale) and the highly electropositive group I metal (1.2 - 0.9) on electronegativity scale) (Bradley 1958; Bradley 2001).

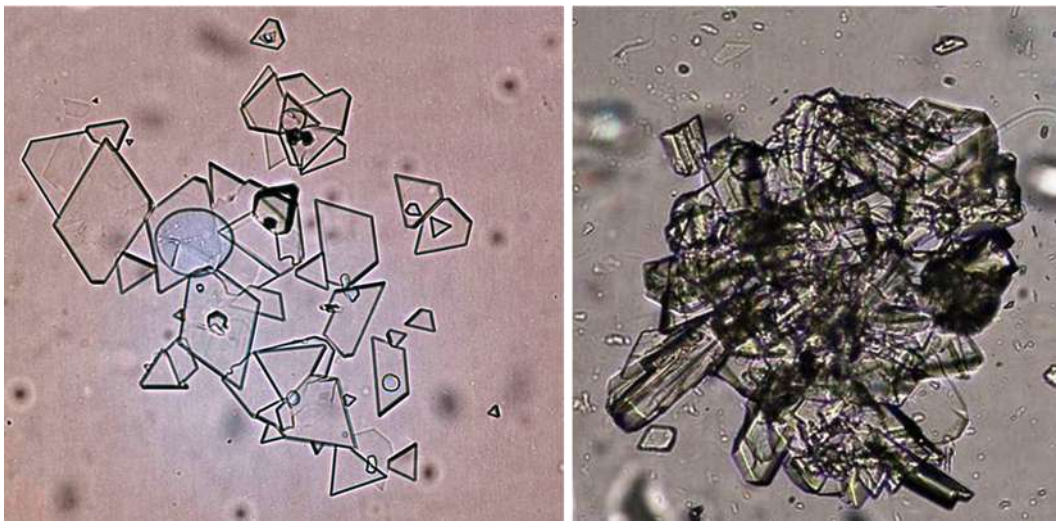

Fig. 4.1 Sodium glycerolate crystal growth from 50 wt% sodium hydroxide solution and glycerol at 3:1 mole ratio. Image viewed under Nikon Eclipse E400 microscope with 10x/0.25, WO 10.5 objective

(a)

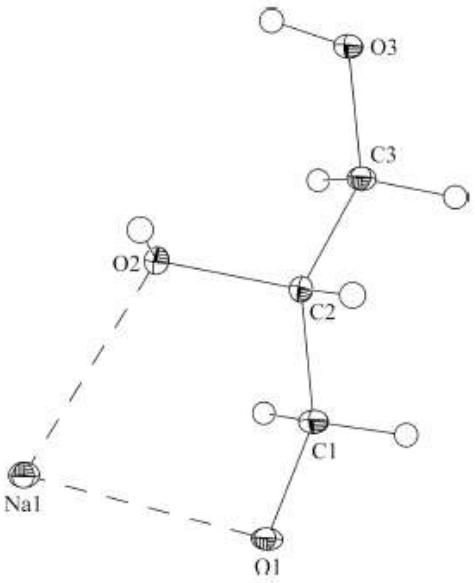

(b)

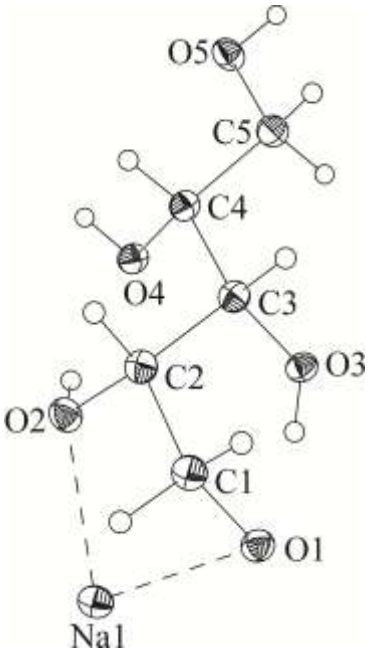

Fig. 4.2 A non-planar asymmetric five-membered ring formed by intra-molecular Na-O bonding within vicinal hydroxyl groups of (a) H_2gl^- and (b) H_4xl^- ligands

Ionic bonding ($Na^{\delta+}$--$O_1^{\delta-}$) is observed at C_1 where deprotonation of hydroxyl group occurs. Nevertheless, Na-O bonding has also demonstrated metal covalent expansion (multiple bonding by mono-valent sodium metal) due to the attenuation in polarity of metal-oxygen bonds (Mehrotra 1988). Example of such bonding can be observed at C_2 where sodium ion is coordinated to the hydroxo (O_2) group. Such covalent expansion enables stable chelation of metal to the adjacent oxygen within the same molecule. This phenomenon explains why the presence of 1,2-diol structure (vicinal hydroxyl group) is a crucial factor for a stable metal chelate formation (Rich *et al*., 1991). In the same crystal report, it is also mentioned that:

> "The negatively charged O atom of the glycerolate anion is in equatorial position, and the O atom of the hydroxo group, attached to the secondary C atom occupies an axial position completing a five-membered non-planar chelate ring."

Therefore, the stereochemistry of the hydroxyl group within the polyol plays a role in metal covalence expansion. In this context, the equatorial and axial position of the vicinal hydroxyl groups within glycerol molecule reduced the conformational steric hindrance, which favours metal chelate bonding.

Besides intra-molecular sodium-oxygen bonding, Schatte *et al.* (2010) also revealed inter-molecular Na---O bonding between H_2Gl^- ligands *via* metal covalence expansion as illustrated in Fig. 4.2 (c). The author commented that:

> "The other symmetry-related H_2gl^- ligands form essentially monodentate attachments to the Na^+ ion. Therefore, each sodium ion (Na^+) is coordinated by five O atoms leading to formation of pseudo-five-membered chelate rings possessing distorted trigonal-bipyramidal geometry. Therefore, each H_2gl^- is bonded to four Na^+ ions. Meanwhile the ligands are connected to each other *via* two strong intermolecular O-H---O hydrogen bonds."

This bonding pattern is shown in Fig. 4.3. Sodium xylitolate structure has the similar inter-molecular bonding except that each sodium ion is coordinated to four H_4xl^- ligands through six oxygen atoms (Fig. 4.4).

In brief, both polyol-derived sodium alkoxide structures are coordinated by inter- and intra-molecular Na---O covalent bonds between adjacent units. Meanwhile, the strong intra-molecular hydrogen bonding between donor hydroxyl and acceptor alkoxido moiety within the H_2gl^- and H_4xl^- ligands has further enhanced the stability of the polymeric structure. The crystal structure elucidation has also demonstrated that glycerolate compound excludes both water and free glycerol from the structure which provides an advantage in the efficient production of dry catalysts for transesterification reactions. The result of the crystal report also confirms the earlier proposed structure by Fairbourne *et al.* (1921) who described the alkoxide compound formed from 1:1 mole ratio of NaOH: Glycerol as $C_3H_7O_3Na$ (mono-sodium substituted glycerolate).

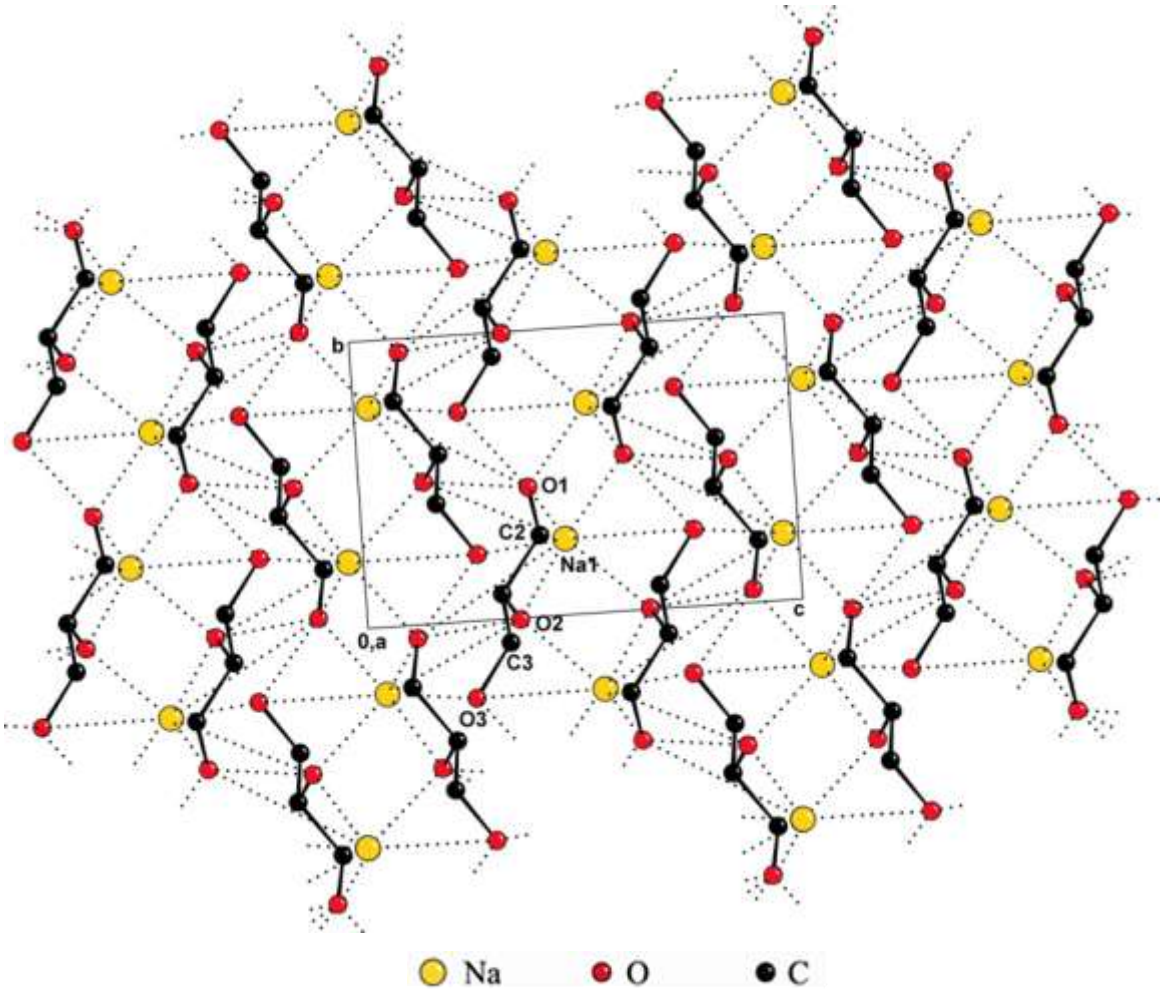

Fig. 4.3 Mono-sodium glycerolate structure $[Na(C_3H_7O_3)]_n$ showing the intra-and inter-molecular Na----O and intra-molecular O(H)----O contacts leading to a polymeric sheet-like structure. Hydrogen atoms attached to carbons have been omitted for clarity (Schatte *et al*., 2010)

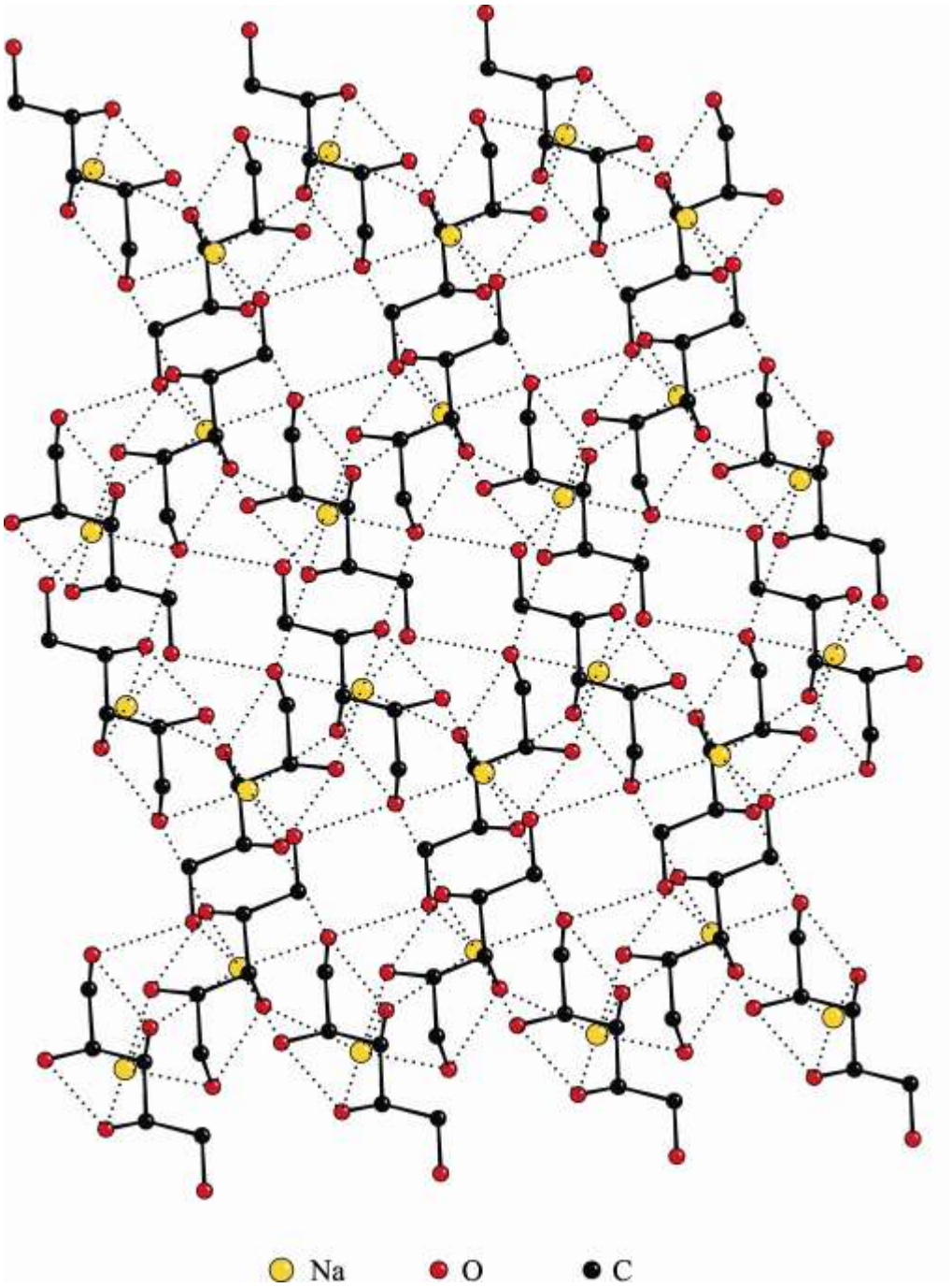

Fig. 4.4 Mono-sodium xylitolate structure $[Na(C_5H_{11}O_5)]_n$ showing the intra-and inter-molecular Na----O and intra-molecular O(H)----O contacts leading to a polymeric sheet-like structure. Hydrogen atoms attached to carbons have been omitted for clarity

4.4.2 Powder diffraction patterns for sodium alkoxide catalysts

The analyses of the samples (sodium glycerolate at 2:1 and 3:1 mole ratio) were performed by overlapping the powder diffraction pattern of the samples with sodium glycerolate, NaOH, glycerol and NaCl in which the reference patterns (Fig. 4.5) that were retrieved from recognized crystallographic databases mentioned in section 4.2.3. From the powder diffraction patterns (Fig. 4.6), it was observed that both samples synthesized at different ratios were comparable since the respective patterns match closely. The sample patterns closely resembled the sodium glycerolate powder diffraction data even though some peaks corresponded with the NaOH pattern. As a result, the conclusion was that the compounds contained sodium glycerolate [CH_2(OH)-CH(OH)-CH_2ONa] and varying amounts of NaOH. Additionally, the unassigned peaks present may be attributed to either additional sodium glycerolate derivatives (di- or trisodium glycerolate) or NaOH × *n* H_2O compounds (*n* = 1 to 7).

The powder derived from mixing 1,2-propanediol and sodium hydroxide solution produced the diffraction pattern presented in Fig 4.7. The pattern produced from this powder is distinguishable from the pattern of NaOH. The powder contains peaks at 30 ^{o}, 55^o and 80^o which may be related to the pattern of NaOH in the powder. This finding indicates the formation of an alkoxide compound and likely the presence of NaOH in the final product, possibly occurring as an adduct. The same description also applied to 1,3-propanediol derived alkoxide (Fig. 4.7). The powder diffraction pattern differs greatly from the NaOH reagent which indicates formation of a new compound. The starting materials, 1,2-propanediol, and 1,3-propane diol exist as liquids at room temperature from which a diffraction pattern is not available for comparison. Powder diffraction of powders derived from the dehydration of solutions of xylitol and sodium hydroxide produces patterns that are unlike published pattern of NaOH (Fig. 4.8). Additionally the pattern was unlike that of xylitol proving formation of new bonding within the powdered sample. Powder produced from sorbitol and sodium hydroxide (not shown) produced a broad peak indicating an amorphous structure of the powder.

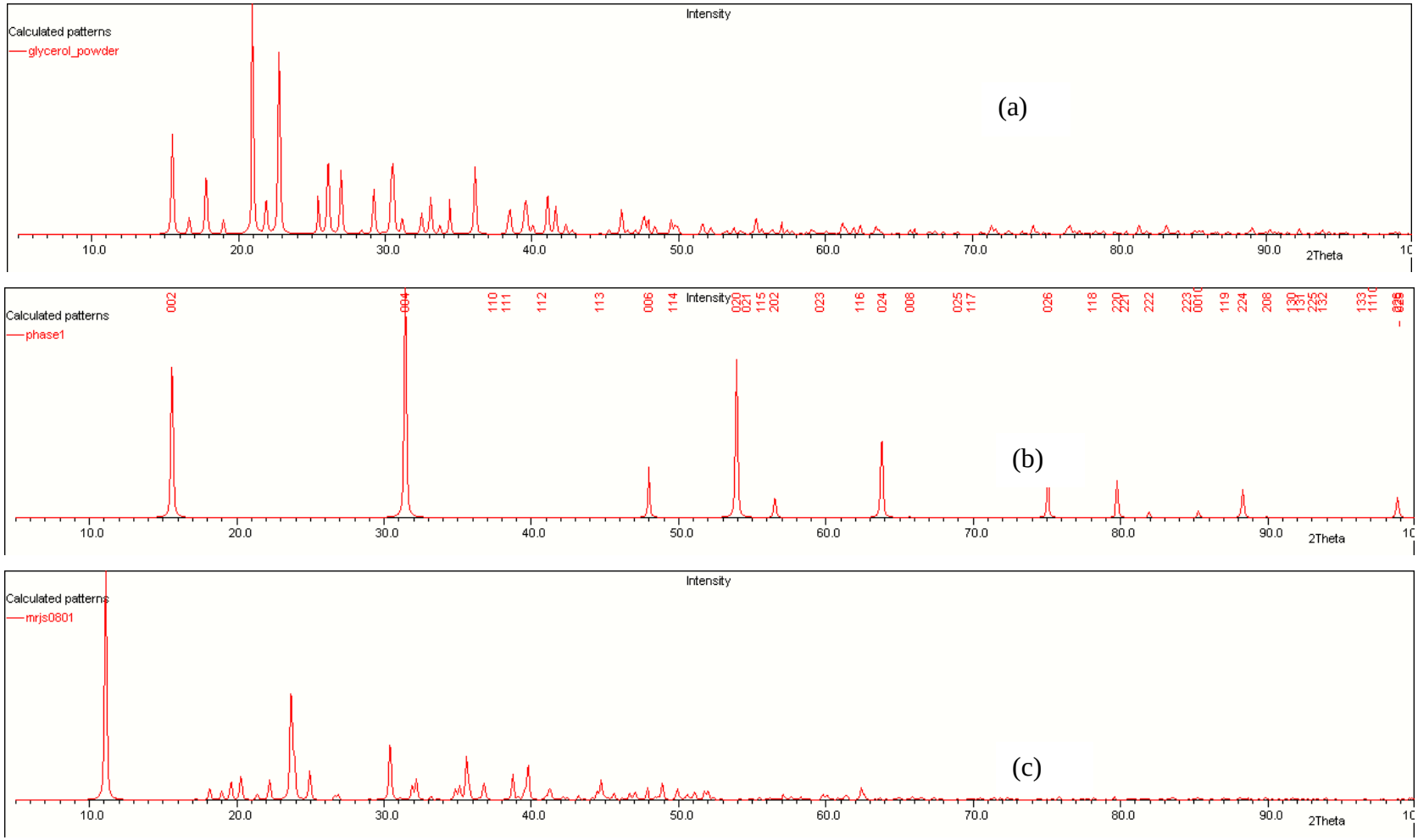

Fig. 4.5 Powder diffraction pattern for (a) glycerol; (b) sodium hydroxide and (c) sodium glycerolate

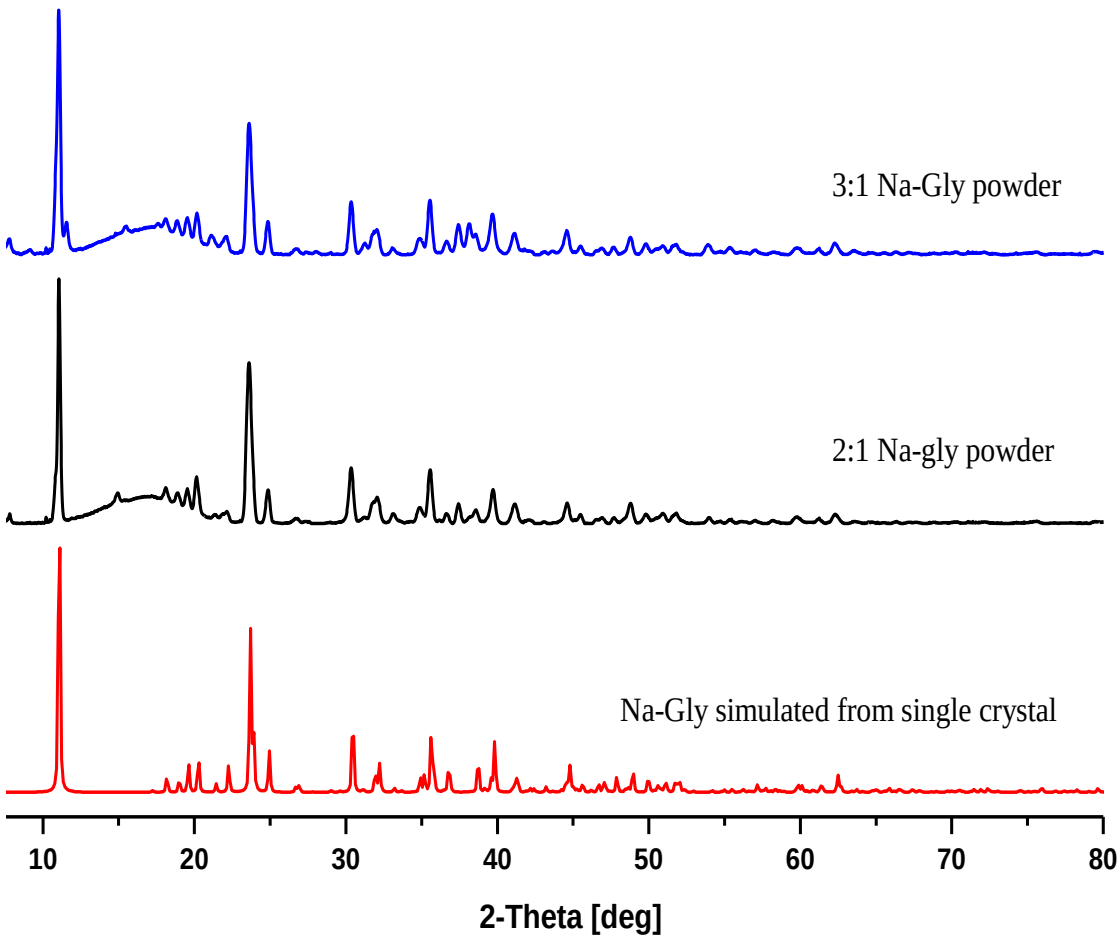

Fig. 4.6 Powder diffraction pattern of Sodium glycerolate catalysts at different mole ratio

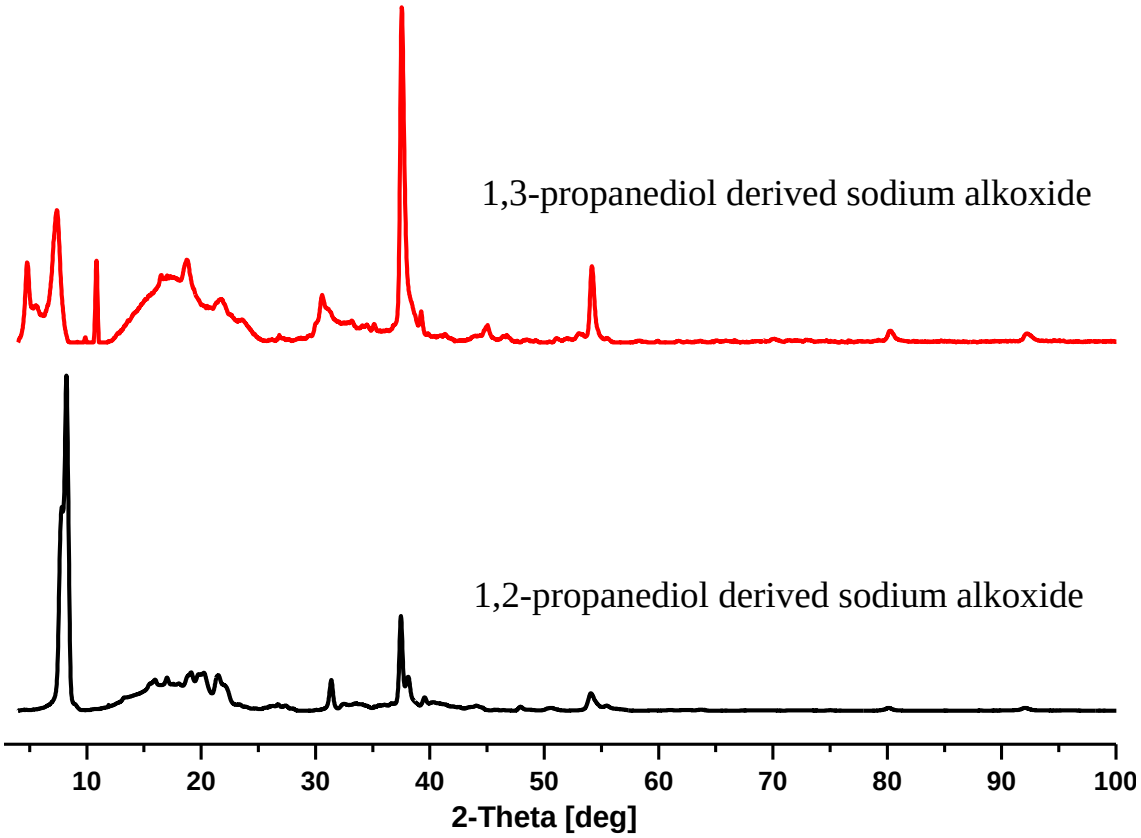

Fig. 4.7 Powder diffraction pattern for glycol-derived sodium alkoxide at 3:1 mole ratio

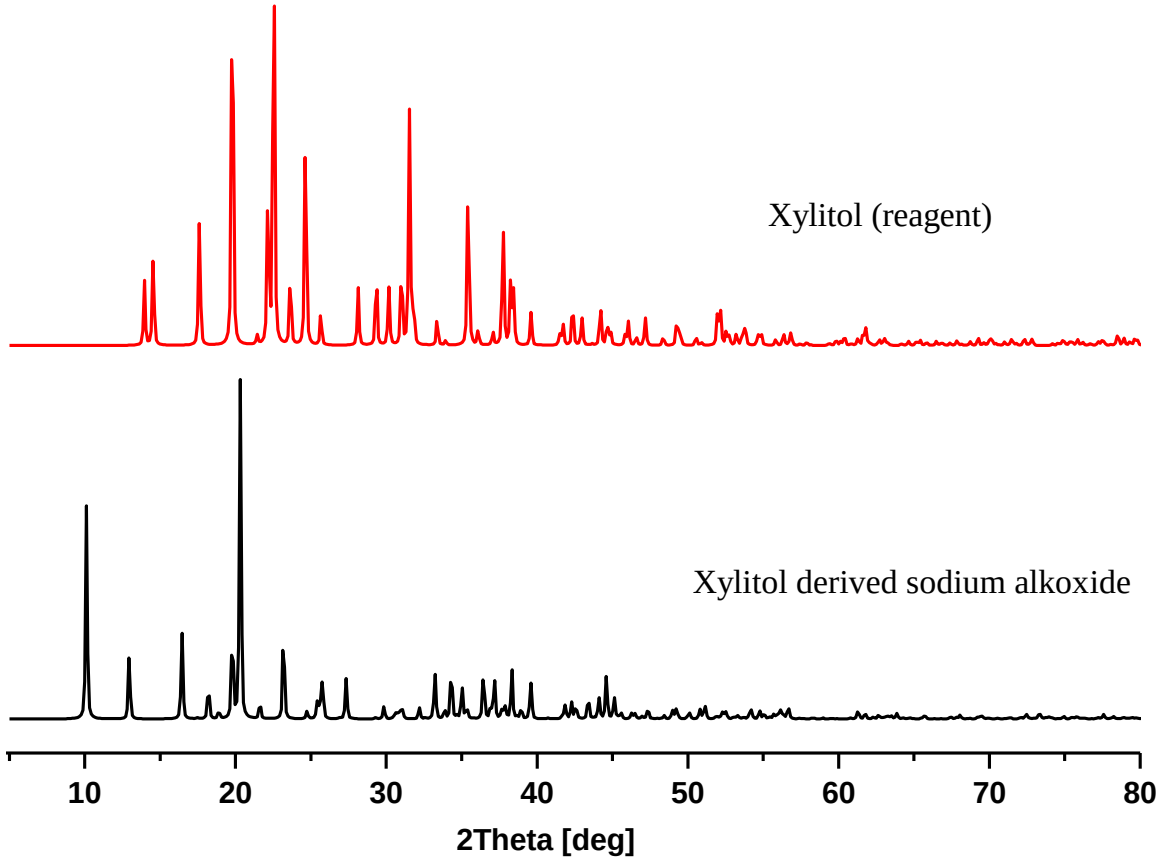

Fig. 4.8 Powder diffraction patterns for xylitol-derived sodium alkoxide at 3:1 mole ratio as compared to original reagent pattern

4.4.3 Sodium, carbon and hydrogen content in wt%

The sodium, carbon and hydrogen content (wt %) derived from ICP-AES and elemental analyses comprise Table 4.2. It is observed that both sodium alkoxide derived from 1,3-propanediol at 2:1 and 3:1 mole ratios produced significantly lower C, H content than would be predicted. Theoretically, the elemental content should appear comparable to the 1,2-propanediol derived alkoxide counterpart because the diol compounds are isomers having the same molecular weight. This result can be associated with evaporation of 1,3-propanediol during the second stage of vacuum dehydration. A published patent describes a process for purifying a carbonyl containing 1,3-propanediol by distillation of the 1,3-propanediol under basic condition (Kelsey 1994). 1,3-Propanediol can be distilled from a 1 N NaOH solution at 124°C (oil bath 150 – 155°C) under a vacuum pressure 80 – 90 mbar (Kelsey 1994). In the current experiment, the second stage of dehydration involved heating to120°C under vacuum pressure (68 mbar). The experimental conditions have caused partial evaporation of the glycol producing a powder with a lower carbon and hydrogen content than expected.

Despite the fact that 1,2-propanediol boils at 120°C under atmospheric pressure 80 mbar (Budavari, 1989), the diol compound does not appear to evaporate under the experimental conditions. This phenomenon can likely be attributed to the vicinal hydroxyl moieties in 1,2-propanediol that bind with sodium metal forming a stable high boiling complex in the solid state. Therefore, hydrogen bonding within the molecule likely prevented glycol evaporation during heating under vacuum pressure. The hydroxyl groups of 1,3-propanediol are less favorable for metal chelation. Consequently, partial evaporation of 1,3-propanediol occurred due to the lack of a vicinal 1,2-diol conformation. Therefore, the end product was not covalently linked to sodium as compared to its counterpart.

Table 4.2 Sodium, carbon and hydrogen content in wt% for polyol-derived sodium alkoxide catalysts derived from different mole ratios of base and polyols

	2: 1 NaOH: Polyol mole ratio			**3: 1 NaOH: Polyol mole ratio**		
	Na (wt%)	**C (wt%)**	**H (wt%)**	**Na (wt%)**	**C (wt%)**	**H (wt%)**
Na-O-glycerol	25.1±2.7	22.3±1.0	6.0±0.3	33.9±2.3	19.3±1.2	5.3±0.0
Na-O-1,2-PD	32.0±2.2	23.4±0.5	6.1±0.2	35.8±2.2	21.1±0.7	5.1±0.1
Na-O-1,3-PD	39.1±2.1	17.6±0.1	3.6±0.3	41.6±2.1	15.7±0.7	4.5±0.3
Na-O-Xylitol	21.2±2.5	30.0±0.2	5.3±0.1	24.0±2.6	20.2±0.0	5.9±0.3
Na-O-Sorbitol	14.9±3.0	31.8±0.0	6.1±0.2	21.3±2.7	22.8±0.2	5.9±0.1

4.4.4 Polyol-derived sodium alkoxide product composition

Elemental analysis for sodium, carbon, hydrogen and oxygen content has provided reference data set for estimation of the composition of powders. Oxygen content was calculated by subtracting the other elements (Na, C and H) from 100 wt%. Calculation using mathematical models based on stoichiometric molecular weight provided the best fitting of the empirical formulae as summarized in Table 4.3. Generally, sodium alkoxide derived from different polyols are constituted from mono-sodium substituted alkoxide and other adducts such as NaOH. Even though extreme care was taken during material transfer of these compounds, such as processing samples in an inert atmosphere, these alkoxides are easily hydrated due to their high water affinity. It is difficult to produce a completely dry powder or maintain a powder in a dried state.

Empirical formulae indicate that the powders were mono-sodium substituted alkoxides except for 3:1 xylitolate and sorbitolate, which were likely to be hydrated during sample transfer for elemental analysis. The composition of sodium glycerolate produced at 3 to 1 mole ratio of NaOH to alcohol is in agreement with the single crystal structure where mono-sodium substituted crystals were observed. In addition, the results verify Gross (1926) who reported in 1926 that di-sodium substituted alkoxide was not produced when double the molecular quantity of caustic soda was employed in the synthesis of alkoxide from glycerol, 1,2-propanediol and 1,3-propanediol. However, pure sodium metal and absolute alcohol (eg. ethanol) were used as the starting materials to derive mono-sodium glycerolate from glycerol (Gross, 1926). Subsequently, the crystals of mono-sodium glycerolate was triturated with more sodium ethoxide under absolute alcohol and boiled for several hours to produce di-sodium substituted compound.

This elaborate method for catalyst synthesis is both time consuming and costly as compared with the current method, which utilizes a less costly base, sodium hydroxide. According to Table 4.3, an assumption is made regarding deprotonation of

the primary hydroxyl group where a sodium ion is attached with *via* ionic bonding. The assumption is based on the observation that the primary hydroxyl group has a more polarized M-O bond than occurs when bonded with a secondary hydroxyl group. In these structures deprotonation occurs more easily. Deprotonation is accomplished by sodium ion displacement of the proton. Also important to alkoxide formation is the adoption of structural conformations where steric hindrance is minimized. For example, in 1,2-propanediol derived alkoxide, the presence of methyl group adjacent to the secondary hydroxyl group causes steric hindrance and thus sodium ion is more likely to attach to the terminal OH group. Nevertheless, single crystal structure of the alkoxide compounds is necessary to further verify such assumptions. Unfortunately, most of the alkoxide crystals (except sodium glycerolate and xylitolate) are not available to confirm the actual deprotonation and sodium ion displacement position.

Table 4.3 Estimated product composition (in mole) of polyol-derived sodium alkoxides by Excel solver program

Polyol type	2:1 (NaOH:alkoxide) mole ratio	3:1 (NaOH:alkoxide) mole ratio
Glycerol	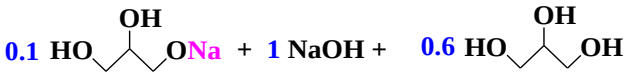	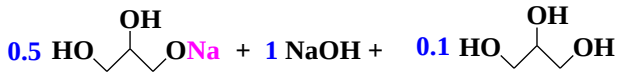
1,2-Propanediol	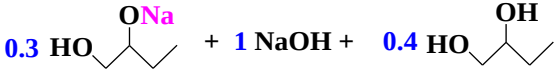	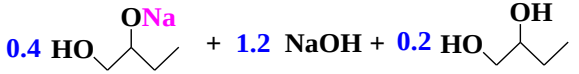
1,3-Propanediol	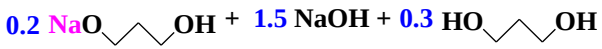	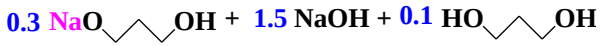
Xylitol	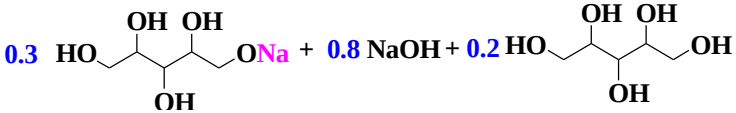	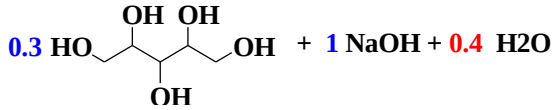
Sorbitol	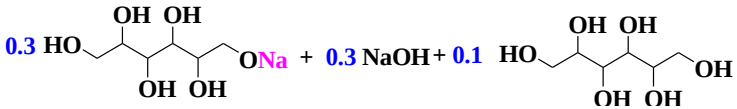	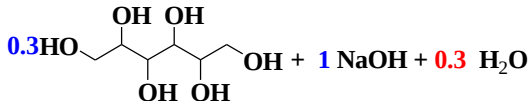

4.5 Connection to the Next Study

From this chapter, we reported a unique crystal structure of a sodium monoalkoxide of xylitol. The crystal structure of this novel compound was similar to that of the mono-sodium alkoxide of glycerol. The formation of these compounds presents a possible mechanism whereby polyols accelerate drying of sodium hydroxide solutions as was reported in chapter 3 of this thesis. It is likely that the formation of insoluble mono-alkoxides lowers the amount of dissolved solutes thus improving drying rates.

X-ray diffraction patterns and elemental analyses results indicate that all dried products of aqueous solutions of NaOH and polyol contained mixtures of mono-sodium alkoxide and hydroxide. It is likely that a portion of the sodium hydroxide occurred as an adduct with the polyol or the alkoxide and does not occur as crystalline sodium hydroxide. This novel group of strongly basic materials has never been reported previously and their efficiency as catalysts is unknown. In Chapter 5, the polyol-derived sodium alkoxide/hydroxide catalysts are described as catalysts for biodiesel production. The kinetics and biodiesel yield of transesterification reactions catalyzed by the new catalysts and sodium methoxide will be compared.

CHAPTER 5.
SODIUM ALKOXIDE/HYDROXIDE CATALYSTS IN TRANSESTERIFICATION REACTIONS

5.1 Abstract

Alkoxide/hydroxide catalysts prepared from solutions of sodium hydroxide and polyols at 3:1 mole ratio were efficient catalysts of transesterification of triglyceride (TG). Based on the amount of sodium hydroxide used in alkoxide catalyst production, just 0.36 wt % of NaOH by weight of TG was sufficient to produce a high yield of biodiesel. Reaction conditions were also strictly controlled at 6:1 (methanol to oil) mole ratio at 60°C. Under the specified condition these catalysts achieved reaction rates and yields similar or superior to those achieved with the conventional catalyst sodium methoxide, added at a constant mole ratio of sodium base to TG. At 2 min after the addition of the alcohol/ catalyst solution, the reactions achieved satisfactory yield (62.4 to 70.5 %) when compared to the sodium methoxide catalyst (62.4 %). After 1.5 h transesterification reactions, similar biodiesel yield is recorded for all catalysts (95 – 97 wt%). As a result, the product yield is similar for all catalysts, but the reactivity varied from among catalysts throughout the reaction. Comparison of the polyol-derived sodium alkoxide/hydroxide catalyst reactivity during initial stage of reaction at increasing order is as follows: sorbitol < xylitol < sodium methoxide < 1,2-propanediol < 1,3-propanediol < glycerol.

5.2 Hypothesis

Anhydrous sodium alkoxide base compounds produced by drying solutions of sodium hydroxide and polyols will efficiently catalyze TG transesterification reactions.

Alkoxide base will afford comparable or even better reaction rate and yield as compared to the commonly used homogeneous catalyst (sodium methoxide). Therefore, sodium alkoxide catalysts derived from polyols can be used as an alternative to sodium methoxide as a commercial alkali base.

5.3 Methods

5.3.1 Preparation of sodium methoxide solution

Fresh sodium methoxide solution is prepared by reacting sodium metal with dried methanol according to equation [5.1]. All glassware had undergone flame drying prior to use. Dried methanol was prepared by first refluxing methanol (Sigma Aldrich, Oakville, Canada) with anhydrous magnesium sulfate (EMD chemicals, Gibbstown USA) in a round bottom flask to minimize formation of sodium hydroxide. During drying the round bottom flask was connected to a condenser with a collecting flask and stopper. The reflux apparatus was flushed with argon gas for 15 min to eliminate all the air (moisture) before methanol reflux was initiated. The solvent was allowed to reflux at 60°C for 10 min before collecting the purified methanol in the sample flask.

$$2Na + 2\ CH_3OH \longrightarrow 2\ NaOCH_3 + H_2 \qquad [5.1]$$

A portion of sodium metal (Sigma Aldrich, Oakville, Canada) was cut and rinsed with hexane to remove excessive paraffin oil adhering to the metal. The metal (10.04g) was weighed quickly then placed in freshly distilled methanol (90.00 g) to afford a 31 wt% sodium methoxide solution in methanol. The resulting sodium methoxide solution (3.0484 g) was weighed and utilized as a catalyst in transesterification reactions. The weighed sodium methoxide solution contained 0.945g $NaOCH_3$ (0.0175 mol) in methanol.

5.3.2 Transesterification reactions

A kinetic study of the transesterification reaction of TG can elucidate parameters that determine the extent of a reaction at any given time under particular reaction conditions. The results can then be used to evaluate catalyst efficiency. All reactions were conducted at 60°C, 0.0175 mole sodium methoxide (equivalent to the mole concentration of base for all catalysts) and 6:1 mole ratio of methanol to TG. The weight of 1 mol TG was determined from the calculated average molecular weight of canola oil (885.46 g/mol) assuming canola oil was pure triolein (van Gerpen 2004). All glassware had undergone flame drying prior to use. Transesterification reactions were performed in a 500 mL three-necked flask equipped with a reflux condenser, a thermometer, and a sampling port. The flask was immersed in a constant temperature oil bath equipped with a temperature controller that was capable of maintaining the temperature within ±0.1 ° C. Agitation was provided with a magnetic stirrer, which was set at a constant speed (1000 rpm) throughout the experiment. Initially, the flask was filled with 193.00 g canola oil and heated to the desired temperature (60°C). A known amount of polyol-derived alkoxide (the catalyst prepared from 0.0175 mole sodium hydroxide) was dissolved in the required amount of methanol (42.00 g). This methanolic alkoxide was then injected into the reaction flask through a septum at sampling port at which point the reaction was assumed to have started. A timer was set to start simultaneously to record the reaction time for the kinetic study.

Samples (1 mL) were removed at regular intervals (0.5, 1, 2, 3, 4, 5, 6, 7, 8, 10, 15, 20, 25, 30, 60, 90 min) with a syringe (±0.01 mL). Each sample was neutralized immediately after removal using hydrochloric acid (1 N) to quench any ongoing reaction. The samples were then transferred to 5mm i.d. NMR tubes and deuterated chloroform ($CDCl_3$) was added to provide both a locking signal and small residual amount of chloroform, which acts as a reference for chemical shift. ^{1}H Nuclear Magnetic Resonance spectra (Bruker 500 MHz Avance NMR spectrometer, Milton Canada) were recorded (spectral width, 10,330.58 Hz; data points, 32,768; pulse width, 6.05 μs (90^o); pulse delay, 1.79 s and number of scans, 128). The raw free induction decay (fid) data were then converted into frequency domain by Fourier transform (ACD Labs version 11). The

yields for the transesterification reactions are obtained directly from the areas of the selected signals:

$$Y\% = 100 \times (2A_1/3A_2) \quad [5.2]$$

where A_1 = area of the methoxy group; and A_2 = area of the α-carbonyl methylene group (Gelbard *et al*., 1995). The NMR integration data was then analysed using data analysis software (OriginPro version 8.0; OriginLab Corporation; Northampton, USA) to enable analysis of biodiesel yield (wt%) versus time (in log scale, s). More details regarding quantification of fatty acid methyl ester are discussed in the literature review section 2.4.3.

Two-way analysis of variance (ANOVA) was conducted to assess whether the differences among sample means are statistically different at the three reaction phases. Phase I represents initial stage at the first minute; phase II range from 2 – 20 min; and phase III range from 20 – 90 min. The mathematical models are optimized using the Numerical Algorithms Group (NAG) functions as embodied in the OriginPro (version 8.0) data analysis software (OriginLab Corporation; Northampton, USA). Appendix E has detailed information of two-way ANOVA analysis including tables and means comparison results.

5.4 Results and Discussion

5.4.1 Comparisons of transesterification reactions catalyzed by sodium methoxide and sodium alkoxide/hydroxide derived from polyols

Transesterification is a three-step reversible reaction with each step initiated by an attack on the carbonyl carbon atom of the TG, DG or MG molecule by the methoxide ion ($^{-}OCH_3$). Ma and Hannah (1999) previously published mechanism for homogeneous base catalyzed transesterification of triglycerides (see Fig. 2.3). Similar to most homogeneous

base catalyzed reactions in methanol, the methoxide anion is the catalyst that enables the transesterification reaction (see Fig. 5.1).

In the current study, the catalysts are likely mixtures of alkoxides of polyols and sodium hydroxide. These alkaline mixtures react with methanol solution to produce methoxide anions. The quantity of methoxide anion released depends on the concentration of polyol alkoxide, and sodium hydroxide as well as the dissociation constant of these species in methanol. Due to the strong basicity of sodium, its dissociation constant is likely high. In this sense, the methoxide ion concentration depends directly on the alkoxide/hydroxide catalyst concentration.

The presence of polyols in large quantities is not desirable in the transesterification reaction as their presence might lead to the formation of polyol esters. Nevertheless, in the current study only small concentrations of polyols (<0.5 wt %) are added with the catalyst and, thus, reaction equilibrium should not be affected. The presence of polyols in small quantities might help to stabilize the immiscible oil/methanol phase by formation of emulsifiers such as diglyceride, monoglyceride or glycol esters, which could facilitate the transesterification reaction by enhancing the mixing of the two phases. In general, the base catalysed (0.5 wt% sodium methoxide) transesterification reactions at methanol:TG ratio of 6:1 using soybean and sunflower oils achieved 60 - 80% ester after 1 min of reaction time (Freedman *et al*., 1984).

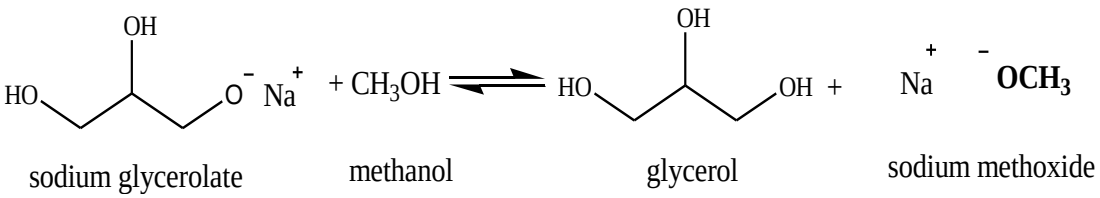

Fig. 5.1 Sodium glycerolate dissolves in methanol to produce methoxide ion as catalytic agent

Since the base catalyzed reaction occurs rapidly, it is reasonable to evaluate and compare the reaction efficiency during the first 2 minutes of reaction. According to Fig. 5.2, transesterification reactions catalyzed by sodium glycerolate/hydroxide produced similar biodiesel yield at 1:1, 2:1 and 3:1 mole ratio. However, the graph shows a lower reaction rate during the first 2 min of the reaction catalyzed by glycerolate compound (1:1 ratio) when compared to the other catalysts. Nevertheless, the glycerolate catalysts prepared with higher mole ratios of sodium hydroxide to glycerol have similar or better transesterification reaction rates and yield when compared with freshly prepared sodium methoxide. At 120 s (approximately log scale 2.1), the reactions have achieved satisfactory yield (sodium glycerolate/hydroxide 1:1, 62.4 wt%; 2:1, 68.7 wt%; 3:1, 68.7 wt%) when compared to the standard sodium methoxide catalyst (62.4 wt%).

The reaction rate and yield was similar for catalysts produced from 2:1 and 3:1 ratios of sodium hydroxide to 1,2-propanediol (PD) (see Fig. 5.3). The experimental data demonstrated that the efficiency of these catalysts was also comparable to sodium methoxide. The 1:1 compound of this glycol afforded 6% lower biodiesel yield after 1.5 h than catalysts produced with higher ratios of sodium hydroxide to glycol and sodium methoxide catalyzed reaction. At 120 s (log scale 2.08), the reactions achieved satisfactory yield (1,2-PD alkoxide/hydroxide 1:1, 65.4%; 2:1, 69.1%; 3:1, 70.5%) when compared to the sodium methoxide catalyst (62.4%). Similar to its isomer, 1,3-propanediol (Fig. 5.4) derived sodium alkoxide/hydroxide catalyst achieved similar biodiesel yield patterns and was comparable to the catalytic efficiency of sodium methoxide (see figure 18). At 120 seconds (log scale 2.08), the reactions attained satisfactory yield (1,3-PD alkoxide/hydroxide 1:1, 58.0%; 2:1, 72.1%; 3:1, 66.7%) as compared to the standard sodium methoxide catalyst (62.4%).

Alkoxide derived from three moles of sodium hydroxide solution and one of xylitol produced a similar yield of methyl ester after 1.5 h when compared to sodium methoxide and the reaction progressed at the same rate through the first 5 minutes of the reaction (see Fig. 5.5). The alkoxide/hydroxide compounds produced at 1:1 and 2:1

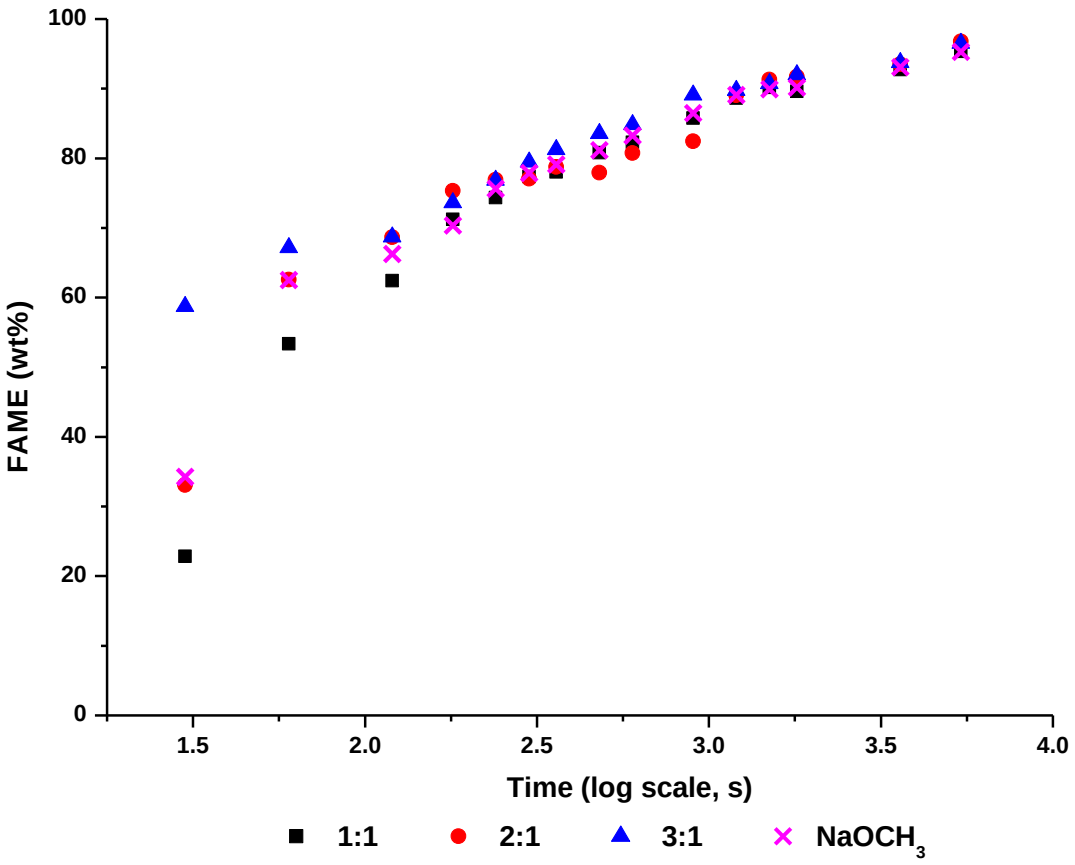

Fig. 5.2 Fatty acid methyl ester production (wt%) during the transesterification of canola oil (6:1 methanol to oil mole ratio at 60°C) catalyzed by glycerol derived sodium alkoxide/hydroxide and sodium methoxide;

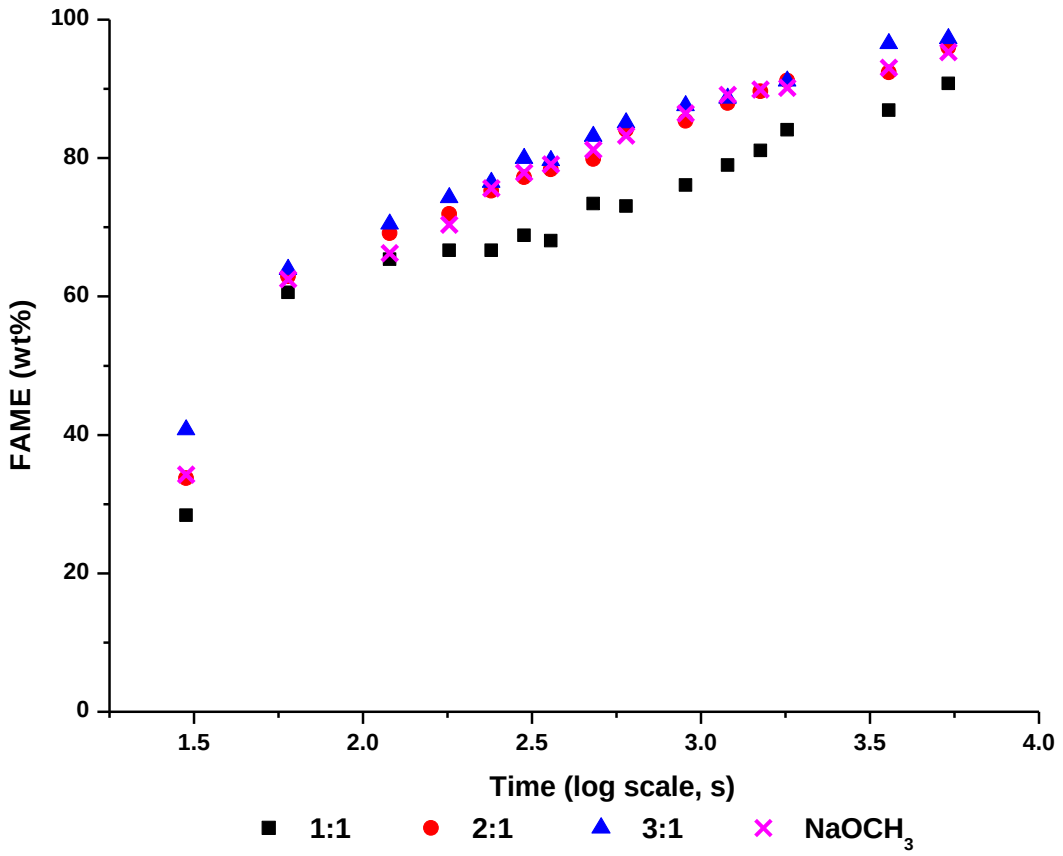

Fig. 5.3 Fatty acid methyl ester production (wt%) during the transesterification of canola oil (6:1 methanol to oil mole ratio at 60°C) catalyzed by 1,2-propanediol derived sodium alkoxide/hydroxide and sodium methoxide

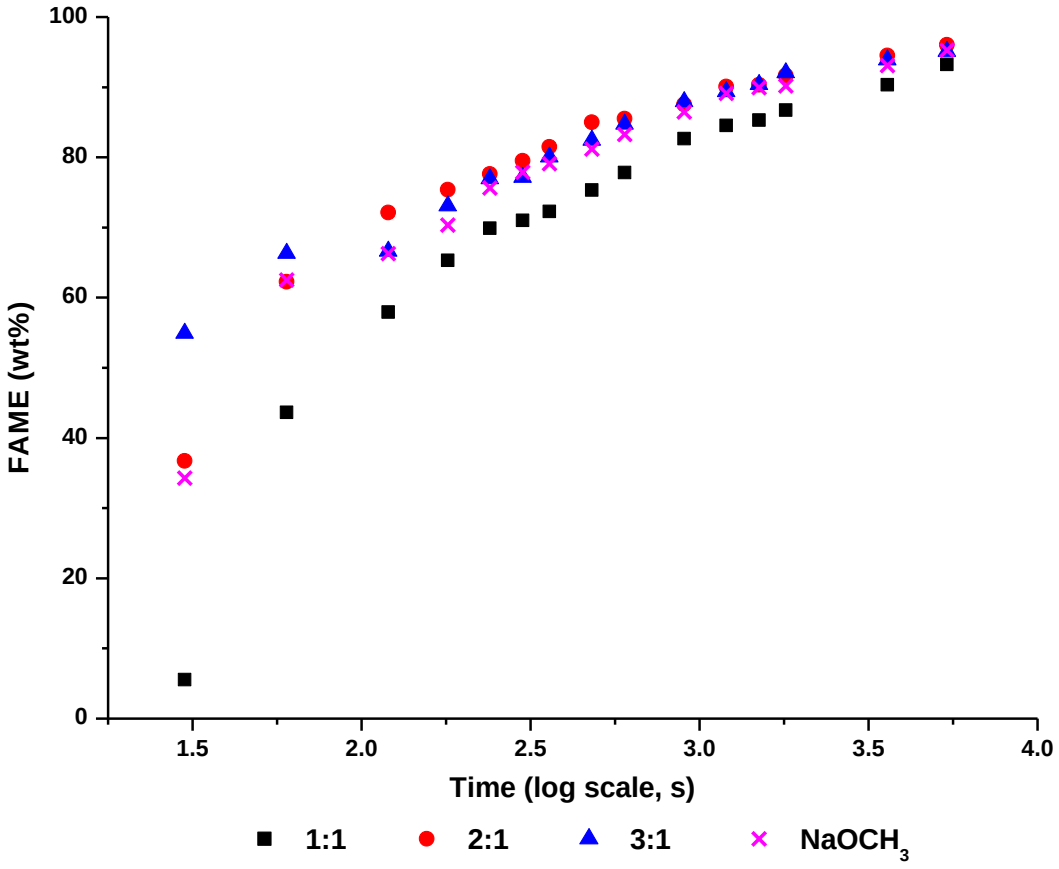

Fig. 5.4 Fatty acid methyl ester production (wt%) during the transesterification of canola oil (6:1 methanol to oil mole ratio at 60°C) catalyzed by 1,3-propanediol derived sodium alkoxide/hydroxide and sodium methoxide

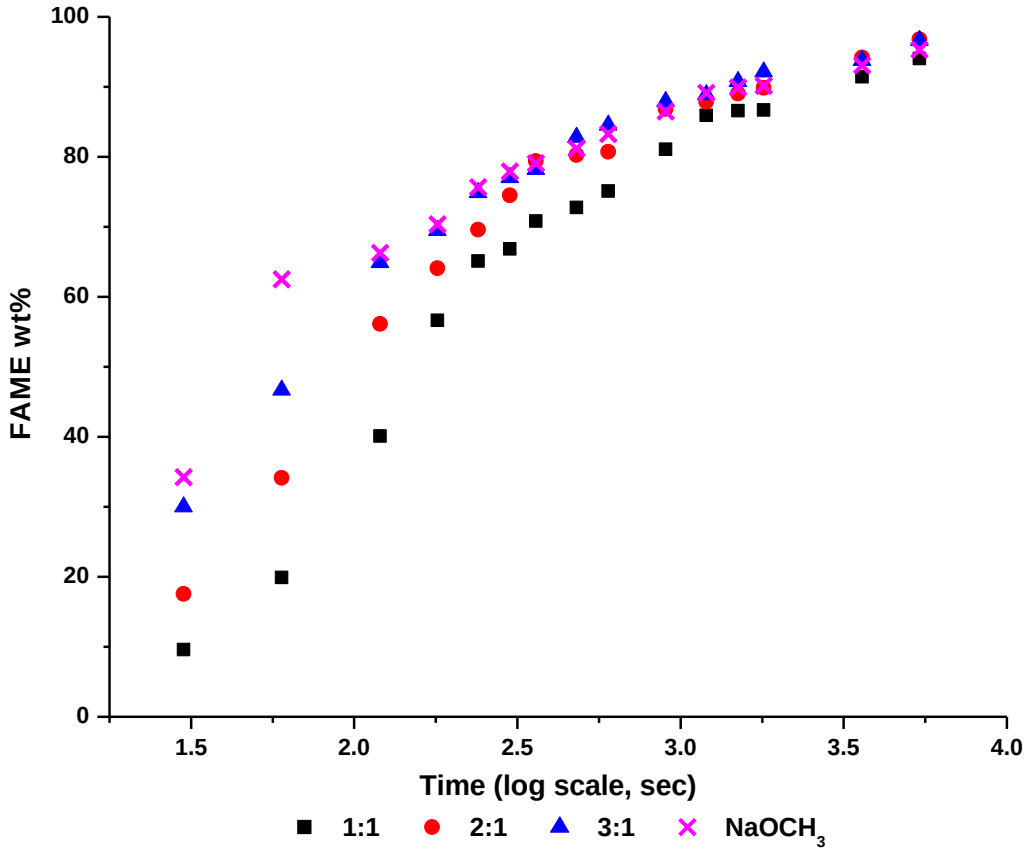

Fig. 5.5 Fatty acid methyl ester production (wt%) during the transesterification of canola oil (6:1 methanol to oil mole ratio at 60°C) catalyzed by xylitol derived sodium alkoxide/hydroxide and sodium methoxide

mole ratios produced less ester during the first 10 min of the reaction. For example at 120 s (log scale 2.08), the reactions had achieved relatively lower yield from xylitol alkoxide/hydroxide 1:1 (40.1 wt%) and 2:1 (56.1 wt%) compared to the standard sodium methoxide catalyst (62.4 wt%). Nevertheless, the reactions catalyzed by all three xylitol derived alkoxide catalysts produced comparable biodiesel yields (~95 wt%) compared with sodium methoxide after 1.5h.

The sorbitol derived sodium alkoxide/hydroxide demonstrated similar biodiesel yield trends to those observed for xylitol. All three alkoxide/hydroxide catalysts at different mole ratio had lower biodiesel yield as compared to sodium methoxide after 10 min of reaction (see Figure 5.6). Nevertheless, the reactions catalyzed by all sorbitol derived alkoxide/hydroxide catalysts achieved 95 wt% of the fatty acid methyl ester yield after 1.5 h. At 120 s (log scale 2.08), the reactions achieved relatively lower yields from sorbitol-alkoxide/hydroxide 1:1, 2:1 and 3:1 of 26.3 wt%, 52.1 wt% and 51.9 wt% respectively as compared to the standard sodium methoxide catalyst (62.4 wt%).

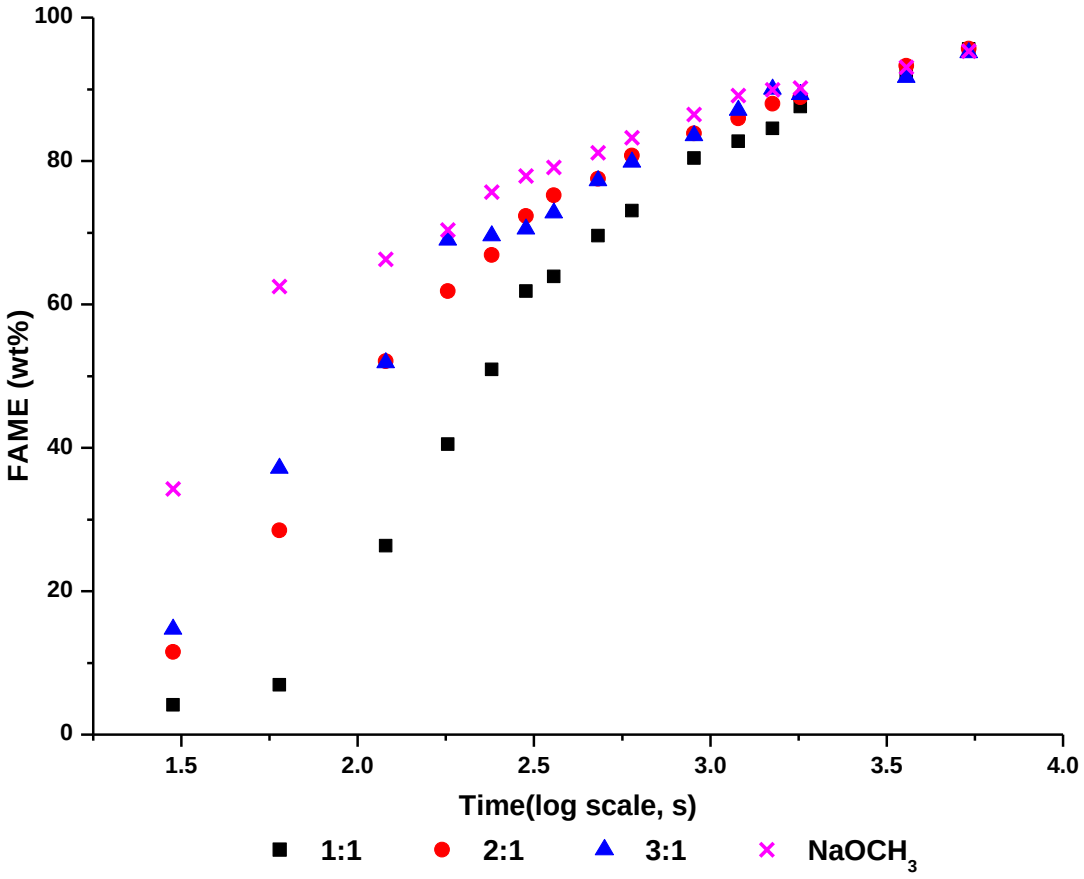

Fig. 5.6 Fatty acid methyl ester production (wt%) during the transesterification of canola oil (6:1 methanol to oil mole ratio at 60°C) catalyzed by sorbitol derived sodium-alkoxide/hydroxide and sodium methoxide

To conclude, the 3:1 and 2:1 catalysts of glycerol and glycols produced similar or superior reaction rate and yield when compared with sodium methoxide. The base compounds synthesized at 1:1 mole ratio of NaOH: polyol achieved relatively lower reaction rates and may not be preferred in biodiesel synthesis. Although the higher concentration of polyol helped drying process during catalyst synthesis, the transesterification reaction rate responds negatively to high ratios of polyol to sodium hydroxide. In general, the catalysts produced from higher polyols, sorbitol and xylitol, produced lower reaction rates than achieved by sodium methoxide. The 3 to 1 mole ratio of NaOH:Polyol has demonstrated consistently high performance in transesterification reaction as compared to catalysts synthesized at other mole ratios.

5.4.2 Comparison of catalytic reactivity

5.4.2.1 Biodiesel yield at different phases of transesterification

As described above sodium alkoxide catalysts prepared with 3:1 ratio NaOH to polyol consistently produced higher biodiesel yields in the initial reaction stage than catalysts prepared with lower ratios of NaOH to polyol. The reaction progress data (Fig.5.7) may be used to further evaluate catalytic reactivity and efficiency. An S-shape curve is often observed in a plot of ester percentage *vs*. time (Boocock *et al*., 1996). Slow ester formation initially, and prior to reaction completion, are effects of mass transfer limitations. In the current study, mass transfer limitation at the initial stages of the reactions was not apparent, possibly due to thorough mixing *via* mechanical stirring at 1000 rpm and heating. These aspects of the reaction conditions were sufficient to maintain effective mass transfer (Murugesan *et al*., 2009; Vicente *et al*., 2005). In the current study substrate concentration and other experimental conditions were held constant. Therefore, the slope of linear fit of percent methyl ester *vs.* log of time (Fig. 5.8) may be calculated to evaluate catalytic activity at each phase of the reaction: Phase I represents initial stage at the first minute; phase II range from 2 – 20 min; and phase III range from 20 – 90 min. As time proceeds, the reaction rate decreases significantly

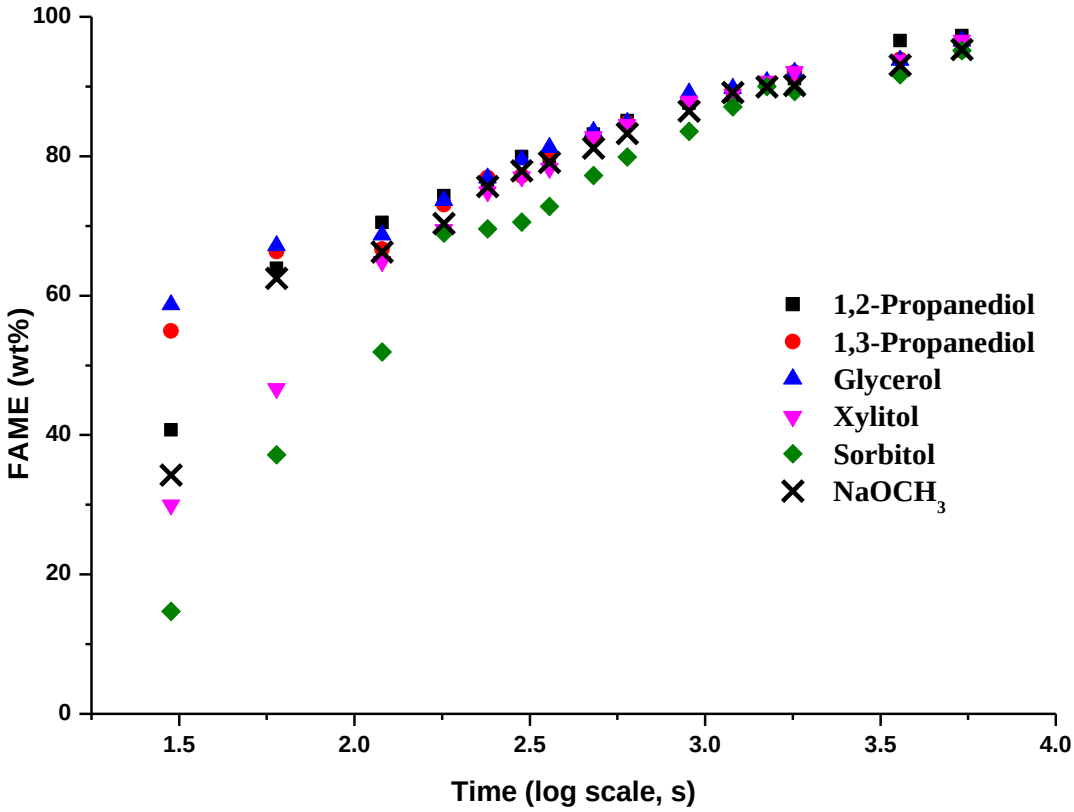

Fig. 5.7 Fatty acid methyl ester production (wt%) during the transesterification of canola oil (6:1 methanol to oil mole ratio at 60°C) catalyzed by polyol derived sodium alkoxide/hydroxide catalysts and sodium methoxide

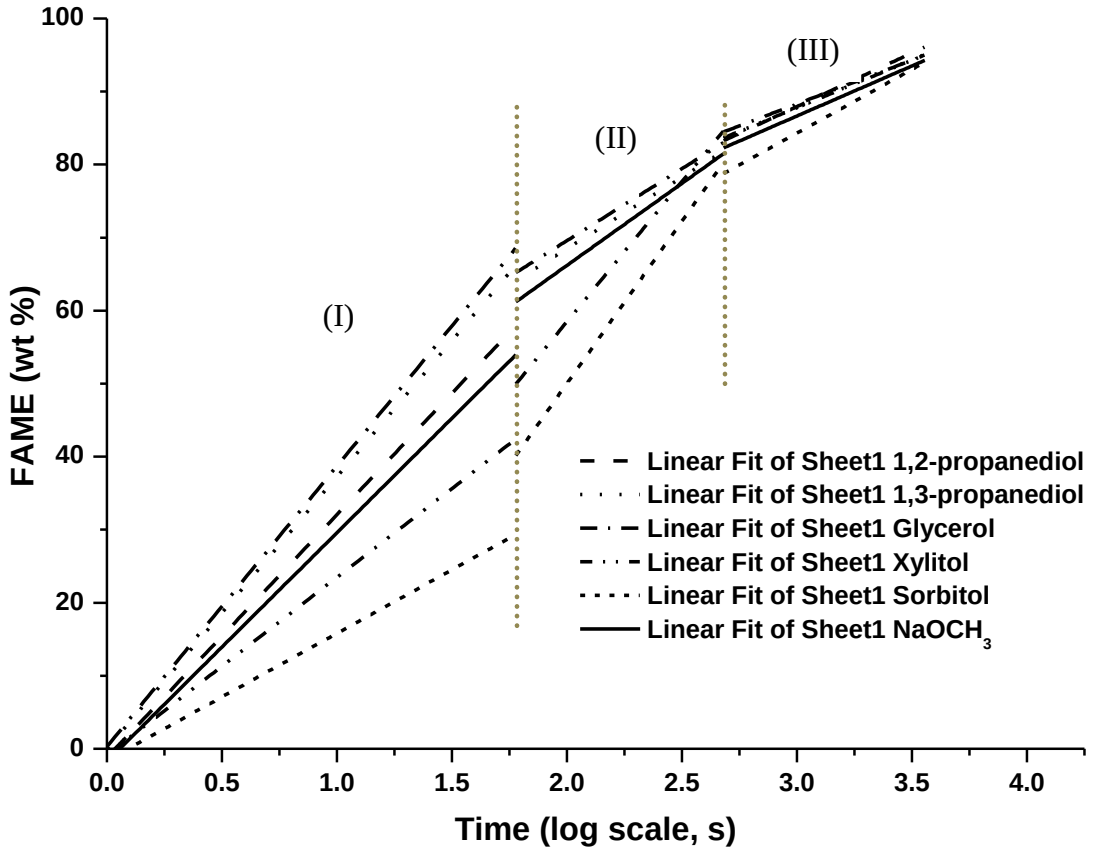

Fig. 5.8 Linear curve fit of biodiesel yield (in log scale, second). Transesterification (6:1 methanol to oil mole ratio at 60°C) catalyzed by various polyol-derived sodium alkoxide/hydroxide catalysts (3:1 mole ratio of NaOH: Polyol)

(decreasing slope from phase I to III) as a result of the depletion of substrate (oil and methanol) and catalyst concentration.

The slope of linear curve fit was directly proportional to the rate of reaction and hence, indicated the relative catalytic reactivity at a particular time. According to Table 5.1, comparison of the polyol-derived sodium alkoxide/hydroxide catalysts reactivity during initial stage of reaction at increasing order is as follows: sorbitol < xylitol < sodium methoxide < 1,2-propanediol < 1,3-propanediol < glycerol. At the beginning of the reaction, glycerol, 1,2- and 1,3-propanediol derived sodium alkoxide/hydroxide catalyzed reactions have achieved relatively higher biodiesel yield as compared to other alkoxide catalysts (~20 wt% higher than sodium methoxide catalyzed reaction). Increase yield can be attributed to the presence of glycerol (0.2 wt %) at the initial stage that potentially form monoacylglyceride (MG) and diacylglyceride (DG) compounds as a result of interesterification with the TG under alkaline conditions. (Bancquart *et al*., 2001; Martinello *et al*., 2005). The MG and DG have been known for their emulsifying properties due to the presence of both hydrophilic and hydrophobic moieties in their structures. A low concentration of emulsifying agent could stabilize the oil-methanol phase that would, in turn, facilitate the mixture of the two insoluble phases for the transesterification reaction. In addition, glycols (0.2 wt %) could also form monoesters which are emulsification agents with potential for promoting the mixing of oil with methanol (Shaw and Lo, 1994).

Alkoxide/hydroxides derived from sorbitol and xylitol induced relatively low reaction rates at the beginning of the reactions as compared to other polyols. The lower reaction rate may be associated with the polarity of the polyols. Given that xylitol and sorbitol have the highest number of hydroxyl groups per mole, the two compounds would be expected to preferentially reside in the more polar methanol phase. Consequently, interesterification of alkyl groups with TAG might be less pronounced than for smaller polyols. Thus these compounds would be less likely to produce a useful emulsifying agent.

Table 5.1 Statistical analysis of the linear curve fit of biodiesel yield

Sodium Alkoxide	**Slope I**	**R square I**	**Slope II**	**R square II**	**Slope III**	**R square III**
1,2-PD	33.27	0.9149	21.13	0.9902	13.79	0.9987
1,3- PD	37.26	0.9876	19.60	0.9060	11.70	0.9432
Glycerol	38.41	0.9964	19.72	0.9397	11.65	0.9198
Xylitol	24.34	0.9962	23.69	0.9422	12.55	0.9435
Sorbitol	17.41	0.9661	44.44	0.9113	16.18	0.8837
$NaOCH_3$	31.32	0.8148	22.46	0.9631	12.82	0.9360

However, as the reactions proceeded with time, the oil-methanol phases were thoroughly mixed *via* mechanical stirring and eventually the biodiesel reaction mixtures also achieved >95 wt % yield.

In stages II and III, sorbitol and xylitol derived base catalysts are more reactive than the other catalysts. This observation can be explained by comparing the remaining substrate concentration for each catalyst in the later stages of the reaction. Both xylitol and sorbitol catalyzed reactions are much slower than their counterparts at the beginning. Hence, the remaining substrate concentration is relatively higher than others in stage II and III. Therefore, reaction rate increased during these latter stages particularly when the oil-methanol phase was thoroughly mixed by external stirring. At the end of all transesterification reactions, similar biodiesel yield is recorded for all catalysts (95 – 97 wt%). As a result, the production yield is similar for all catalysts, but the reactivity varied from one to another throughout the process.

5.4.3 Two-way analysis of variance (ANOVA)

In this statistical model, the sample means were assessed based on two factors, the polyol type (Factor A) and sodium hydroxide to polyol ratio (Factor B). For the purpose of increasing the power of the statistical analysis data was grouped. The first group included lower polyols 1,2-propanediol and its isomer compound, 1,3-propanediol, which were used as replicates based on their similar structure. Similarly xylitol and sorbitol, both with more than three hydroxyl moieties, were grouped as replicates. Glycerol stood alone as the third group for comparison in this model. Factor B (catalyst ratio) was NaOH to polyol mole ratio (1:1, 2:1 and 3:1). The response data were the slope values of the linear curve fit of biodiesel product yield at each reaction phase vs the logarithm of time (Table E.1). The slope values were further adjusted (Table E.2) by considering the remaining substrate concentration for mean comparisons.

From two-way ANOVA analysis, the polyol type had the most significant impact ($p < 0.05$) during phase I of transesterification reaction. Alkoxide catalyst

synthesized from glycerol and diols (mean slope value of 0.31 and 0.29 respectively) are much more reactive than xylitol/sorbitol derived alkoxide (mean slope value of 0.14). As the reactions proceed to phase III, the catalyst type has no impact on the reaction as the mean slope values do not differ significantly ($p > 0.05$). In terms of catalyst ratio comparison, the effect is significant only at the initial stage of reaction. In phase I, catalysts prepared from 1:1 base to polyol mole ratio are much less reactive (mean slope value of 0.16) when compared to its counterpart synthesized from 2:1 and 3:1 mole ratio (mean value of 0.24 and 0.30, respectively). However, the data are not significantly different as the reactions proceed further. The ANOVA results also indicated that catalysts prepared from 2:1 and 3:1 mole ratio has similar reactivity throughout the reaction ($p < 0.05$).

5.4.4 Industry standard for base catalyst loading

Equivalent mole amounts of sodium methoxide (0.0175 mol; 0.5 wt %) and sodium hydroxide (0.0175 mol; 0.36 wt% in all polyol derived sodium alkoxide synthesis) were investigated in this research. Literature shows that catalyst loading for sodium hydroxide and sodium methoxide of 1 wt% and 0.5 wt%, respectively produce equivalent biodiesel yield under reaction conditions of 6:1 methanol to TG mole ratio at a temperature of 60°C (Freedman *et al*., 1984). Despite the sodium hydroxide loading used in this experiment being lower than the actual optimized value (1 wt %), the reactions catalyzed by the polyol derived sodium alkoxide have successfully achieved a comparable biodiesel yield with sodium methoxide at 0.5 wt %. Moreover, the alkoxide catalysts have successfully achieved high biodiesel yield (> 95 wt %) in a single stage transesterification reaction. In conclusion, the sodium alkoxide/hydroxide catalysts derived from polyols have demonstrated promising qualities for use by industry. These catalysts may serve as an alternative solution to lower the cost of biodiesel plant operation without compromising production efficiency.

CHAPTER 6.
GENERAL DISCUSSION

The results of this thesis support the concept that solutions of aqueous sodium hydroxide can used to produce catalysts that might displace sodium methoxide as the catalyst for industrial biodiesel production. The implications of this research on the biodiesel industry must be seen in context of the many effects of substituting 50 wt% aqueous sodium hydroxide for solutions of methanolic sodium methoxide (30 wt%). Cost comparison between 30 wt% sodium methylate and 50 wt% sodium hydroxide solutions in biodiesel production is presented in Table 6.1 (refer to Appendix F for calculation). In terms of the biodiesel catalyst cost, 50 wt % NaOH solution ($0.008/mole NaOH) is much less expensive than 30 wt% sodium methoxide solution ($0.128/mole NaOMe). By considering the total shipment charges, the cost of using aqueous NaOH solution will become even more economical.

This study has proven that polyols help in drying of sodium hydroxide and thus the catalyst loading of < 0.5 wt% is sufficient to produce biodiesel at an equivalent sodium methoxide concentration. In comparison, one shipping tank containing 100 tonnes of sodium hydroxide can produce 12,500 tonnes of biodiesel (0.4 wt% catalyst loading); whereas the equivalent shipment of 30 wt% sodium methoxide only produce 6,000 tonnes biodiesel (0.5 wt% catalyst loading) as presented in Table 6.1. Therefore, with the shipping advantage and effective drying of 50 wt% NaOH by polyols, development of these alkoxide/hydroxide compounds helps to reduce the cost of biodiesel catalyst without compromising the reaction efficiency.

In the future it is recommended that research into the production of alkoxides from polyols be expanded. For example, other group I metals, such as potassium and lithium, should be studied as should the formation of alkoxides from other polyols like

Table 6.1 Base catalyst cost per mole and biodiesel production capacity

Base catalysts	**Base Catalyst cost (per mole)**	**Biodiesel production capacity* (tonnes)**
30 wt% sodium methoxide	$ 0.128	6,000
50 wt% sodium hydroxide	$ 0.008	12,500

* per 100 tonnes of base catalysts used

erythritol, mannitol or ethylene glycol. The wide range of polyol reagents with unique structural conformation or ramification of alkyl group can be tailor-made to suit many specific applications for base-catalyzed organic reactions. In biodiesel production, glycerol recovered as a by-product may be purified and recycled for preparation of these potential base catalysts, meanwhile reducing the cost of biodiesel operation. A larger scale pilot plant study is recommended to investigate the economic feasibility for synthesis and application of these alkoxide/hydroxide catalysts.

CHAPTER 7.
GENERAL CONCLUSIONS

Alkoxide/hydroxide base catalysts prepared by heating sodium hydroxide solution and polyols under vacuum pressure have properties that are largely related to the polyols used in their production. Catalyst derived from 1,2-propanediol, glycerol and xylitol are hygroscopic, anhydrous white powders while the 1,3-propanediol-derived sodium alkoxide/hydroxide has an off-white and slightly yellowish color. Sorbitol-derived alkoxide/hydroxide is also white but has a glassy texture. Gravimetric analysis of water mass loss shows that drying under heat and vacuum removes all of the free water plus additional water of reaction of polyols (deprotonated hydroxyl group) and sodium hydroxide during formation of sodium alkoxide/hydroxide compounds.

Polyols aid the evaporation of aqueous base solutions. This is primarily due to the reaction of these polyols with the base to become insoluble complexes during drying. The drying rate is more rapid for higher molecular weight polyols like sorbitol and xylitol while lower molecular weight polyols glycerol, 1,2-propanediol, and 1,3-propadiol dried more slowly. The drying trend is influenced by the ability of the polyols to form ion-chelating complexes. The availability of vicinal hydroxyl groups plays an important role in formation of a stable metal-ion chelate. The study demonstrated the dehydration rate of 50 wt% aqueous NaOH solution added with polyols is, in decreasing order, xylitol> sorbitol> glycerol> 1,2-propanediol> 1,3-propanediol > NaOH control.

Several attempts were made to obtain single crystals of the sodium alkoxide compound from a series of polyol/base solutions at different mole ratios. Two crystals

were successfully derived and were suited for x-ray diffraction analysis. The colorless and monoclinic crystal of sodium glycerolate was identified with molecular formula $[Na(C_3H_7O_3)]n$ or $Na[H_2gl^-]$. Crystal derived from sodium xylitolate was colorless and has a rod shape. The molecular formula was recognised as $[Na(C_5H_{11}O_5)]n$ or $Na[H_4xl^-]$. Both H_2gl^- and H_4xl^- anion are basic ligand which has multiple functions in the molecular bonding. In general, the ionic Na-O bonding was found at C_1 where deprotonation occurs at the primary hydroxyl group. In addition, metal covalent expansion enabled formation of strong inter- and intra-molecular Na----O connections. Meanwhile, the ligands are linked to each other *via* strong O—H-----O hydrogen bonds. These strong inter- and intra-molecular bonds have stabilized the polymeric alkoxide structure. This thesis provides the first description of the synthesis of the xylitolate and its structure.

In powder diffraction analysis, diffraction patterns demonstrated that new materials were obtained from the synthesis steps since all alkoxide patterns differ from the original reagents. Nonetheless, presence of diffraction peaks corresponding to NaOH peaks indicates that the final compound may have incorporated NaOH as a crystal or as adducts. Sodium glycerolate/hydroxide powder, prepared by mixing 1 mole of aqueous sodium hydroxide with 1 mole of glycerol and drying the solution, produced a diffraction pattern that was indistinguishable from the pattern derived from the pattern projected to arise from a single crystal. Sorbitol derived alkoxide/hydroxide was an amorphous material that did not produce a useful diffraction pattern.

Elemental analysis has shown that the alkoxide compounds contain mono-sodium alkoxides that likely occur as adducts with sodium hydroxide. Analysis of elemental composition indicated that water was at most a minor component. Sodium glycerolate/hydroxide synthesized at base:poyol mole ratio of 3:1 was substantially anhydrous. The 1,3-propanediol sodium alkoxide/hydroxide had lower C and H content than theoretically possible. Evaporation of the polyol under the experimental conditions may have led to this observation. Curiously while 1,3-propanediol appeared to evaporate during the drying experiment, it’s molecular isomer (1,2-propanediol), which

has a relatively lower boiling point, did not. This may be explained by the vicinal hydroxyl groups in 1,2-propanediol. This structure produces an alkoxide chelate complex that is not volatile. The vicinal position of OH moieties favors metal chelation, which in turn prevents evaporation of the corresponding glycol.

Transesterification reactions catalyzed by sodium alkoxide/hydroxide catalysts (prepared at 2:1 and 3:1 mole ratio of sodium hydroxide to polyol) were observed to have similar reaction rates and yields when compared with reactions catalyzed by sodium methoxide (mole ratio of sodium base to TG being constant). The compounds synthesized at 1:1 base: alcohol ratio achieved relatively lower reaction rates. Generally, the yield of ester produced is similar for all catalysts approaching the end of reaction (after 1.5 hours), but the reactivity varied from one to another throughout the process. During the initial stages of reaction (first 2 min), sodium alkoxide/hydroxide catalyst strength in order of increasing reactivity is as follows: sorbitol < xylitol < sodium methoxide< 1,2-propanediol < 1,3-propanediol < glycerol. This result can be associated with release of these polyols in small quantity (<0.5%) as a result of methanol solvation to liberate the methoxide ion as catalytic agent. Presence of these polyols at the beginning of reaction may help to stabilize the immiscible oil/methanol phase by formation of emulsifier compounds (such as glycerol esters or glycol esters) that in return facilitate the transesterification reaction.

All polyol-derived alkoxide/hydroxide catalysts investigated in these studies were capable of achieving >95 wt% of biodiesel yield after 1.5 h in a single step transesterification reaction. Literature shows that catalyst loading for sodium hydroxide and sodium methoxide of 1 wt% and 0.5 wt%, respectively produce equivalent biodiesel yield under reaction conditions of 6:1 methanol to TG mole ratio at a temperature of 60°C (Freedman *et al*., 1984). Despite the sodium hydroxide loading (0.36 wt%) used to prepare the polyol alkoxide/hydroxide being lower than the actual optimized value (1 wt %), the reactions catalyzed by the polyol derived sodium alkoxide have successfully achieved a comparable biodiesel yield with sodium methoxide at 0.5 wt %.

LIST OF REFERENCES

Allred, A. L. (1961). Electronegativity values from thermochemical data. *Journal of Inorganic and Nuclear Chemistry*, *17*(3-4), 215-221.

Bancquart, S., Vanhove, C., Pouilloux, Y., and Barrault, J. (2001). Glycerol transesterification with methyl stearate over solid basic catalysts: I. Relationship between activity and basicity. *Applied Catalysis A: General*, *218*(1-2), 1-11.

Basu, H. N., and Norris, M. E. (1996). Process for production of esters for use as a diesel fuel substitute using a non-alkaline catalyst. US Patent 5,525,126

Bender, M. L. (1960). Mechanisms of catalysis of nucleophilic reactions of carboxylic Acid Derivatives. *Chemical Reviews*, *60*(1), 53-113.

Bochu, J. L. (2004). POUDRIX-MP:Multiphases version of POUDRIX-V2. *Powder diffraction diagram simulation program for standard X ray source, synchrotron radiation or neutrons.* : Laboratoire des Matériaux et du Génie Physique, Ecole Nationale Supérieure de Physique de Grenoble (INPG).

Boocock, D. G. B., Konar, S. K., Mao, V., and Sidi, H. (1996). Fast one-phase oil-rich processes for the preparation of vegetable oil methyl esters. *Biomass and Bioenergy*, *11*(1), 43-50.

Bradley, D. C. (1958). A structural theory for metal alkoxide polymers. *Nature 182*(4644), 1211-1214

Bradley, D. C. (1960). Progress in Inorganic Chemistry. *F. A. Cotton*, vol. 2 (pp. 303-361). New York: Interscience publishers.

Bradley, D. C. (1989). Metal alkoxides as precursors for electronic and ceramic materials. *Chemical Reviews*, *89*(6), 1317-1322.

Bradley, D. C. (2001). *Alkoxo and aryloxo derivatives of metals*. San Diego: Academic Press.

Bradley, D. C., Mehrotra, R. C., and Gaur, D. P. (1978). *Metal alkoxides*. London ; New York: Academic Press.

Brinker, C. J., and Scherer, G. W. (1990). *Sol-gel science : the physics and chemistry of sol-gel processing*. Boston: Academic Press.

Budavari, S. (1996). *The Merck index : an encyclopedia of chemicals, drugs, and biologicals*. Whitehouse Station, NJ: Merck.

Budavari, S. (1989). *The Merck index : an encyclopedia of chemicals, drugs, and biologicals*. Rahway, U.S.A.: Merck.

Cole-Hamilton, D. J., and Tooze, R. P. (2006). *Catalyst separation, recovery and recycling chemistry and process design*. Dordrecht: Springer.

Crabtree, R. H. (2009). *The organometallic chemistry of the transition metals*. Hoboken, N.J.: Wiley.

Creighton, H. J. (1926). Process for electrolytically reducing sugars to alcohol. US Patent 1,612,361

Darnoko, D., and Cheryan, M. (2000). Kinetics of palm oil transesterification in a batch reactor. *Journal of the American Oil Chemists' Society*, *77*(12), 1263-1267.

Dasari, M. A., Kiatsimkul, P. P., Sutterlin, W. R., and Suppes, G. J. (2005). Low-pressure hydrogenolysis of glycerol to propylene glycol. *Applied Catalysis A: General*, *281*(1-2), 225-231.

Dimmig, T., Radig, W., Knoll, C., and Dittmar, T. (1999). 13C-NMR Spektroskopie zur Bestimmung von

Dong, C. (1999). PowderX. Beijing, China, Institute of Physics, Chinese Academy of Sciences. Umsatz und Reaktionskinetik der Umesterung von Triglyceriden zu Methylestern. *Chem. Tech. (Leipzig)*, *1*(51), 326–329.

Drakin, S. I., Kurmalieva, R. K., and Karapet'yants, M. K. (1967). Methanol solvates of alkali metal methoxides. *Theoretical and Experimental Chemistry*, *2*(1), 40-44.

Engelhaupt, E. (2007). Biodiesel boom creates glut of glycerin. *Environmental Science & Technology*, *41*(15), 5175-5175.

Fairbourne, A. T. H. (1921). A monosodium glyceroxide: its structure and application. *Journal of Chemical Society. Trans.*, *119*, 1035-1040.

Farrugia, L. (1999). WinGX suite for small-molecule single-crystal crystallography. *Journal of Applied Crystallography 32*(4), 837-838.

Feuge, R., and Gros, A. (1949). Modification of vegetable oils. VII. Alkali catalyzed interesterification of peanut oil with ethanol. *Journal of the American Oil Chemists' Society*, *26*(3), 97-102.

Fisher, N., and McElvain, S. M. (1934). The Acetoacetic Ester Condensation. VII. The Condensation of Various Alkyl Acetates. *Journal of the American Chemical Society*, *56*(8), 1766-1769.

Forcrand, D. (1887). Bibasic glyceroxide. *Comt. Rend, 106*, 665-667.

Forcrand, D. (1887). Polybasic glyceroxide. *Compt. Rend., 107*, 269-272.

Fraser-Reid, B. O., Tatsuta, K., Thiem, J., Allscher, T., Klüfers, P., and Mayer, P. (2008). Carbohydrate-Metal Complexes: Structural Chemistry of Stable Solution Species. *Glycoscience* (pp. 1077-1139): Springer Berlin Heidelberg.

Freedman, B., Butterfield, R., and Pryde, E. (1986). Transesterification kinetics of soybean oil 1. *Journal of the American Oil Chemists' Society*, *63*(10), 1375-1380.

Freedman, B., Pryde, E., and Mounts, T. (1984). Variables affecting the yields of fatty esters from transesterified vegetable oils. *Journal of the American Oil Chemists' Society*, *61*(10), 1638-1643.

Gelbard, G., O. Brès, R.M. Vargas, F. Vielfaure, and Schuchardt, U. F. (1995). 1H Nuclear Magnetic Resonance Determination of the Yield of the Transesterification of Rapeseed Oil with Methanol. *Journal of the American Oil Chemists' Society*, *72*, 1239–1241.

Ghesti, G. F., de Macedo, J. L., Resck, I. S. S., Dias, J. A., and Dias, S. l. C. u. L. (2007). FT-Raman Spectroscopy Quantification of Biodiesel in a Progressive Soybean Oil Transesterification Reaction and Its Correlation with ^{1}H NMR Spectroscopy Methods. *Energy & Fuels*, *21*(5), 2475-2480.

Gjaldbaek, J. C. (1948). On the reaction between carbon monoxide and alcohol catalyzed by alcoholate; the propyl- and butyl alcohols; the solubility of carbon monoxide in secondary and tertiary butyl alcohol. *Acta chemica Scandinavica*, *2*(8), 683-692.

Granjo, J. F. O., Duarte, B. P. D., Oliveira, N. M. C., Rita Maria, C. A. O. d. N., and Evaristo, C. B. Jr. (2009). Kinetic models for the homogeneous alkaline and acid catalysis in biodiesel production. *Computer Aided Chemical Engineering*, vol. Volume 27 (pp. 483-488): Elsevier.

Gross, F. C. (1926). A new method for the preparation of alkali glyceroxides. *Soc. Chem. Ind.*, 320T - 321T.

Gyurcsik, B., and Nagy, L. (2000). Carbohydrates as ligands: coordination equilibria and structure of the metal complexes. *Coordination Chemistry Reviews*, *203*(1), 81-149.

Haas, T., Neher, A., Arntz, D., Klenk, H., and Girke, W. (1995). Process for the production of 1,2 and 1,3-propanediol. US Patent 5, 426, 249

Halbig, P. (1931). Process of preparing alkali metal aliphatic monohydroxy alcoholates. US Patent 1,910,331

Horn, M., and Horns, U. (2000). Alkoxides, Metal. *Kirk-Othmer Encyclopedia of Chemical Technology*: John Wiley & Sons, Inc.

Huheey, J. E. (1971). Electronegativity, acids, and bases. IV. Concerning the inductive effect of alkyl groups. *The Journal of Organic Chemistry*, *36*(1), 204-205.

Kapicak, L. A., and Schreck, D. J. (2008). Biodiesel process and catalyst therefor. US 2010/0048941 A1

Karabinos, J. V., and Ballun, A. T. (1953). Direct Reduction of Aldoses and Ketoses by Raney Nickel. *Journal of the American Chemical Society*, *75*(18), 4501-4502.

Kelsey, D. R. (1994). Purification of 1,3-propanediol. US Patent 5,527,973.

Knothe, G. (2000). Monitoring a progressing transesterification reaction by fiber-optic near infrared spectroscopy with correlation to ¹H nuclear magnetic resonance spectroscopy. *Journal of the American Oil Chemists' Society*, *77*(5), 489-493.

Kohno, S., Yamatsu, I., and Ueyama, S. (1971). Preparation of Xylitol. US Patent 3,558,725

Kool, C. M. H., Westen, H. A. V., and Hartstra, L. (1952). Process of the hydrolytic hydrogenation of carbohydrates in an acid medium. US Patent 2,609,39

Kramis, C. J. (1959). Production of sodium methoxide. US Patent 2,877,274

Krisnangkura, K., and Simamaharnnop, R. (1992). Continuous transmethylation of palm oil in an organic solvent. *Journal of the American Oil Chemists' Society*, *69*(2), 166-169.

Kyrides, L. P. (1929). Alkali metal alcoholates. US Patent 1,712,830

Lawrance, G. A., Robertson, M. J., Sutrisno, and von Nagy-Felsobuki, E. I. (2002). Complexation of a four-strand tetraalcohol with labile metal ions probed by electrospray mass spectrometry. *Inorganica Chimica Acta*, *328*(1), 159-168.

Lawson, M. E. (2000). *Sugar Alcohols*. John Wiley & Sons, Inc.

Leeuwen, P. W. N. M. (2004). Homogeneous catalysis understanding the art. (pp. xiii, 407 p.). Dordrecht ; Boston: Kluwer Academic Publishers.

Letts, E. A. (1872). Ueber eine Verbindung von natrium mit Glycerin. *Ber.*, *5*, 159.

Liebig, J. (1837). Ueber die Aethertheorie, in besonderer Rücksicht auf die vorhergehende Abhandlung Zeise's. *Annalen der Pharmacie*, *23*(1), 12-42.

Liu, K.-S. (1994). Preparation of fatty acid methyl esters for gas-chromatographic analysis of lipids in biological materials. *Journal of the American Oil Chemists' Society*, *71*(11), 1179-1187.

Loder, D. J., and Lee, D. D. (1939). Preparation of alkali metal alkoxides. US Patent 2,278,550

Ludwig, S., and Manfred, E. (1997). Preparation of 1, 2-propanediol. US Patent 5,616,817

Ma, F., Clements, L. D., and Hanna, M. A. (1998). The effect of catalyst, free fatty acids, and water on Transesterification of beef tallow. *Transactions of the ASABE*, vol. 41(5) (pp. 1261-1264).

Ma, F., and Hanna, M. A. (1999). Biodiesel production: a review. *Bioresource Technology*, *70*(1), 1-15.

Marjanovic, A. V., Stamenkovic, O. S., Todorovic, Z. B., Lazic, M. L., and Veljkovic, V. B. (2010). Kinetics of the base-catalyzed sunflower oil ethanolysis. *Fuel*, *89*(3), 665-671.

Martinello, M. A., Molina, F., and Pramparo, M. (2005). Purification of crude monoglycerides by two stages molecular distillation. *2nd Mercosur Congress on Chemical Engineering*. Rio de Janeiro, Brazil.

McCabe, W. L., Smith, J. C., and Harriott, P. (1993). *Unit operations of chemical engineering*. New York: McGraw-Hill.

Mehrotra, R. C. (1988). Synthesis and reactions of metal alkoxides. *Journal of Non-Crystalline Solids*, *100*(1-3), 1-15.

Meyer, R. H., and Johnson, A. K. (1957). Method for making anhydrous alkali metal alcoholates. US Patent 2,796,443

Mills, J. A. (1962). Association of polyhydroxy compounds with cations in solution. *Biochemical and biophysical research communications 6*, 418-421.

Moore, W. J. (1962). *Physical chemistry*. Englewood Cliffs, N.J.: Prentice-Hall.

Morgenstern, M., Cline, J., Meyer, S., and Cataldo, S. (2006). Determination of the kinetics of biodiesel production using proton nuclear magnetic resonance spectroscopy (1H NMR). *Energy & Fuels, 20*(4), 1350-1353.

Morrison, L. R. (2000). *Glycerol*. John Wiley & Sons, Inc.

Murugesan, A., Umarani, C., Chinnusamy, T. R., Krishnan, M., Subramanian, R., and Neduzchezhain, N. (2009). Production and analysis of bio-diesel from non-edible oils--A review. *Renewable and Sustainable Energy Reviews*, *13*(4), 825-834.

Turnova, N.Y. and Novoselova, A. V. (1965). Alcohol derivatives of the alkali and alkaline earth metals, magnesium, and thallium (I). *Russian Chemical Reviews*, *34*(3), 161.

Noiroj, K., Intarapong, P., Luengnaruemitchai, A., and Jai-In, S. (2009). A comparative study of KOH/Al2O3 and KOH/NaY catalysts forbiodiesel production *via* transesterification from palm oil. *Renewable Energy 34*(4),1145-1150.

Olson, E. T., and Twining, R. H. (1931). Method for making alkali metal alcoholates. US Patent 1,978,647

Onishi, H., and Suzuki, T. (1969). Microbial production of xylitol from glucose. *Applied and Environmental Microbiology*, *18*(6), 1031-1035.

Parsons, T. E. (2000). *Glycols, Other Glycols*. John Wiley & Sons, Inc.

PospIsilová, M., Polásek, M., and Procházka, J. (1997). Separation and determination of pharmaceutically important polyols in dosage forms by capillary isotachophoresis. *Journal of Chromatography A, 772*(1-2), 277-282.

Reaney, J. T., Liu, Y. D., and Westcott, N. D. (2002). Method for commercial preparation of conjugated linoleic acid. US Patent 6,414,171

Reaney, M., Shen, J., and Soveran, D. W. (2010). Process for the production of polyol base catalysts. US 2010/0305344 A1

Reaney, M. J. T., and Westcott, N. D. (2007). Methods for preparation and use of strong base catalysts. WO 2007/022621 A2

Rendleman, J. A. (1966). Alkali Metal Complexes of Carbohydrates. I. Interaction of alkali metal salts with carbohydrates in alcoholic media. *The Journal of Organic Chemistry*, *31*(6), 1839-1845.

Rendleman, J. A. (1967). Complexes of Alkali Metals and Alkaline-Earth Metals with Carbohydrates. *Advances in Carbohydrate Chemistry*, vol. Volume 21 (pp. 209-271): Academic Press.

Saka, S., and Kusdiana, D. (2001). Biodiesel fuel from rapeseed oil as prepared in supercritical methanol. *Fuel*, *80*(2), 225-231.

Rich, H. W., Hegetschweiler, K., Streit, H. M., Erni, I., and Schneider, W. (1991). Mononuclear, oligonuclear and polynuclear iron(III) complexes with polyalcohols formed in alkaline aqueous media. *Inorganica Chimica Acta*, *187*(1), 9-15.

Schatte, G., Shen, J. H., Reaney, M., and Sammynaiken, R. (2010). Poly[μ]-2,3-dihydroxypropan-1-olato-sodium]. *Acta Crystallographica Section E*, *66*(6), m634-m635.

Schatte, G., Shen, J. H., Reaney, M., and Sammynaiken, R. (2011). Poly[-(1,3-dihydroxypropan-2-olato)-potassium]. *Acta Crystallographica Section E*, *67*(2), m141-m142.

Sharma, Y. C., Singh, B., and Upadhyay, S. N. (2008). Advancements in development and characterization of biodiesel: A review. *Fuel*, *87*(12), 2355-2373.

Shaw, J.-F., and Lo, S. (1994). Production of propylene glycol fatty acid monoesters by lipase-catalyzed reactions in organic solvents. *Journal of the American Oil Chemists' Society*, *71*(7), 715-719.

Srivastava, A., and Prasad, R. (2000). Triglycerides-based diesel fuels. *Renewable and Sustainable Energy Reviews*, *4*(2), 111-133.

Stehr, H. (1967). Neubestimmung der Kristallstrukturen des dimorphen Natriumhydroxids, NaOH, bei verschiedenen Temperaturen mit Röntgenstrahl- und Neutronenbeugung. *Zeitschrift für Kristallographie*, *125*(125), 332-359.

Thamsen, J. (1952). The acidic dissociation constants of glucose, mannitol and Ssorbitol, as measured by means of the hydrogen electrode and the glass electrode at 0 degrees and 18 degrees C. *Acta Chem. Scand.*, 270-284.

Tower, R. S. (1963). Processes for preparing organo-metallic compounds. US Patent 3,094,546

Turova, N. Y. (2002). *The chemistry of metal alkoxides*. Boston: Kluwer Academic Publishers.

Turova, N. Y., and Novoselova, A. V. (1965). Alcohol derivatives of the alkali and akaline earth metals, magnesium, and thalium(I). *Russian Chemical Reviews*, *34*(3), 161.

Ullmann, F. (1953). Enzyklopadie der technischen chemie. vol. 3 (p. 280). Munchen: Urban and Schwarzenberg.

van Gerpen, J. V., Shanks, B., pruszko, R., Chements, D., and Knothe, G. (2004). Biodiesel Production Technology. (pp. 1-22). Colarado: National Renewable Energy Laboratory.

Vicente, G., Martínez, M., and Aracil, J. (2004). Integrated biodiesel production: a comparison of different homogeneous catalysts systems. *Bioresource Technology*, *92*(3), 297-305.

Vicente, G., Martínez, M., Aracil, J., and Esteban, A. (2005). Kinetics of sunflower oil methanolysis. *Industrial & Engineering Chemistry Research*, *44*(15), 5447-5454.

Weiss, E. (1993). Structures of organo alkali metalcomplexes and related compounds. *Angewandte Chemie International Edition in English*, *32*(11), 1501-1523.

Wheatley, P. J. (1960). A physicochemical investigation of the methoxides of lithium, sodium, and potassium. *Journal of Chemical Society*, 4270- 4274.

Wright, J. D., and Sommerdijk, N. A. J. M. (2001). *Sol-gel materials : chemistry and applications*. Amsterdam: Gordon and Breach Science Publishers.

APPENDIX A

POWDER DIFFRACTION DATA AND IMAGES

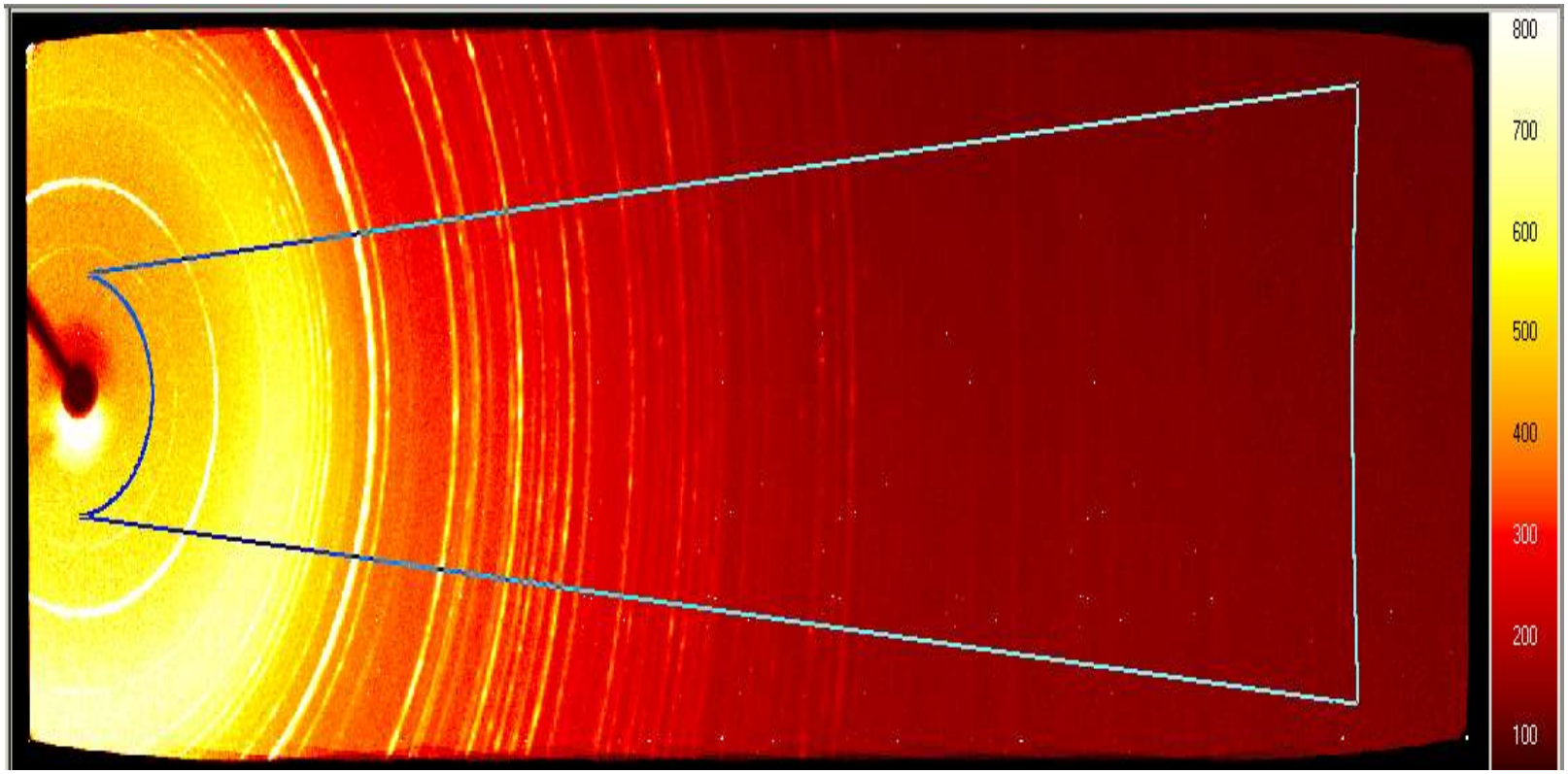

Fig. A.1 Powder Diffraction Images for Sodium glycerolate at 3:1 mole ratio

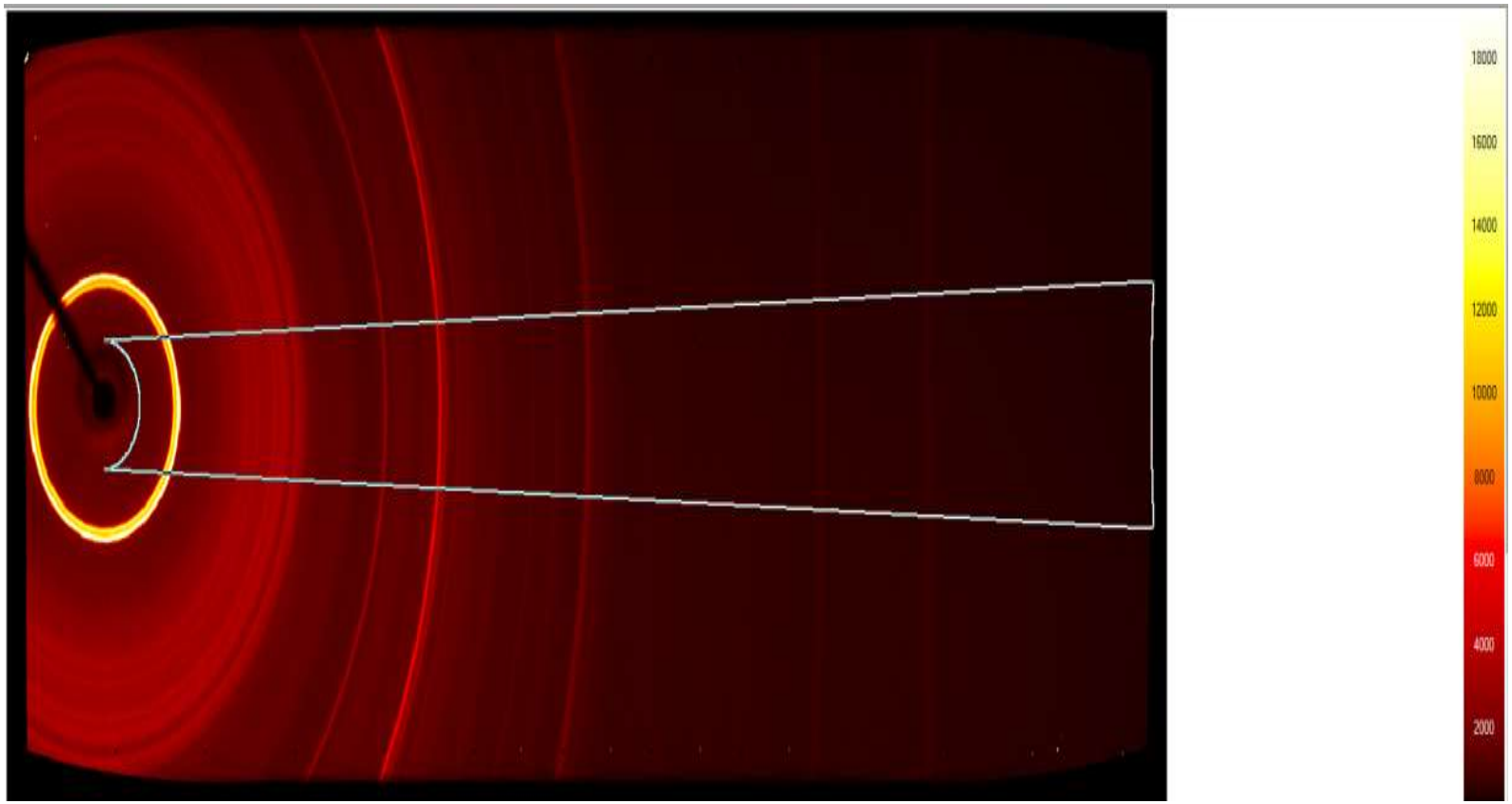

Fig.A.2 Powder Diffraction Images for 1,2-Propanediol derived Sodium alkoxide at 3:1 mole ratio

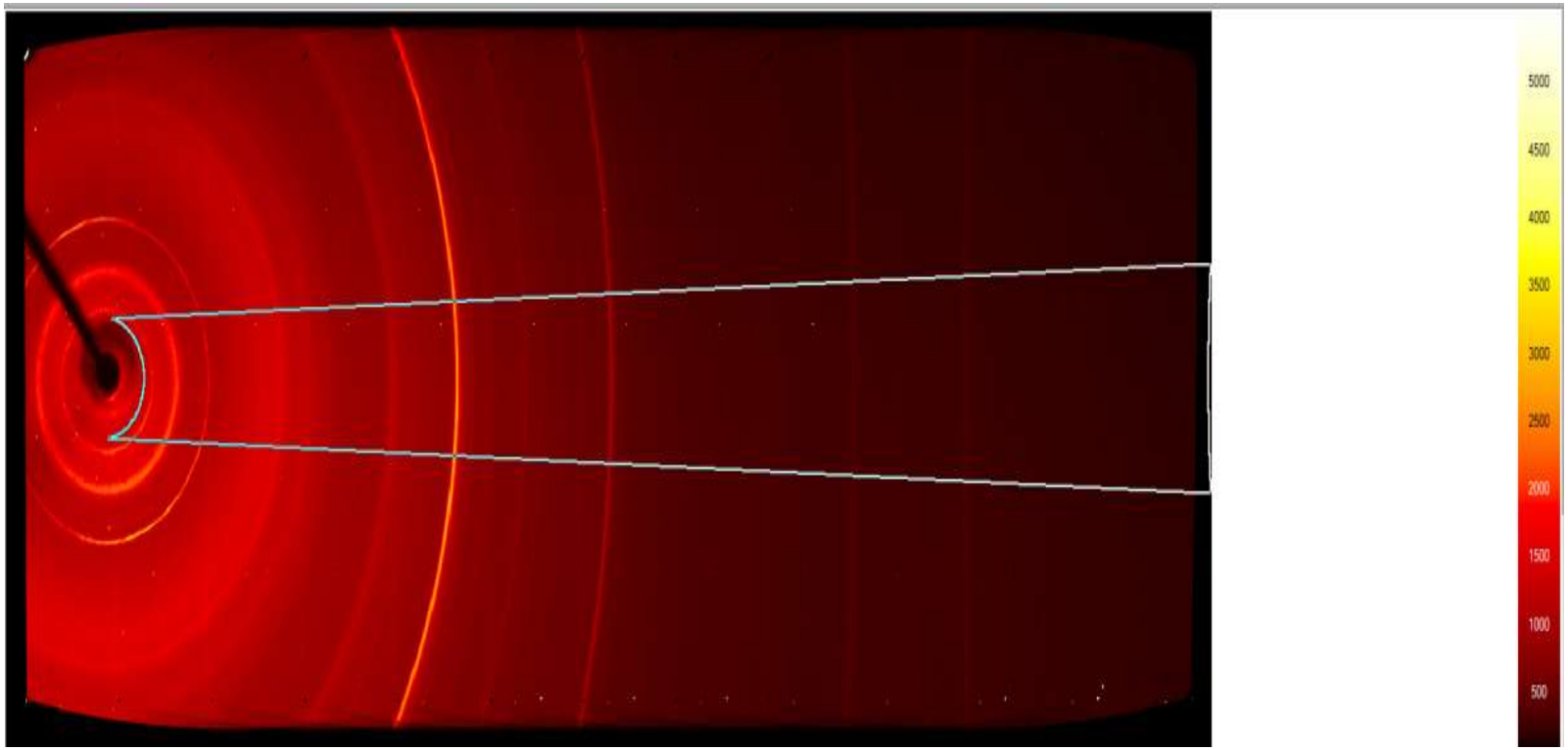

Fig.A.3 Powder Diffraction Images for 1,3-Propanediol derived Sodium alkoxide at 3:1 mole ratio

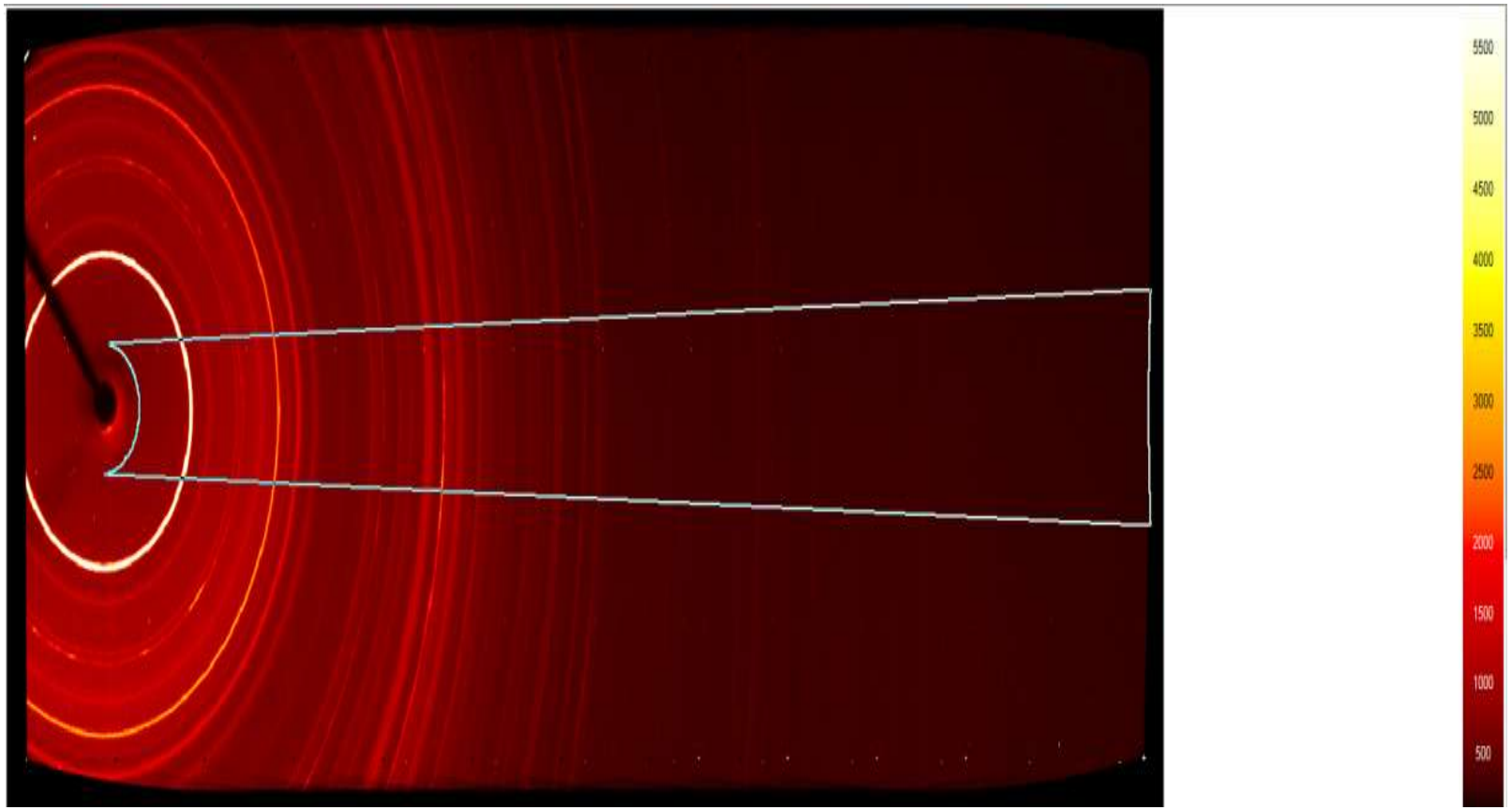

Fig. A.4 Powder Diffraction Images for xylitol derived Sodium alkoxide at 3:1 mole ratio

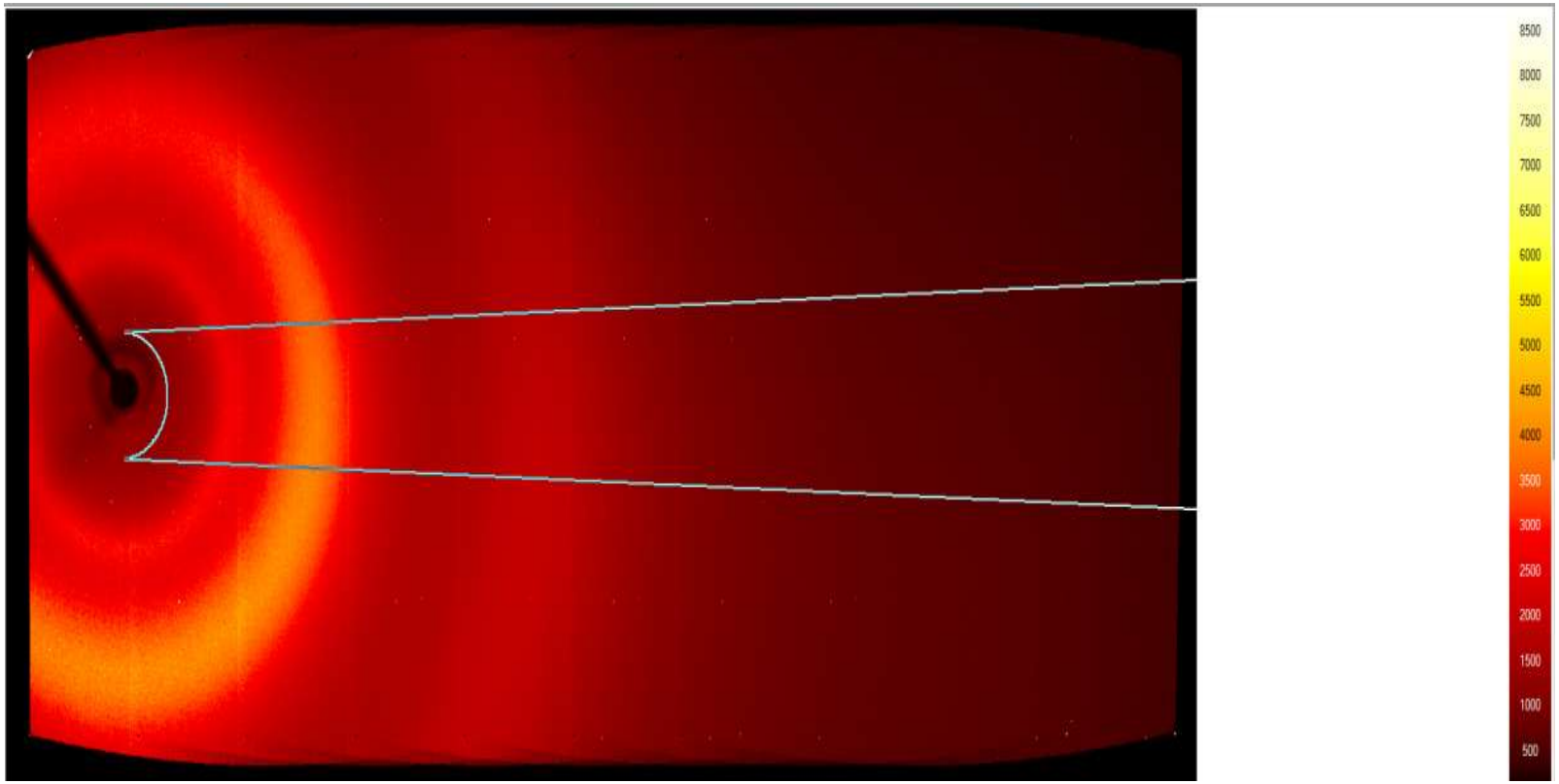

Fig. A.5 Powder Diffraction Images for sorbitol derived Sodium alkoxide at 3:1 mole ratio

APPENDIX B

SINGLE CRYSTAL DATA FOR MONO-SODIUM XYLITOLATE

Table B.1 Crystal data and structure refinement for mono-sodium xylitolate

A. Crystal Data

Identification code	mrfc_1368 / fc1368
Empirical formula	$C_5H_{11}Na_1O_5$
Formula weight	174.13
Crystal Color, Habit	colorless, rod
Crystal dimensions (mm)	$0.16 \times 0.09 \times 0.04$
Crystal system	monoclinic
Space group	$P2_1/c$ [No. 14]
Unit cell parameters[a]	
a (Å)	8.8191(4)
b (Å)	5.8646(3)
c (Å)	13.7820(7)
□ (°)	90
□ (°)	97.564(2)
□ (°)	90
V (Å^3)	706.61(6)
Z[b]	4
F(000)	368
Density (□$_{calcd}$)	1.637 Mg/m^3
Absorption coefficient (□)	1.764 mm^{-1}

B. Data Collection and Refinement Conditions

Diffractometer	Proteum R Smart 6000 diffractometer (Bruker AXS)[c]
Radiation	monochromated Cu K□
Wavelength (Mo K□)	1.54184 Å
Temperature	-100(2) °C [173(2) K]
Scan type	ϕ and □ (0.5º per frame, 20 s exposure/frame)
Theta range for data collection	5.06 to 65.13°
Completeness to theta = 65.13°	97.0%
Reflections collected[d]	1526
Index ranges	$-10 \le h \le 10$, $-5 \le k \le 6$, $-15 \le l \le 16$
Independent reflections [$F_o^2 \ge -3\square(F_o^2)$][e]	1173 [$R_{int} = 0.0557$][f]
Observed reflections [$F_o^2 > 2\square(F_o^2)$][g]	1092
Absorption correction method	multi-scan [SCALEPACK]
Range of transmission factors (max./min.)	0.9264-0.7631 [from SHELXL97-2]
Anomalous Dispersion	For all non-hydrogen atoms
Structure solution method	Direct methods (SIR-2004)[h]
Refinement method	Full-matrix least-squares on F^2 (SHELXL97-2)[i]
Function Minimized	$\Sigma w(\|F_o\|^2 - \|kF_c\|^2)^2$ (k: overall scale factor)
Weighing scheme, w	$w = [\square(F_o^2) + (0.0752\ P)^2 + (0.1423\ P)]^{-1}$
$w = [\square(F_o^2) + (a\ P)^2 + (b\ P)]^{-1}$	
P-factor	$[\mathrm{Max}(F_o^2, 0) + 2\ F_c^2]/3$
Data / restraints / parameters	1173 [$F_o^2 \ge -3\square(F_o^2)$] / 0 / 117
Reflection (observed)/parameter ratio	10:1
Reflection (data)/parameter ratio	9:1
Goodness-of-fit on F^2	1.180
$GooF = \{\Sigma[w(F_o^2 - F_c^2)^2]/(n - p)\}^{1/2}$	

n: number of reflections, *p*: number of parameters

Final *R* indices

$R_1 = [\Sigma\|\|F_o\|-\|F_c\|\|]/[\Sigma\|F_o\|]$ for $[F_o^2 > 2\sigma(F_o^2)]$[i]	0.0481
$wR_2 = \{[\Sigma w(F_o^2-F_c^2)^2]/[\Sigma w(F_o^2)^2]\}^{1/2}$ [all data]	0.1236
Max. Shift/Error in Final Cycle	0.000
Extinction coefficient (x)[j]	0.026(3)
Largest difference peak and hole	0.319 and -0.382 $e^-/Å^3$

---

[a] Obtained from least-squares refinement of XYZ-centroids of 3281 reflections above 20 $\sigma(I)$ with 10.11° < 2θ < 129.9°.

[b] *Z* is the number of formula units per unit cell. Comparison of *Z* with the multiplicity of the general position n_a of the space group will then require that the asymmetric unit is Z/n_a times the formula unit. The asymmetric unit is the minimum group of atoms whose positions, together with those generated by the symmetry operations of the space group generate the complete contents of the unit cell.

[c] *Proteum R Smart 6000 diffractometer* (rotating anode; Bruker AXS).

[d] Number of reflections after truncation or rejection (before merging).

[e] The criterion for the independent or unique reflections $[F_o^2 \geq -3\sigma(F_o^2)]$ was taken from:
G. M. Sheldrick, *SHELXL-93, Program for the Solution of Crystal Structures;* University of Göttingen: Göttingen, Germany 1993.

[f] $R_{int} = [\Sigma|F_o^2-F_o^2(\text{mean})|]/[\Sigma|F_o^2|]$

[g] The criterion for the observed reflections $[F_o^2 > 2\sigma(F_o^2)]$ is equivalent to $[I > 2\sigma(I)]$: *I* is proportional to F_o^2.

[h] M. C. Burla, R. Caliandro, M. Camalli, B. Carrozzini, G. L. Cascarano, L. De Caro, C. Giacovazzo, G. Polidori and R. Spagna, *SIR-2004: an improved tool for crystal structure determination and refinement*; *J. Appl. Crystallogr.* 2005**, 38,** 381-388.

[i] G. M. Sheldrick, *SHELXL97-2, Program for the Solution of Crystal Structures;* University of Göttingen, Göttingen, Germany 1997.
Function minimized: $\Sigma w(|F_o|^2-|kF_c|^2)^2$; *k*: overall scale factor.

Refinement on F_o^2 for all reflections (all of these having $F_o^2 \geq -3\sigma(F_o^2)$). Weighted *R*-factors wR_2 and the values for *GooF* are based on F_o^2; conventional *R*-factors R_1 are based on F_o, with F_o set to zero for negative F_o^2. The observed criterion of $F_o^2 > 2\sigma(F_o^2)$ is used only for calculating R_1, and is not relevant to the choice of reflections for refinement. *R*-factors based on F_o^2 are statistically about twice as large as those based on F_o, and *R*-factors based on ALL data will be even larger.

[j] $F_c^* = kF_c[1 + x\{0.001F_c^2\lambda^3/\sin(2\theta)\}]^{-1/4}$, where *k* is the overall scale factor and F_c^* the corrected value.
Extinction is an effect of dynamical diffraction whereby the incident beam is weakened as it passes through the crystal. Part of the incident beam may be reflected twice so that it returns to its original direction but it is out of phase with

the main beam, thus reducing the intensity of the latter (*primary extinction*). When the crystal is mosaic, part of the beam will be diffracted by one mosaic block and therefore not available for diffraction by the following block that is accurately aligned with the first. The second block contributes less than expected to the diffracted beam (*secondary extinction*). The effect of extinction is evidenced by a tendency for $|F_o|$ to be systematically smaller than $|F_c|$ for intense reflections. The above expression for the extinction is empirical and represents a compromise to cover both primary and secondary extinction. For the analysis of variance and *.fcf* output file, the F_o^2 values are brought onto the absolute scale of F_c^2 by dividing them by the scale factor(s) and the extinction factor.

Table B.2 Atomic coordinates ($\times 10^4$), equivalent isotropic displacement parameters ($Å^2 \times 10^3$) and site occupancy factors for *mrfc_1368*. U(eq) is defined as one third of the trace of the orthogonalized U^{ij} tensor.

Atom	**x**	**y**	**z**	**U(eq)**
Na(1)	4154(1)	-448(1)	3425(1)	28(1)
O(1)	3053(1)	3279(2)	3964(1)	25(1)
O(2)	2452(2)	992(2)	2128(1)	28(1)
O(3)	3787(1)	5580(2)	2475(1)	24(1)
O(4)	3475(1)	3435(2)	681(1)	25(1)
O(5)	2743(1)	7385(2)	-536(1)	29(1)
C(1)	1572(2)	2960(3)	3453(1)	25(1)
C(2)	1598(2)	2969(3)	2348(1)	24(1)
C(3)	2274(2)	5145(3)	1974(1)	23(1)
C(4)	2347(2)	5075(3)	865(1)	23(1)
C(5)	2701(2)	7419(3)	494(1)	27(1)

Table B.3(a) Interatomic Distances [Å] for mono-sodium xylitolate

Na(1)-O(5)*	2.3154(13)
Na(1)-O(2)	2.3363(13)
Na(1)-O(4)’	2.3750(13)
Na(1)-O(3)’	2.4070(12)
Na(1)-O(1)	2.5417(13)
Na(1)-O(3)$^{\#}$	2.6716(13)
O(1)-C(1)	1.4131(19)
O(2)-C(2)	1.437(2)
O(2)-H(21)	0.77(3)
O(3)-C(3)	1.4422(19)
O(3)-Na(1)**	2.4071(12)
O(3)-Na(1)$^{\#\#}$	2.6716(13)
O(3)-H(31)	0.83(3)
O(4)-C(4)	1.430(2)
O(4)-Na(1)**	2.3750(13)
O(4)-H(41)	0.89(3)
O(5)-C(5)	1.424(2)
O(5)-Na(1)”	2.3153(13)
O(5)-H(51)	0.83(3)
C(1)-C(2)	1.526(2)
C(2)-C(3)	1.526(2)
C(3)-C(4)	1.539(2)
C(4)-C(5)	1.514(2)

Symmetry transformations used to generate equivalent atoms:
*: x, -y + ½, z + ½; ’: -x + 1, y - ½, -z + ½; $^{\#}$; x, y - 1, z; **: -x + 1, y + ½, -z + ½;
$^{\#\#}$: x, y + 1, z; ”: x, -y + ½, z - ½

Table B.3(b) Interatomic Angles [°] for mono-sodium xylitolate

O(5)*-Na(1)-O(2)	107.88(5)
O(5)*-Na(1)-O(4)’	92.98(5)
O(2)-Na(1)-O(4)’	158.43(5)
O(5)*-Na(1)-O(3)’	160.95(5)
O(2)-Na(1)-O(3)’	88.13(5)
O(4)’-Na(1)-O(3)’	70.38(4)
O(5)*-Na(1)-O(1)	89.09(5)
O(2)-Na(1)-O(1)	71.42(4)
O(4)’-Na(1)-O(1)	115.46(4)
O(3)’-Na(1)-O(1)	106.18(5)
O(5)*-Na(1)-O(3)$^{\#}$	80.49(4)
O(2)-Na(1)-O(3)$^{\#}$	85.15(4)
O(4)’-Na(1)-O(3)$^{\#}$	93.17(4)
O(3)’-Na(1)-O(3)$^{\#}$	90.95(3)
O(1)-Na(1)-O(3)$^{\#}$	150.09(4)
C(1)-O(1)-Na(1)	95.97(9)
C(2)-O(2)-Na(1)	115.57(9)
C(2)-O(2)-H(21)	110(2)
Na(1)-O(2)-H(21)	108(2)
C(3)-O(3)-Na(1)**	114.99(9)
C(3)-O(3)-Na(1)$^{\#\#}$	115.69(9)
Na(1)**-O(3)-Na(1)$^{\#\#}$	114.83(5)
C(3)-O(3)-H(31)	104.3(18)
Na(1)**-O(3)-H(31)	111.2(18)
Na(1)$^{\#\#}$-O(3)-H(31)	92.9(18)
C(4)-O(4)-H(41)	110.5(17)
Na(1)**-O(4)-H(41)	129.5(17)
C(5)-O(5)-Na(1)”	135.18(10)
C(5)-O(5)-H(51)	106.8(17)

Na(1)”-O(5)-H(51)	101.3(17)
O(1)-C(1)-C(2)	111.26(13)
O(2)-C(2)-C(1)	106.57(13)
O(2)-C(2)-C(3)	111.41(13)
C(1)-C(2)-C(3)	113.44(13)
O(3)-C(3)-C(2)	111.34(13)
O(3)-C(3)-C(4)	108.82(12)
C(2)-C(3)-C(4)	112.48(14)
O(4)-C(4)-C(5)	111.81(13)
O(4)-C(4)-C(3)	108.42(13)
C(5)-C(4)-C(3)	110.43(13)
O(5)-C(5)-C(4)	110.95(13)

Symmetry transformations used to generate equivalent atoms:
*: x, -y + ½, z + ½; ’: -x + 1, y - ½, -z + ½; #; x, y - 1, z; **: -x + 1, y + ½, -z + ½;
##: x, y + 1, z; ”: x, -y + ½, z - ½

Table B.3(c) Intra- and Intermolecular Na···O-C contacts [Å] for mono-sodium xylitolate

---

r_{vdW}(Na) + r_{vdW} (O) = (2.30 + 1.50) [Å] = 3.80 [Å] (Bondi)[1)]

Intramolecular contacts:

Na(1)…O(1)	2.5417(13)
Na(1)…O(2)	2.3363(13)

Intermolecular contacts:

Na(1)…O(5)*	2.3154(13)
Na(1)…O(4)’	2.3750(13)
Na(1)…O(3)’	2.4070(12)
Na(1)…O(3)$^{\#}$	2.6716(13)

Symmetry transformations used to generate equivalent atoms:

*: x, -y + ½, z + ½; ’: -x + 1, y - ½, -z + ½; $^{\#}$: x, y - 1, z

Table B. 4 Anisotropic displacement parameters ($Å^2 \times 10^3$) for mono-sodium xylitolate. The anisotropic displacement factor exponent takes the form:

$[-2\pi^2(h^2a^{*2}U_{11} + k^2b^{*2}U_{22} + l^2c^{*2}U_{33} + 2klb^*c^*U_{23} + 2hla^*c^*U_{13} + 2hka^*b^*U_{12})]$

Atom	**U^{11}**	**U^{22}**	**U^{33}**	**U^{23}**	**U^{13}**	**U^{12}**
Na(1)	25(1)	30(1)	29(1)	4(1)	6(1)	1(1)
O(1)	25(1)	27(1)	23(1)	1(1)	3(1)	-2(1)
O(2)	35(1)	24(1)	26(1)	-1(1)	8(1)	2(1)
O(3)	21(1)	28(1)	22(1)	1(1)	2(1)	-2(1)
O(4)	26(1)	27(1)	22(1)	-2(1)	4(1)	4(1)
O(5)	41(1)	24(1)	23(1)	2(1)	11(1)	3(1)
C(1)	24(1)	26(1)	25(1)	1(1)	6(1)	-1(1)
C(2)	22(1)	25(1)	25(1)	0(1)	3(1)	0(1)
C(3)	20(1)	25(1)	24(1)	-1(1)	3(1)	0(1)
C(4)	22(1)	25(1)	22(1)	-1(1)	3(1)	1(1)
C(5)	34(1)	26(1)	21(1)	0(1)	7(1)	2(1)

Table B.5 Hydrogen coordinates ($\times 10^4$) and isotropic displacement parameters ($Å^2 \times 10^3$) for mono-sodium xylitolate

Atom	**x**	**y**	**z**	**U(eq)**
H(21)	2910(30)	1260(50)	1700(20)	51(8)
H(31)	3830(30)	4830(50)	2990(20)	47(7)
H(41)	3280(30)	2900(50)	75(19)	50(7)
H(51)	2850(30)	8720(50)	-706(18)	42(6)
H(1A)	891	4192	3629	30
H(1B)	1154	1489	3650	30
H(2)	525	2803	2018	29
H(3)	1602	6449	2110	28
H(4)	1330	4574	525	28
H(5A)	1911	8511	648	32
H(5B)	3702	7940	831	32

Table B.6 Selected torsion angles [°] for *mrfc_1368.*

O(5)*-Na(1)-O(1)-C(1)	-72.93(9)
O(2)-Na(1)-O(1)-C(1)	36.30(9)
O(4)'-Na(1)-O(1)-C(1)	-165.80(9)
O(3)'-Na(1)-O(1)-C(1)	118.63(9)
O(3)$^{\#}$-Na(1)-O(1)-C(1)	-3.96(14)
C(4)'-Na(1)-O(1)-C(1)	170.23(9)
O(5)*-Na(1)-O(2)-C(2)	76.09(11)
O(4)'-Na(1)-O(2)-C(2)	-119.19(16)
O(3)'-Na(1)-O(2)-C(2)	-114.43(11)
O(1)-Na(1)-O(2)-C(2)	-6.66(10)
O(3)$^{\#}$-Na(1)-O(2)-C(2)	154.47(11)
Na(1)-O(1)-C(1)-C(2)	-65.61(13)
Na(1)-O(2)-C(2)-C(1)	-23.05(15)
Na(1)-O(2)-C(2)-C(3)	101.18(13)
O(1)-C(1)-C(2)-O(2)	65.75(16)
O(1)-C(1)-C(2)-C(3)	-57.22(18)
Na(1)**-O(3)-C(3)-C(2)	101.31(12)
Na(1)$^{\#\#}$-O(3)-C(3)-C(2)	-121.10(12)
Na(1)**-O(3)-C(3)-C(4)	-23.22(15)
Na(1)$^{\#\#}$-O(3)-C(3)-C(4)	114.38(12)
O(2)-C(2)-C(3)-O(3)	-64.99(16)
C(1)-C(2)-C(3)-O(3)	55.27(17)
O(2)-C(2)-C(3)-C(4)	57.45(17)
C(1)-C(2)-C(3)-C(4)	177.71(13)
Na(1)**-O(4)-C(4)-C(5)	63.36(13)
Na(1)**-O(4)-C(4)-C(3)	-58.62(13)
O(3)-C(3)-C(4)-O(4)	54.68(16)
C(2)-C(3)-C(4)-O(4)	-69.17(16)
O(3)-C(3)-C(4)-C(5)	-68.14(17)
C(2)-C(3)-C(4)-C(5)	168.01(13)

Na(1)”-O(5)-C(5)-C(4)	-59.0(2)
O(4)-C(4)-C(5)-O(5)	60.34(17)
C(3)-C(4)-C(5)-O(5)	-178.84(12)

Symmetry transformations used to generate equivalent atoms:
*: x, -y + ½, z + ½; ’: -x + 1, y - ½, -z + ½; #; x, y - 1, z; **: -x + 1, y + ½, -z + ½;
##: x, y + 1, z; ”: x, -y + ½, z - ½

Table B.7 Intra- and Intermolecular O(H)···O contacts [Å] for *mrfc_1368*.

D-H···A	***D-A***	***H···A***	***H···A***	***D-H···A***
O2-H21···O4	0.77(3)	2.01(3)	2.7052(17)	150(3)
O3-H31···O1	0.83(3)	1.83(3)	2.6078(16)	156(3)
O4-H41···O1*	0.89(3)	1.67(3)	2.5522(16)	175(3)
O5-H51···O1***	0.83(3)	1.83(3)	2.6583(17)	178(2)

Symmetry transformations used to generate equivalent atoms:
*: x, -y + ½, z - ½; ***: x, -y + $^{3}/_{2}$, z - ½

APPENDIX C

EXCEL SOLVER PROGRAM FOR BEST FIT OF PRODUCT COMPOSITION

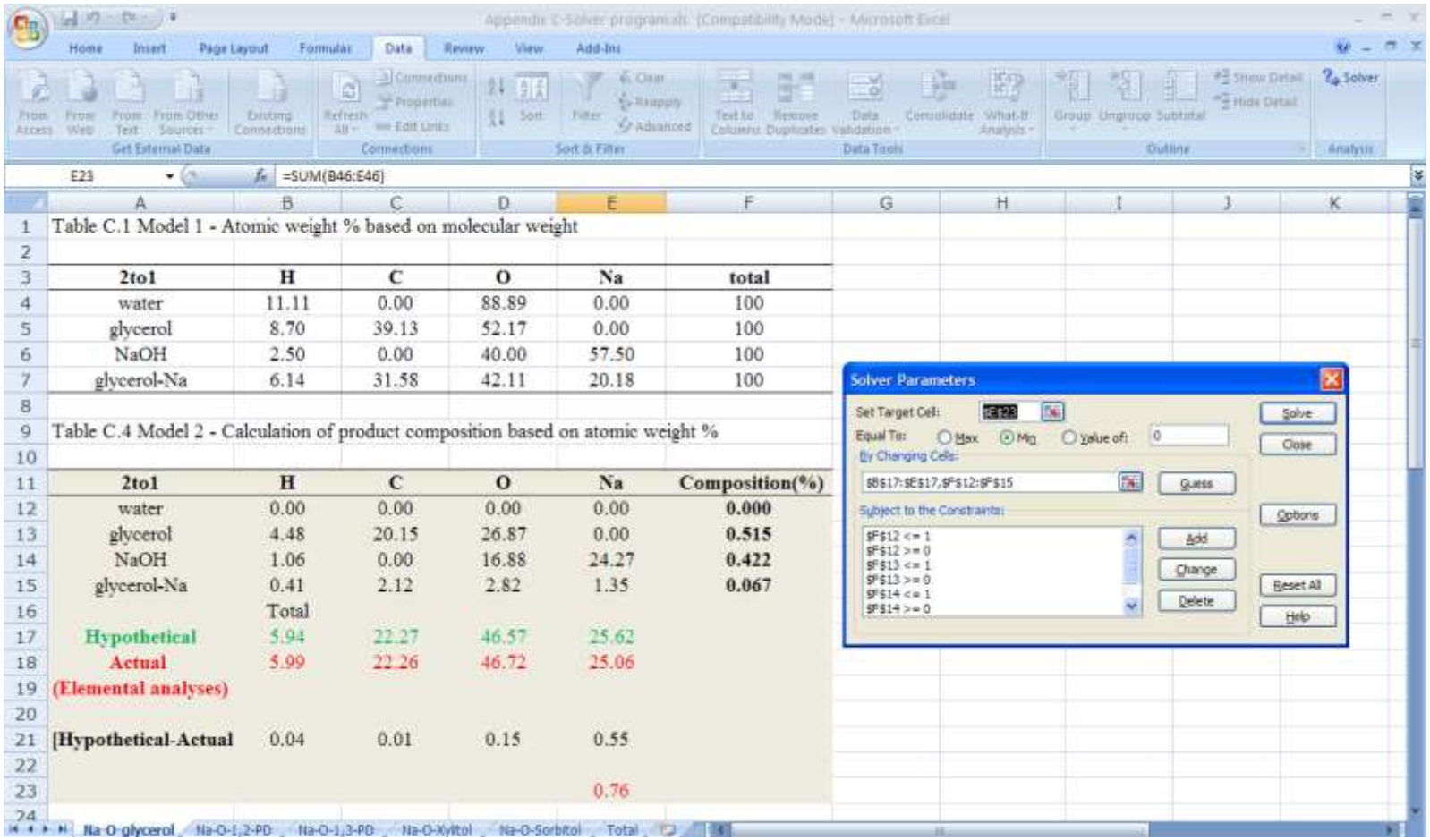

Table C.1 Model 1 - Atomic weight % based on molecular weight

2to1	H	C	O	Na	total
water	11.11	0.00	88.89	0.00	100
glycerol	8.70	39.13	52.17	0.00	100
NaOH	2.50	0.00	40.00	57.50	100
glycerol-Na	6.14	31.58	42.11	20.18	100

Table C.4 Model 2 - Calculation of product composition based on atomic weight %

2to1	H	C	O	Na	Composition(%)
water	0.00	0.00	0.00	0.00	**0.000**
glycerol	4.48	20.15	26.87	0.00	**0.515**
NaOH	1.06	0.00	16.88	24.27	**0.422**
glycerol-Na	0.41	2.12	2.82	1.35	**0.067**
	Total				
Hypothetical	5.94	22.27	46.57	25.62	
Actual	5.99	22.26	46.72	25.06	
(Elemental analyses)					
[Hypothetical-Actual	0.04	0.01	0.15	0.55	
				0.76	

Fig. C.1 Excel solver solution for 2:1 mole ratio glycerol derived sodium alkoxide composition fitting

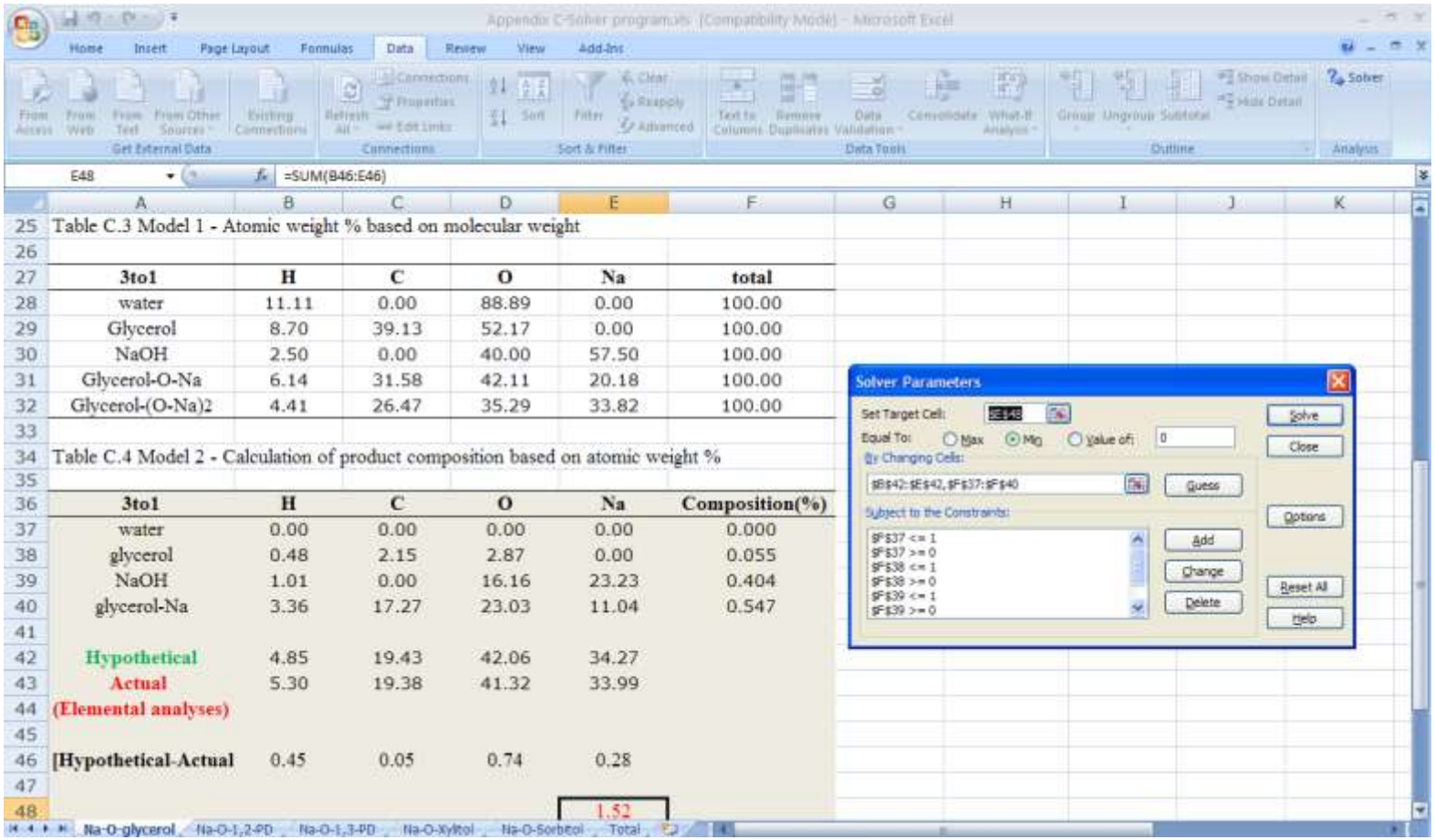

Fig. C.2 Excel solver solution for 3:1 mole ratio glycerol derived sodium alkoxide composition fitting

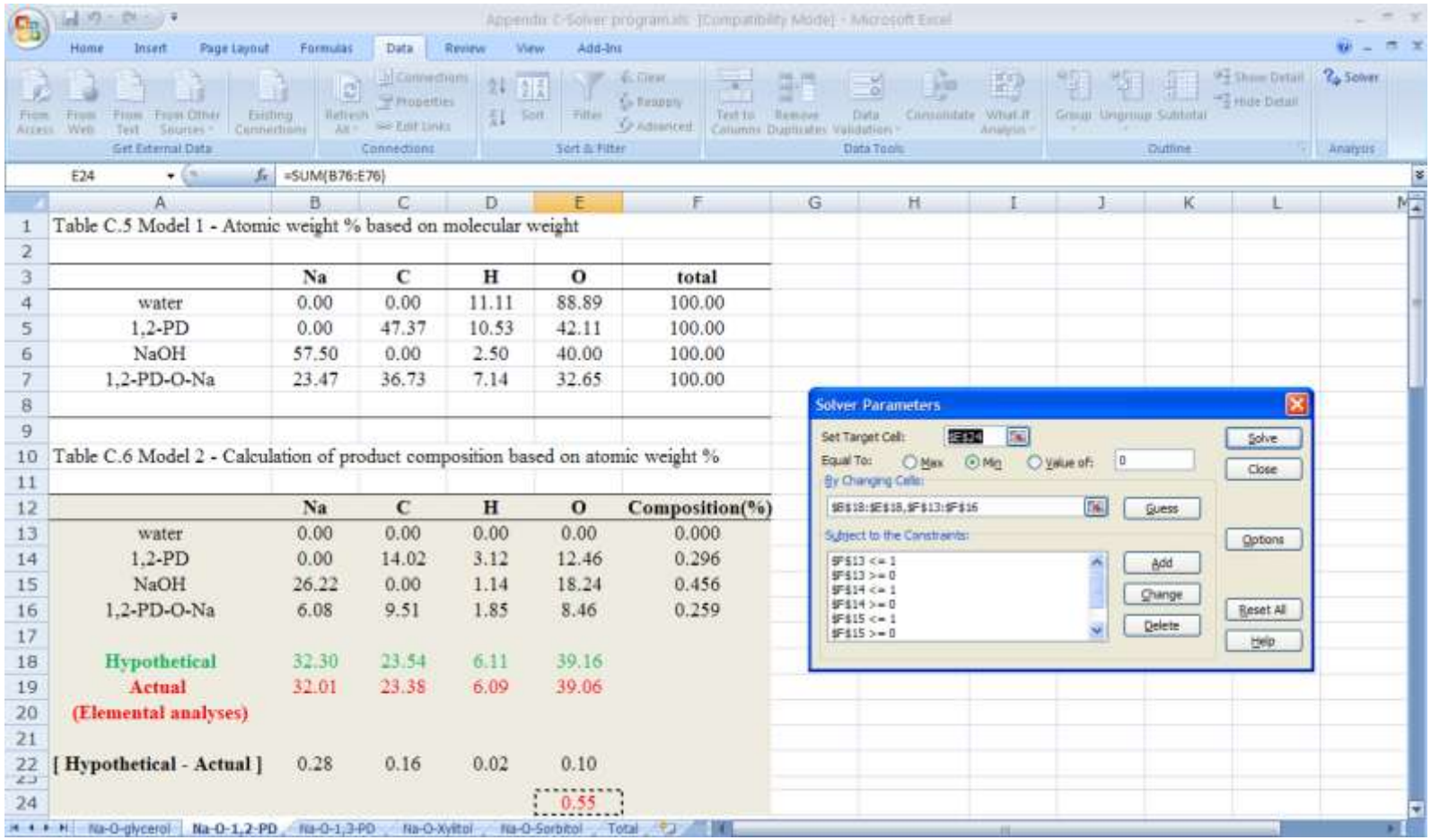

Fig. C.3 Excel solver solution for 2:1 mole ratio 1,2-propanediol derived sodium alkoxide composition fitting

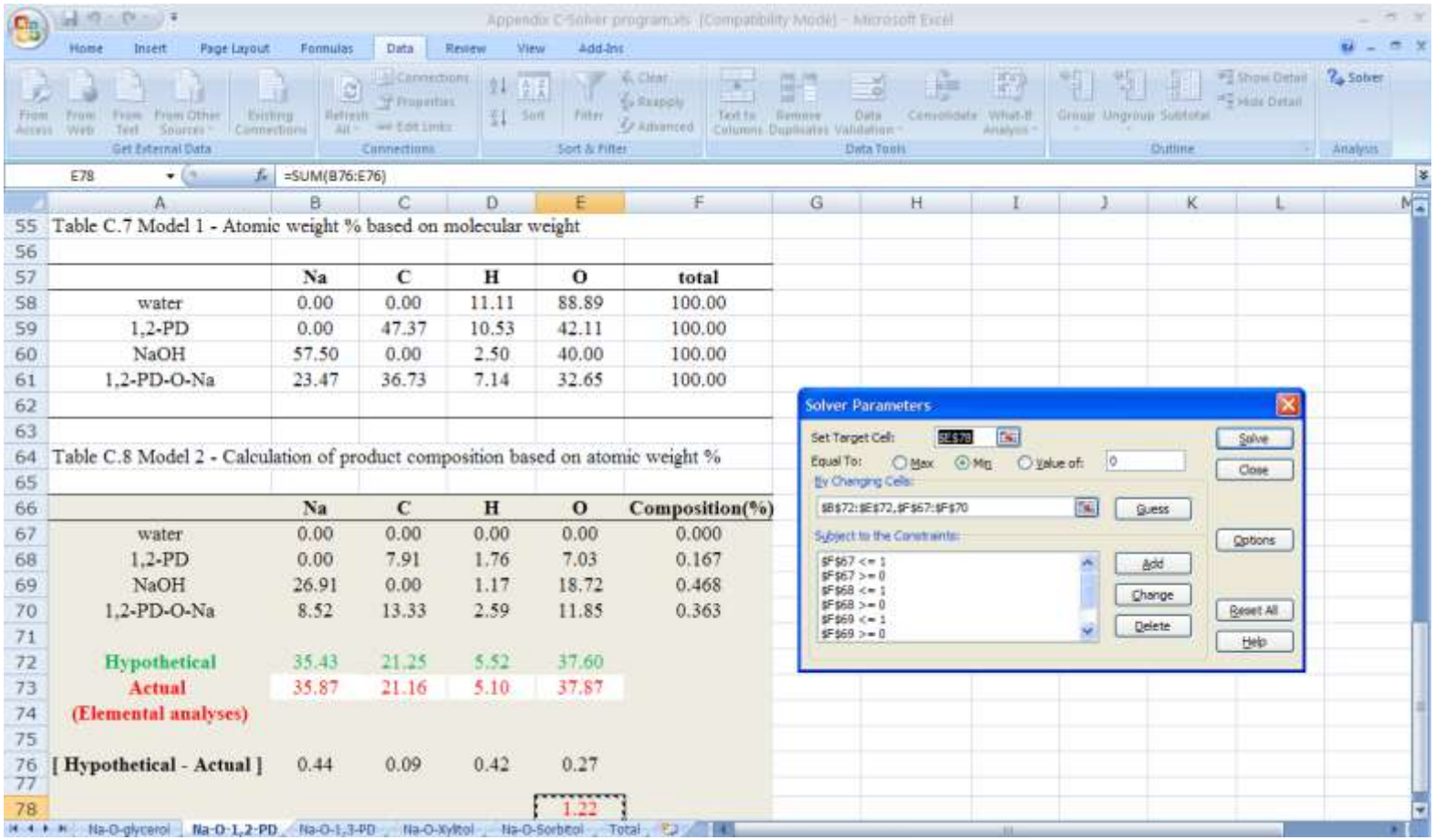

Fig. C.4 Excel solver solution for 3:1 mole ratio 1,2-propanediol derived sodium alkoxide composition fitting

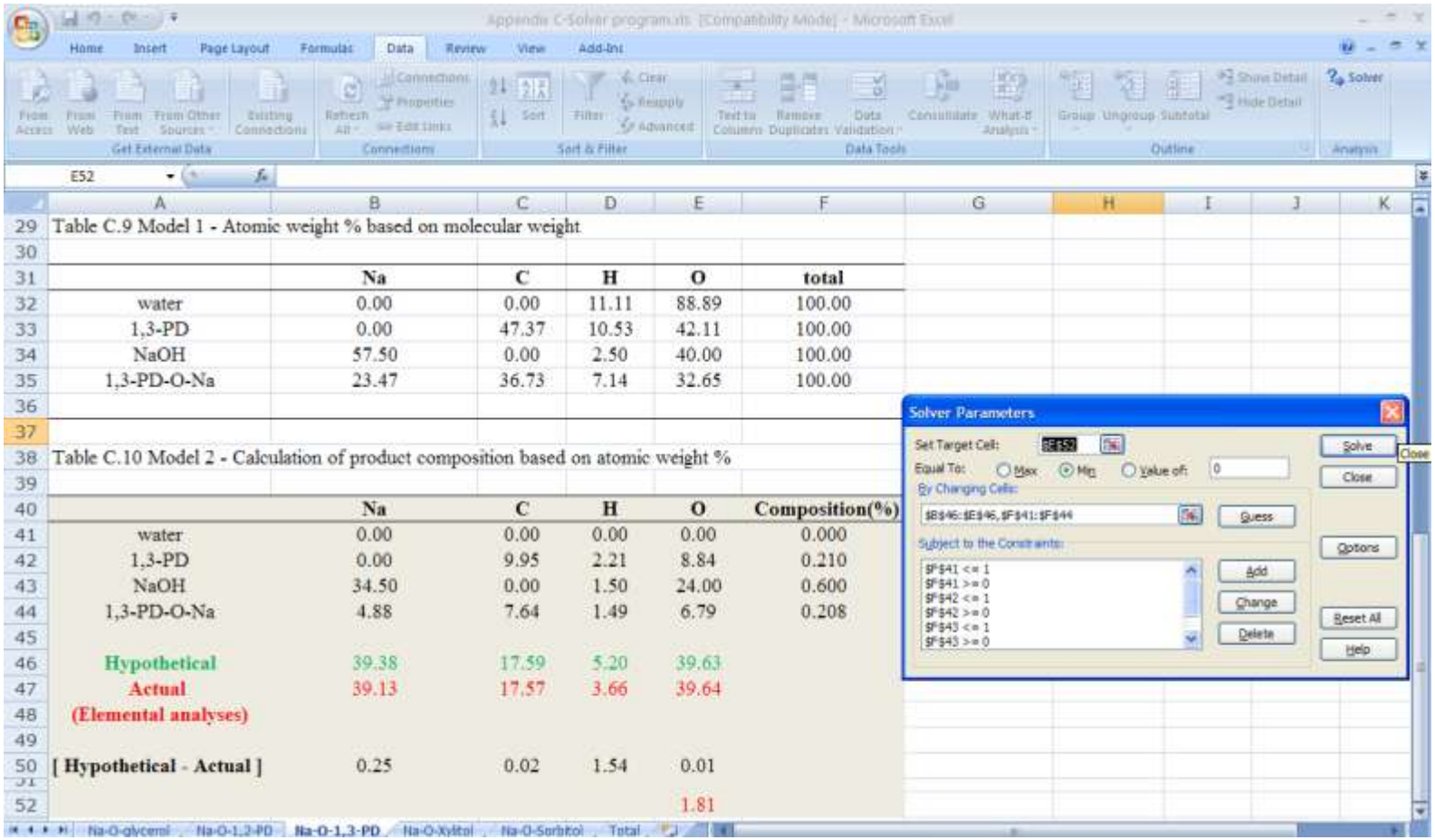

Table C.9 Model 1 - Atomic weight % based on molecular weight

	Na	C	H	O	total
water	0.00	0.00	11.11	88.89	100.00
1,3-PD	0.00	47.37	10.53	42.11	100.00
NaOH	57.50	0.00	2.50	40.00	100.00
1,3-PD-O-Na	23.47	36.73	7.14	32.65	100.00

Table C.10 Model 2 - Calculation of product composition based on atomic weight %

	Na	C	H	O	Composition(%)
water	0.00	0.00	0.00	0.00	0.000
1,3-PD	0.00	9.95	2.21	8.84	0.210
NaOH	34.50	0.00	1.50	24.00	0.600
1,3-PD-O-Na	4.88	7.64	1.49	6.79	0.208
Hypothetical	39.38	17.59	5.20	39.63	
Actual	39.13	17.57	3.66	39.64	
(Elemental analyses)					
[Hypothetical - Actual]	0.25	0.02	1.54	0.01	
				1.81	

Fig. C.5 Excel solver solution for 2:1 mole ratio 1,3-propanediol derived sodium alkoxide composition fitting

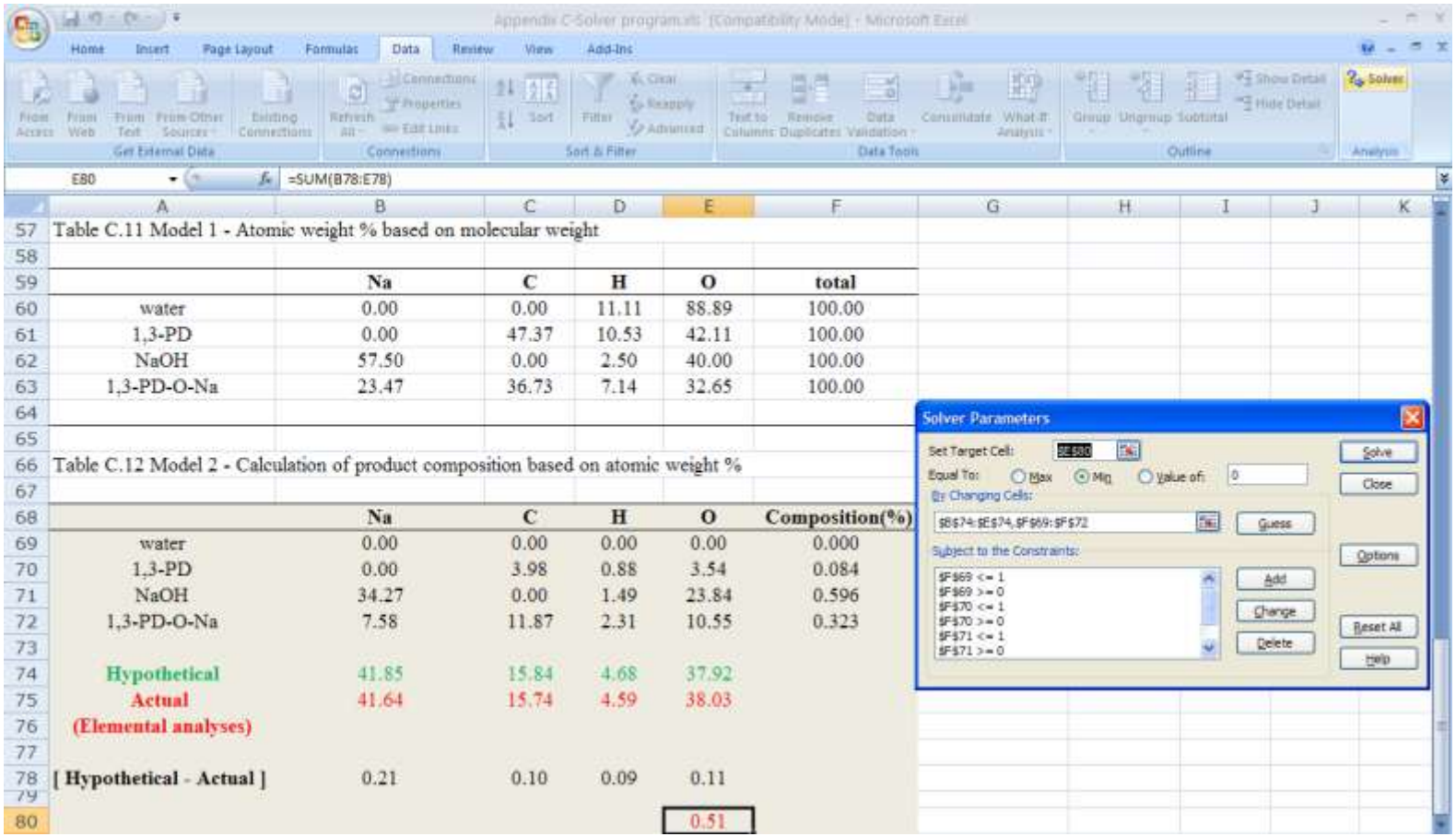

Fig. C.6 Excel solver solution for 3:1 mole ratio 1,3-propanediol derived sodium alkoxide composition fitting

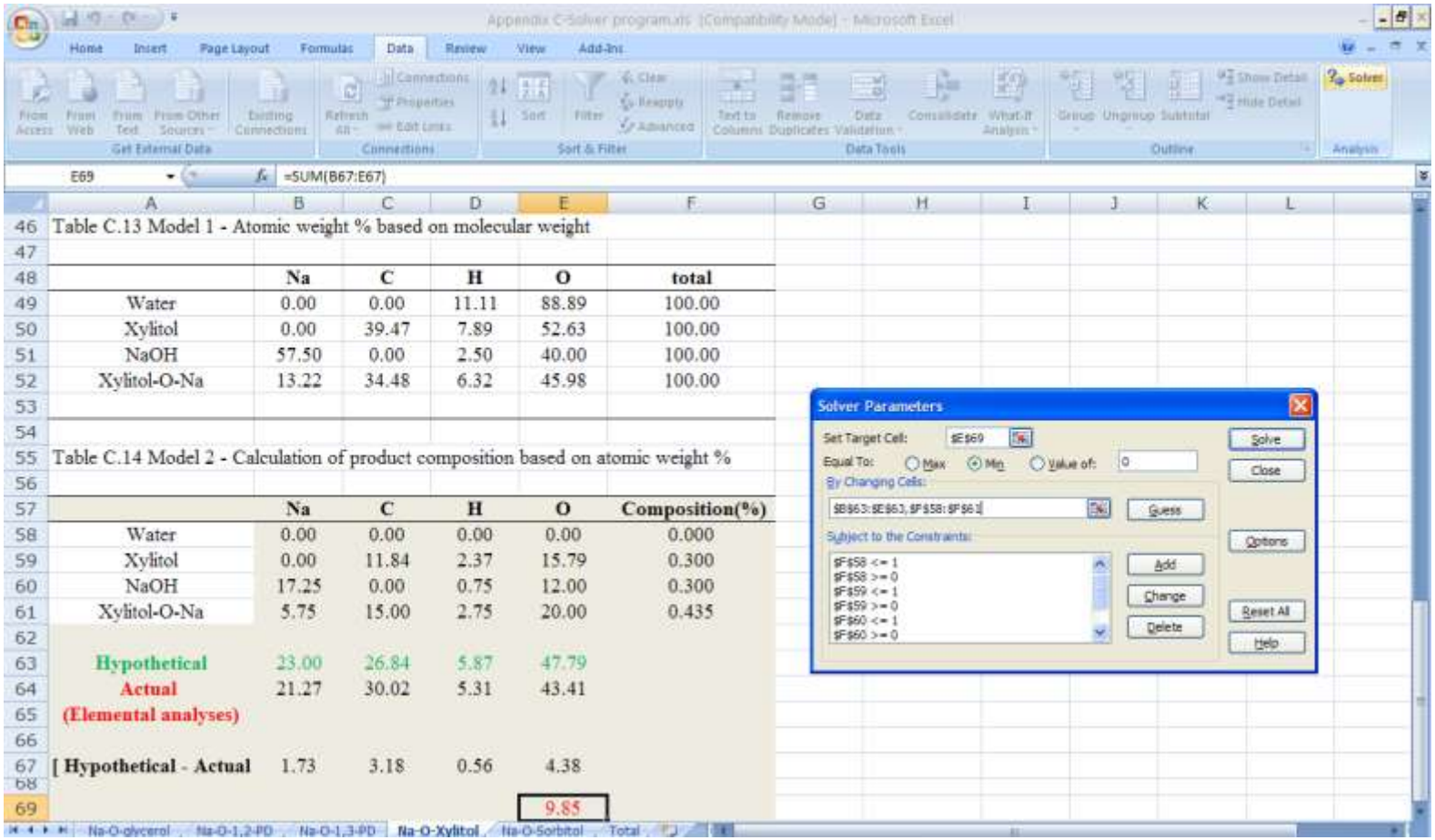

Fig. C.7 Excel solver solution for 2:1 mole ratio xylitol derived sodium alkoxide composition fitting

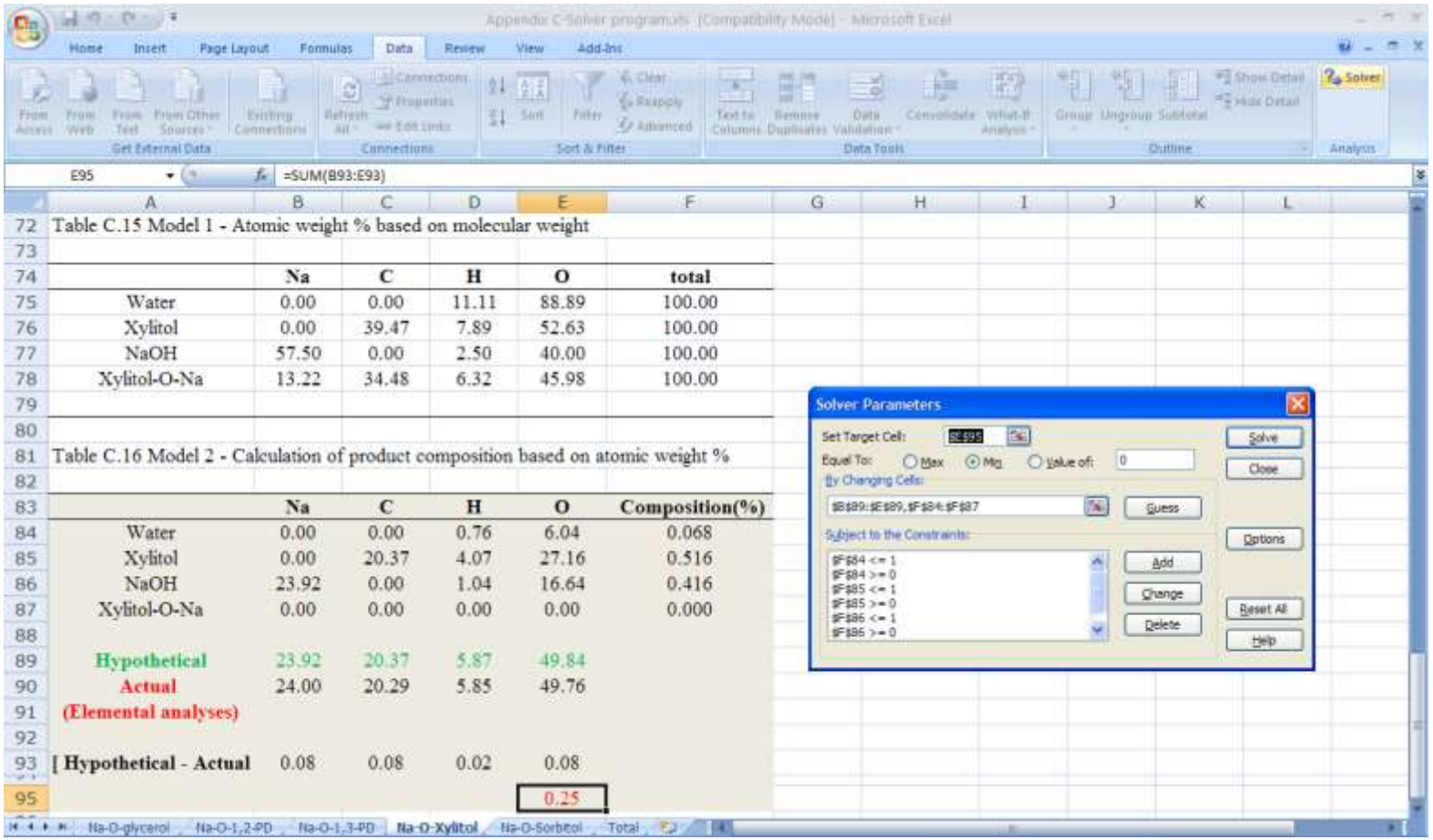

Fig. C.8 Excel solver solution for 3:1 mole ratio xylitol derived sodium alkoxide composition fitting

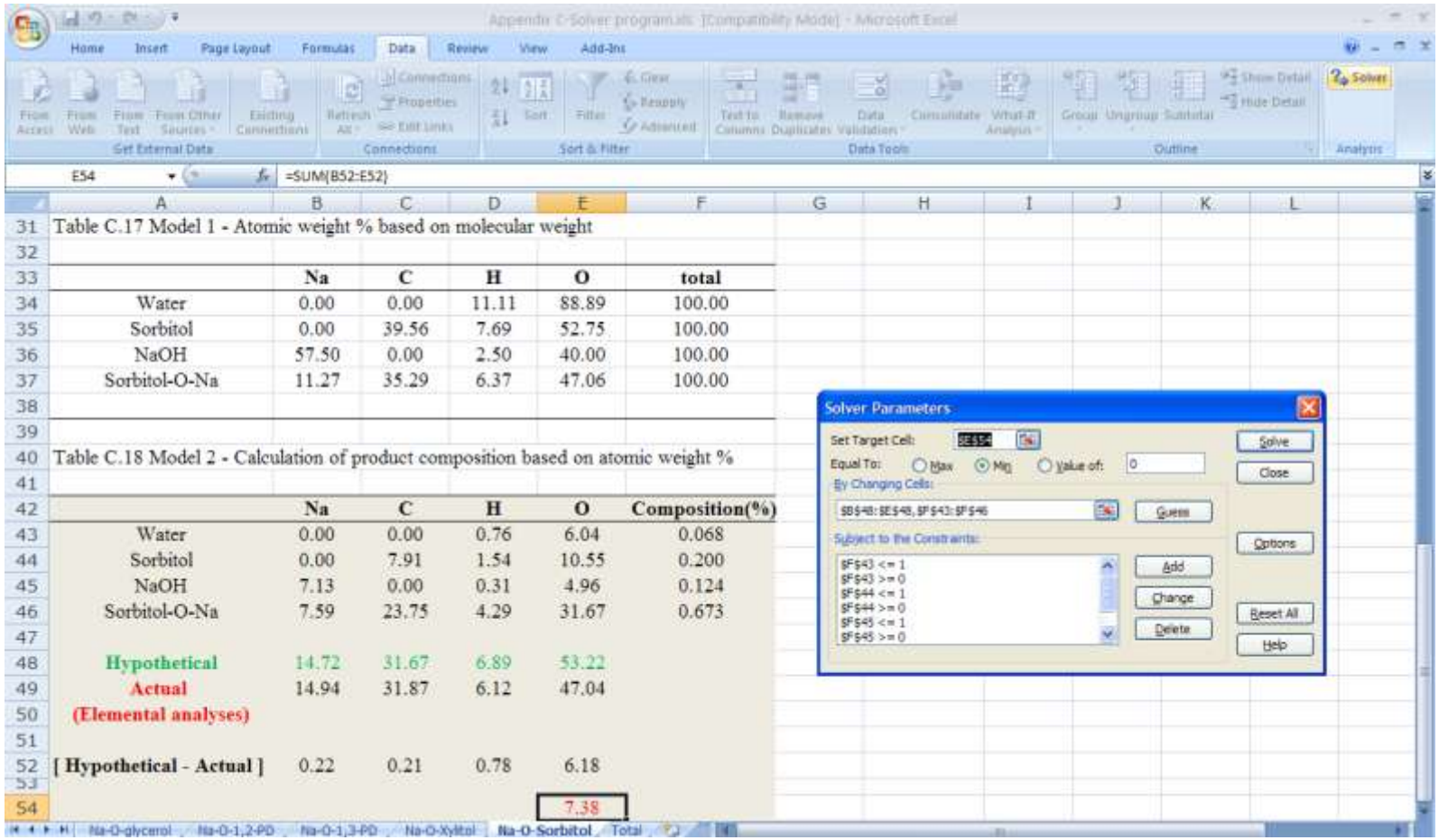

Fig. C.9 Excel solver solution for 2:1 mole ratio sorbitol derived sodium alkoxide composition fitting

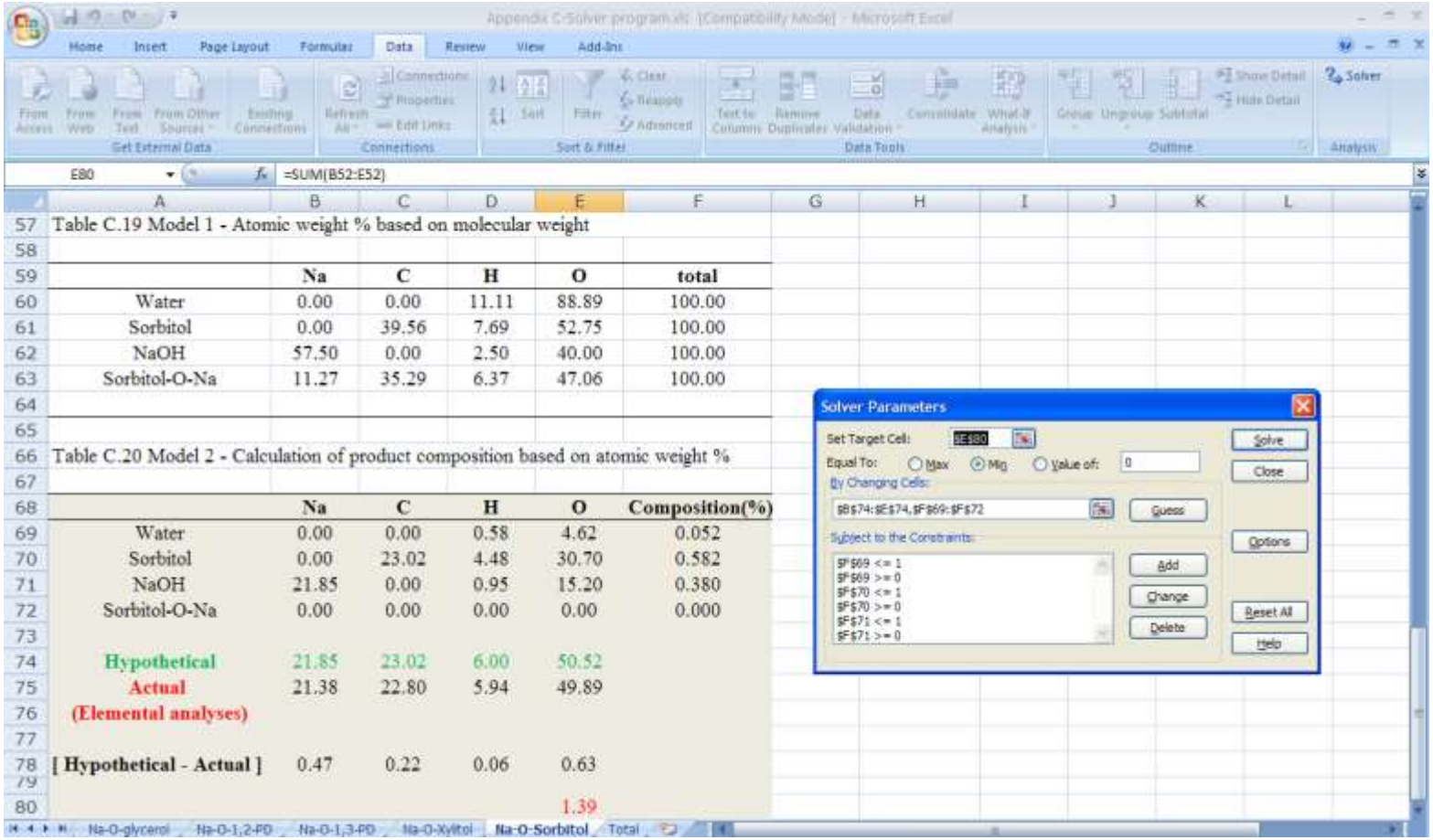

Fig. C.10 Excel solver solution for 3:1 mole ratio sorbitol derived sodium alkoxide composition fitting

APPENDIX D

BIODIESEL YIELD (WT%) IN TRANSESTERIFICATION OF CANOLA OIL CATALYZED BY VARIOUS SODIUM ALKOXIDE CATALYSTS

Table D.1 Fatty acid methyl ester production (wt%) during transesterification of canola oil catalyzed by polyol-derived sodium alkoxide/hydroxide (1: 1 mole ratio) and sodium methoxide

Time (log scale, sec)	1,2-propanediol	1,3-propanediol	Glycerol	Xylitol	Sorbitol	Sodium Methoxide
1.48	28.55	5.56	22.86	9.57	4.12	34.26
1.78	60.57	43.64	53.35	19.90	6.93	62.50
2.08	65.37	57.95	62.41	40.11	26.33	66.26
2.26	66.67	65.32	71.21	56.64	40.52	70.36
2.38	66.67	69.88	74.33	65.10	50.91	75.65
2.48	68.83	71.03	77.39	66.85	61.82	77.89
2.56	68.08	72.27	78.01	70.81	63.90	79.10
2.68	73.41	75.35	80.79	72.75	69.59	81.17
2.78	73.08	77.83	82.29	75.09	73.07	83.26
2.95	76.11	82.65	85.78	81.06	80.41	86.47
3.08	79.00	84.55	88.61	85.91	82.75	89.11
3.18	81.11	85.28	90.18	86.59	84.55	89.92
3.26	84.08	86.73	89.61	86.68	87.56	90.16
3.56	86.90	90.36	92.73	91.44	92.20	93.07
3.73	90.79	93.23	95.33	94.04	95.61	95.29

Table D.2 Fatty acid methyl ester production (wt%) during transesterification of canola oil catalyzed by polyol-derived sodium alkoxide/hydroxide (2: 1 mole ratio) and sodium methoxide

Time (log scale, sec)	**1,2-propanediol**	**1,3-propanediol**	**Glycerol**	**Xylitol**	**Sorbitol**	**Sodium methoxide**
1.48	33.75	36.74	33.07	17.53	11.51	34.26
1.78	62.91	62.24	62.57	34.12	28.47	62.50
2.08	69.13	72.11	68.68	56.10	52.05	66.26
2.26	71.93	75.39	75.33	64.08	61.83	70.36
2.38	75.26	77.64	76.93	69.58	66.89	75.65
2.48	77.23	79.49	77.08	74.51	72.33	77.89
2.56	78.38	81.48	78.76	79.36	75.19	79.10
2.68	79.86	84.97	77.93	80.24	77.51	81.17
2.78	84.07	85.52	80.93	80.71	80.76	83.26
2.95	85.39	87.55	82.42	86.85	83.82	86.47
3.08	87.92	90.08	89.06	87.86	85.95	89.11
3.18	89.64	90.33	91.28	89.05	87.97	89.92
3.26	91.20	91.64	91.72	89.83	88.88	90.16
3.56	92.35	94.53	93.52	94.19	93.26	93.07
3.73	95.98	96.04	96.78	96.77	95.64	95.29

Table D.3 Fatty acid methyl ester production (wt%) during transesterification of canola oil catalyzed by polyol-derived sodium alkoxide/hydroxide (3: 1 mole ratio) and sodium methoxide

Time (log scale, sec)	1,2-propanediol	1,3-propanediol	Glycerol	Xylitol	Sorbitol	Sodium methoxide
1.48	40.73	54.95	58.71	54.48	14.72	34.26
1.78	63.93	66.31	67.19	62.28	37.18	62.50
2.08	70.47	66.65	68.73	64.89	51.89	66.26
2.26	74.31	73.07	73.65	69.48	68.96	70.36
2.38	76.50	76.94	76.88	74.90	69.56	75.65
2.48	79.94	77.18	79.46	77.05	70.53	77.89
2.56	79.64	80.07	81.25	78.23	72.78	79.10
2.68	83.14	82.44	83.58	82.82	77.25	81.17
2.78	85.10	84.73	84.84	84.54	79.87	83.26
2.95	87.58	87.94	89.10	87.90	83.54	86.47
3.08	88.65	89.36	89.75	88.88	87.10	89.11
3.18	89.68	90.41	90.71	90.78	90.02	89.92
3.26	91.14	92.05	92.03	92.12	89.30	90.16
3.56	96.56	93.89	93.77	93.76	91.66	93.07
3.73	97.29	95.10	96.53	96.61	95.13	95.29

APPENDIX E

TWO-WAY ANALYSIS OF VARIANCE (AVOVA)

Table E.1 Statistical analysis of the linear curve fit of biodiesel yield at various base to polyol mole ratio

Polyol alkoxide mole ratio	Slope I	R square I	Slope II	R square II	Slope III	R square I
1 to 1						
1,2-PD	28.05	0.9062	11.82	0.8646	17.48	0.9731
1,3-PD	16.06	0.5680	34.98	0.9534	16.19	0.9650
Glycerol	24.07	0.8787	31.60	0.9734	13.42	0.9465
Xylitol	9.27	0.9118	61.63	0.9521	19.89	0.9242
Sorbitol	3.44	0.9635	73.27	0.9874	24.10	0.9596
$NaOCH_3$	31.33	0.9274	22.47	0.9631	12.82	0.9509
2 to 1						
1,2-PD	31.37	0.7989	19.35	0.9921	13.72	0.9319
1,3-PD	31.76	0.8669	23.88	0.9831	10.94	0.9861
Glycerol	31.10	0.7877	18.57	0.8884	17.66	0.8903
Xylitol	16.85	0.7662	51.94	0.9666	15.72	0.9636
Sorbitol	13.38	0.5817	54.74	0.9593	16.65	0.9829
$NaOCH_3$	31.33	0.8148	22.47	0.9631	12.82	0.9509
3 to 1						
1,2-PD	33.27	0.9149	21.13	0.9902	13.79	0.9987
1,3-PD	37.26	0.9876	19.60	0.9060	11.70	0.9432
Glycerol	38.41	0.9964	19.72	0.9397	11.65	0.9198
Xylitol	24.35	0.9962	23.70	0.9422	12.55	0.9435
Sorbitol	17.41	0.9661	44.45	0.9113	16.18	0.8837
$NaOCH_3$	31.33	0.8148	22.47	0.9631	12.82	0.9360

Table E.2 Adjusted slope value of the linear curve fit of biodiesel yield at various base to polyol mole ratio

Poly-Alkoxide mole ratio	Adjusted slope Phase I	Adjusted slope Phase II	Adjusted slope Phase III
1 to 1			
1,2-PD	0.2805	0.2997	0.6573
1,3-PD	0.1606	0.6207	0.6566
Glycerol	0.2407	0.6773	0.6985
Xylitol	0.0927	0.7695	0.7298
Sorbitol	0.0344	0.7872	0.7924
2 to 1			
1,2-PD	0.3137	0.5217	0.6811
1,3-PD	0.3176	0.6325	0.7279
Glycerol	0.3110	0.4961	0.8002
Xylitol	0.1685	0.7884	0.7955
Sorbitol	0.1338	0.7652	0.7403
3 to 1			
1,2-PD	0.3327	0.5858	0.8181
1,3-PD	0.3726	0.5818	0.6665
Glycerol	0.3841	0.6010	0.7095
Xylitol	0.2435	0.6283	0.7305
Sorbitol	0.1741	0.7076	0.7112

(i) Adjusted slope = $\frac{\text{Slope from linear curve fit}}{[\text{Substrate}]_t}$

(ii) $[\text{Substrate}]_t = (100 - [\text{Biodiesel yield}]_t)$ wt% , t = reaction time

ANOVATwoWay_phase I

Descriptive Statistics

Catalyst type

	N	Mean	SD	SEM	Variance	Missing	NonMissing
1,23-PD	6	0.2963	0.07291	0.02977	0.00532	0	6
Xyl-Sorb-itol	6	0.14117	0.07224	0.02949	0.00522	0	6
Glycerol	3	0.31193	0.0717	0.0414	0.00514	0	3

Catalyst ratio

	N	Mean	SD	SEM	Variance	Missing	NonMissing
1:1	5	0.16178	0.10162	0.04545	0.01033	0	5
2:1	5	0.24893	0.09013	0.04031	0.00812	0	5
3:1	5	0.30141	0.09008	0.04028	0.00811	0	5

Overall

	N	Mean	SD	SEM	Variance	Missing	NonMissing
	15	0.23737	0.10556	0.02726	0.01114	0	15

ANOVA

Overall ANOVA

	DF	Sum of Squares	Mean Square	F Value	P Value
FactorA	2	0.09305	0.04652	35.21028	2.97279E-5
FactorB	2	0.04975	0.02487	18.8247	4.07111E-4
Model	4	0.14279	0.0357	27.01749	2.43034E-5
Error	10	0.01321	0.00132	--	--
Corrected Total	14	0.156	--	--	--

At the 0.05 level, the population means of Factor A are significantly different.
At the 0.05 level, the population means of Factor B are significantly different.

Means Comparisons

Tukey Test

Catalyst type

	MeanDiff	SEM	q Value	Prob	Alpha	Sig	LCL	UCL
Xyl-Sorb-itol 1,23-PD	-0.15513	0.02099	10.45409	6.28877E-5	0.05	1	-0.21266	-0.0976
Glycerol 1,23-PD	0.01563	0.0257	0.85994	0.81903	0.05	0	-0.05483	0.08609
Glycerol Xyl-Sorb-itol	0.17076	0.0257	9.39566	1.54235E-4	0.05	1	0.1003	0.24122

Catalyst ratio

	MeanDiff	SEM	q Value	Prob	Alpha	Sig	LCL	UCL
2:1 1:1	0.08715	0.02299	5.36103	0.00902	0.05	1	0.02413	0.15017
3:1 1:1	0.13963	0.02299	8.58971	3.19465E-4	0.05	1	0.07661	0.20266
3:1 2:1	0.05249	0.02299	3.22868	0.10478	0.05	0	-0.01054	0.11551

Sig equals 1 indicates that the means difference is significant at the 0.05 level.
Sig equals 0 indicates that the means difference is not significant at the 0.05 level.

ANOVATwoWay_phase II

Descriptive Statistics

Catalyst type

	N	Mean	SD	SEM	Variance	Missing	NonMissing
1,23-PD	6	0.5404	0.1241	0.05066	0.0154	0	6
Xyl-Sorb-itol	6	0.74103	0.06262	0.02556	0.00392	0	6
Glycerol	3	0.59147	0.09096	0.05252	0.00827	0	3

Catalyst ratio

	N	Mean	SD	SEM	Variance	Missing	NonMissing
1:1	5	0.63089	0.19723	0.0882	0.0389	0	5
2:1	5	0.6408	0.13457	0.06018	0.01811	0	5
3:1	5	0.6209	0.05176	0.02315	0.00268	0	5

Overall

	N	Mean	SD	SEM	Variance	Missing	NonMissing
	15	0.63086	0.13086	0.03379	0.01712	0	15

ANOVA

Overall ANOVA

	DF	Sum of Squares	Mean Square	F Value	P Value
FactorA	2	0.12657	0.06329	5.64199	0.02289
FactorB	2	9.89604E-4	4.94802E-4	0.04411	0.95703
Model	4	0.12756	0.03189	2.84305	0.08209
Error	10	0.11217	0.01122	--	--
Corrected Total	14	0.23973	--	--	--

At the 0.05 level, the population means of Factor A are significantly different.
At the 0.05 level, the population means of Factor B are not significantly different.

Means Comparisons

Tukey Test

Catalyst type

	MeanDiff	SEM	q Value	Prob	Alpha	Sig	LCL	UCL
Xyl-Sorb-itol 1,23-PD	0.20063	0.06115	4.64008	0.02062	0.05	1	0.033	0.36825
Glycerol 1,23-PD	0.05107	0.07489	0.96441	0.77898	0.05	0	-0.15422	0.25637
Glycerol Xyl-Sorb-itol	-0.14956	0.07489	2.8242	0.16331	0.05	0	-0.35485	0.05574

Catalyst ratio

	MeanDiff	SEM	q Value	Prob	Alpha	Sig	LCL	UCL
2:1 1:1	0.00991	0.06698	0.20917	0.98803	0.05	0	-0.17371	0.19353
3:1 1:1	-0.00999	0.06698	0.21088	0.98783	0.05	0	-0.19361	0.17363
3:1 2:1	-0.0199	0.06698	0.42005	0.95276	0.05	0	-0.20352	0.16373

Sig equals 1 indicates that the means difference is significant at the 0.05 level.
Sig equals 0 indicates that the means difference is not significant at the 0.05 level.

ANOVATwoWay_phaseIII

Descriptive Statistics

Catalyst type

	N	Mean	SD	SEM	Variance	Missing	NonMissing
Glycerol-1,2-PD	6	0.72745	0.06591	0.02691	0.00434	0	6
Xyl-Sorb-itol	6	0.74993	0.03539	0.01445	0.00125	0	6
1,3-PD	3	0.68367	0.03862	0.0223	0.00149	0	3

Catalyst ratio

	N	Mean	SD	SEM	Variance	Missing	NonMissing
1:1	5	0.70693	0.05676	0.02538	0.00322	0	5
2:1	5	0.749	0.04978	0.02226	0.00248	0	5
3:1	5	0.72713	0.05596	0.02502	0.00313	0	5

Overall

	N	Mean	SD	SEM	Variance	Missing	NonMissing
	15	0.72769	0.05329	0.01376	0.00284	0	15

ANOVA

Overall ANOVA

	DF	Sum of Squares	Mean Square	F Value	P Value
FactorA	2	0.00878	0.00439	1.65463	0.23946
FactorB	2	0.00443	0.00221	0.83408	0.46237
Model	4	0.01321	0.0033	1.24436	0.35315
Error	10	0.02654	0.00265	--	--
Corrected Total	14	0.03975	--	--	--

At the 0.05 level, the population means of Factor A are not significantly different.
At the 0.05 level, the population means of Factor B are not significantly different.

Means Comparisons

Tukey Test

Catalyst type

	MeanDiff	SEM	q Value	Prob	Alpha	Sig	LCL	UCL
Xyl-Sorb-itol Glycerol-1,2-PD	0.02248	0.02974	1.06893	0.73708	0.05	0	-0.05906	0.10402
1,3-PD Glycerol-1,2-PD	-0.04379	0.03643	1.69979	0.47858	0.05	0	-0.14365	0.05608
1,3-PD Xyl-Sorb-itol	-0.06627	0.03643	2.57257	0.21279	0.05	0	-0.16613	0.0336

Catalyst ratio

	MeanDiff	SEM	q Value	Prob	Alpha	Sig	LCL	UCL
2:1 1:1	0.04207	0.03258	1.82607	0.43123	0.05	0	-0.04725	0.13139
3:1 1:1	0.02019	0.03258	0.87651	0.81283	0.05	0	-0.06912	0.10951
3:1 2:1	-0.02188	0.03258	0.94956	0.78481	0.05	0	-0.1112	0.06744

Sig equals 1 indicates that the means difference is significant at the 0.05 level.
Sig equals 0 indicates that the means difference is not significant at the 0.05 level.

APPENDIX F:

CALCULATION FOR CATALYSTS COST AND BIODIESEL PRODUCTION CAPACITY

Calculation of biodiesel catalyst cost per mole:

Per tonne of 30 wt% sodium methoxide = $902[*]; Per tonne of methanol = $300[*]; Per tonne of 50 wt% sodium hydroxide = $100[*];

(i) Therefore, cost of 1 kg of sodium methoxide = $\frac{\$902-(0.7x\$300)}{300\ kg}$ = $2.31/kg

1 kg Catalyst contains 18 moles (1000g/ 54gmol^{-1}),

Therefore the cost of sodium methoxide ($/mole) = $2.31/18 moles = ***$0.128/mole***

(ii) Therefore, cost of 1 kg of sodium hydroxide = $\frac{\$100}{500\ kg}$ = $0.20/kg

1 kg Catalyst contains 25 moles (1000g/ 40gmol^{-1}),

Therefore the cost of sodium methoxide ($/mole) = $0.20/25 moles = ***$0.008/mole***

*Source: Price quoted from online international trading company (alibaba.com)

Calculation of biodiesel production capacity over 1 shipment (100 tonnes) of base catalyst:

In 100 tonnes per shipment of 30 wt% sodium methoxide, 0.5 wt% of catalyst loading would generate:

Biodiesel capacity = $\frac{30\ tonnes\ x\ 100\%}{0.6\%}$ = ***6,000 tonnes***

In 100 tonnes per shipment of 50 wt% sodium hydroxide, with 0.4wt% catalyst loading would generate:

Biodiesel capacity = $\frac{50\ tonnes\ x\ 100\%}{0.5\%}$ = ***12,500 tonnes***